UNIVERSIDADE DE LISBOA
FACULDADE DE CIÊNCIAS
DEPARTAMENTO DE FÍSICA

Automating Daily Linac Quality Control using Portal Images

Sara Filipa Coelho Guerreiro

Mestrado Integrado em Engenharia Biomédica e Biofísica
Perfil em Engenharia Clínica e Instrumentação Médica

Dissertação orientada por:
Prof. Doutor Nuno Matela
Doutor Joep Stroom

2018

Nothing in life is to be feared
it is only to be understood.
Now is the time to understand
more, so that we may fear less.

MARIE CURIE

Acknowledgements

Firstly, I would like to start by express my gratitude to all the team of Radiotherapy Department of Champalimaud Foundation for them contribute to turn this experience more enriching and for all the support given to me during this journey. I am particularly grateful to Dra. Sandra Vieira, who introduce me in this project and who gave me the opportunity to be part of this team. Nevertheless, I want to offer my special thanks to my supervisor Dr. Joep Stroom for all the suggestions and encouragement which he provided me. Dr. Joep, allowed me to obtain a better grasp of the required fundamentals and supported my work constantly. I could not be more grateful, more than mentors, Dra. Sandra and Dr. Joep become a real support contributing to my development.

I am also grateful to Prof. Dr. Nuno Matela for having accepted to join me in this project and for guiding my work. Although he was not physically present, he was always ready to solve any situation.

Thank you to my parents, Constância Guerreiro and José Guerreiro, to my sister, Inês, and to my grandparents. They were the key to getting here and they are responsible for the stability, love and attention. Their life stories were the encouragement to overcome myself. There are no words to better describe how fundamental they have been on this journey.

Thank you to my friends for all the help, attention, motivation and for sharing with me all the own insecurities felt during a master thesis. A special thanks to Francisco, who also shared with me the university world and who became a real friend that I will preserve for life.

Last but not least, a special thank you to my friend J.K. who passed away because of cancer 5 years ago. He was a person who has been part of my teenage years and who left us very early making me feel close to the pain of the real problem that cancer is. Today he continues to be an inspiration and the motivation for my work.

Resumo

O aumento da incidência de tumores malignos, representa um dos principais problemas de saúde nos países desenvolvidos e sob o qual especialistas da área da oncologia se debruçam tendo em vista o desenvolvimento de soluções que garantam maior eficácia dos tratamentos, e assim um aumento na qualidade de vida dos pacientes. Atualmente, existem técnicas que permitem a deteção precoce de lesões malignas bem como o tratamento diferenciado e personalizado tendo em conta o perfil sintomatológico e biológico de cada paciente. Neste sentido, a Radioterapia destaca-se como uma das áreas terapêuticas que mais se desenvolveu, devido ao aparecimento de aceleradores lineares que permitem a administração de doses elevadas de radiação com recurso a sistemas dedicados de colimação de feixes e a sistemas de segurança. Contudo, a adoção de tal tecnologia implica a definição de normas e protocolos de segurança conhecidos como protocolos de controlo de qualidade capazes de validar a capacidade dos aceleradores lineares para realizarem os tratamentos para os quais são projetados. O objetivo de tal controlo é a minimização da incerteza associada à irradiação do volume tumoral através de métricas que se relacionam com o desempenho de diversos componentes constituintes dos aceleradores lineares.

O Centro Clínico Champalimaud (CCC), é uma referência a nível internacional que aposta na inovação e nas novas tecnologias. Na vanguarda dos tratamentos administrados incluem-se os tratamentos de radioterapia realizados no Departamento de Radioterapia do CCC. Neste departamento o controlo de qualidade é realizado de acordo com as recomendações da *American Association of Physicists in Medicine* (AAPM) combinadas com recomendações técnicas específicas aos aceleradores lineares utilizados, culminando assim num protocolo vasto, que implica um período de verificações diárias superior a uma hora. De facto, o controlo de qualidade é baseado num processo bastante demorado e principalmente centrado em tarefas manuais que são realizadas diariamente, o que pode conduzir a erros nos processos de medição. Nesse contexto, o projeto desenvolvido no âmbito desta dissertação relaciona-se com a discussão das principais limitações e com a otimização do protocolo de controlo de qualidade adotado atualmente na clínica, de modo a torná-lo mais confiável e eficaz. O objetivo é aliviar o esforço clínico, permitindo que os especialistas se concentrem noutras questões. Portanto, a automação de tais procedimentos apresenta-se como uma solução eficiente para agilizar o processo de controlo de qualidade e assim reduzir os erros a ele associados.

Atualmente, os aceleradores lineares existentes no mercado tendem a disponibilizar sistemas de imagem sofisticados, como o *Electronic Portal Image Device* (EPID), que detetam a radiação proveniente do feixe, permitindo assim gerar representações designadas por imagens portais. Originalmente, tais sistemas de imagem visavam a verificação da posição do paciente durante os tratamentos. Posteriormente, abriu-se portas à utilização das imagens portais tendo em vista outras finalidades, nas quais se destaca a automatização do controlo de qualidade. Em particular, a utilização de imagens portais permite a extração de métricas de performance, baseadas na análise dos valores de intensidade de cada pixel, que avaliam parâmetros relacionados com a qualidade do feixe e parâmetros geométricos, relativos a outros componentes do acelerador, nomeadamente o colimador e a gantry.

Apesar de alguns dos maiores fornecedores de aceleradores lineares desenvolverem e integrarem os seus próprios softwares de análise de imagens portais, como o *Machine Performance Check* (MPC) desenvolvido pela *Varian Medical Systems* (Varian Medical Systems, Inc., Palo Alto, CA), muitas unidades clínicas continuam a privilegiar a criação das suas próprias ferramentas de análise em alternativa às soluções propostas no mercado. Ainda que o MPC tenha sido considerado como uma alternativa numa

fase inicial deste projeto, o conjunto de recursos apresentado por este software não descartou a possibilidade de melhorar o protocolo com a inclusão de novos testes de análise por forma a melhorar a resposta às exigências da clínica.

Neste contexto, o processo de otimização do protocolo de controlo de qualidade implementado no CCC consistiu no desenvolvimento de um software, utilizando a linguagem Python, que permite o armazenamento dos dados por comunicação com base de dados SQL, facilitando a gestão dos dados e respetiva visualização, bem como análises futuras. Além disso, alguns módulos para aquisição e análise de parâmetros numéricos também foram incluídos neste software tendo sido assim desenvolvido o módulo dedicado à manipulação do eletrômetro, o dispositivo utilizado na leitura dos valores de dose, e o módulo responsável pela verificação do posicionamento das lâminas do colimador de múltiplas lâminas (MLC). Em suma, o software desenvolvido combina a componente de armazenamento e gerenciamento de dados com os testes de controlo de qualidade. A gestão mais agilizada dos principais comandos do eletrômetro (usando uma comunicação via conexão RS232) acelera o registro das leituras em formato digital. O uso de imagens de portais adquiridas com o EPID para extrair automaticamente o posicionamento das folhas do MLC reduz a incerteza associada ao erro humano nas medições.

A decisão de inclusão dos dois últimos módulos prendeu-se com conclusões baseadas na análise dos dados do controlo de qualidade e do registo de falhas e na opinião dos profissionais responsáveis pela realização de tais processos, que descreveram a configuração do eletrómetro e o teste MLC como um processo demorado e pouco eficaz, respetivamente. A análise inicial dos dados relativos aos parâmetros verificados no controlo de qualidade ao longo do ano de 2017 e a observação dos dados referentes ao registo de falhas do acelerador linear Edge®, revelaram a ocorrência de 28 falhas relativas ao componente MLC durante este período, sem deteção prévia durante o controlo de qualidade. Este facto, em concordância com as afirmações dos profissionais, contribuiu para o desenvolvimento de um módulo dedicado à análise do posicionamento das lâminas.

Os resultados obtidos utilizando o módulo de leitura da dose mostraram ser os mesmos que os obtidos pelo método manual anteriormente utilizado.

Em relação aos resultados relacionados com o módulo de posicionamento das folhas, a inclinação do colimador e as diferentes distâncias entre as lâminas e o centro de rotação mostraram impacto nas posições finais das lâminas. Além disso, este estudo sugeriu uma sobre-exposição causada pela abertura excessiva das lâminas (cerca de 1,2-1,4 mm na situação considerada). É importante notar que estudos anteriores realizados nesta clínica confirmam esses resultados. No entanto, os mesmos estudos anteriores, quando um componente dinâmico é introduzido no movimento das lâminas, revelaram o comportamento oposto, sugerindo um fechamento das lâminas e, consequentemente, uma subexposição tumoral em relação à contribuição deste componente.

O módulo de análise do posicionamento das lâminas foi ainda sujeito a testes que visavam analisar a performance associada, tendo sido avaliada a precisão do método utilizado na determinação do centro de rotação do colimador, os diferentes métodos de segmentação considerados e, por último, a posição estimada pelo algoritmo. Relativamente à determinação do centro de rotação do colimador, parâmetro utilizado no cálculo do posicionamento das lâminas, o algoritmo mostrou boa aproximação e uma redução do tempo de computação em cerca de 40% quando comparado à função *Starshoot()* incluída no package *Pylinac*, desenhada para o mesmo efeito. No que diz respeito à segmentação de imagem, foram testados diferentes métodos a fim de estabelecer a fronteira física entre a região da lâmina e a região irradiada (região aberta). De entre os diferentes métodos analisados, *Canny Edge Detector*, *Otsu Thresholding* e *Half-Maximum Intensity Value*, o último método apresentado revelou os melhores resultados uma vez que permite a inclusão de técnicas de precisão sub-pixel e se revela independente do tamanho do pixel.

Posteriormente, a estimação da posição das lâminas obtida com recurso ao algoritmo desenvolvido foi comparada com os resultados obtidos através do *garden fence test* revelando uma discrepância de 1.2 mm na distância média entre pares de lâminas. Apesar do resultado obtido ser suficientemente próximo do esperado, 1.4 mm, tendo em conta a precisão que se pretende (aproximadamente 0.1 mm), importa notar que o movimento das próprias lâminas introduz erros no seu posicionamento, mesmo durante aquisições sucessivas. Finalmente, foi mostrado o impacto da inclinação do colimador e dos diferentes posicionamentos das lâminas nos resultados obtidos.

Em suma, este projeto permitiu otimizar o controlo de qualidade diário do CCC dotando a clínica de uma ferramenta capaz de aumentar a eficiência de execução do protocolo e assim, facilitar a gestão dos dados resultantes. Note-se ainda que a introdução do módulo de análise do posicionamento das lâminas e de armazenamento de leituras de dose poderá conduzir a novos projetos de investigação baseados em técnicas de análise de dados.

Palavras-chave: radioterapia; controlo de qualidade; acelerador linear; imagens portais.

Abstract

The increase in the incidence of malignant tumours is one of the main health problems in developed countries. In this context, specialists in the area of oncology are focused on the development of solutions that guarantee greater effectiveness of treatments, and thus an increase in the quality of life of the patients. Currently, there are techniques that allow the early detection of malignant lesions as well as provide differentiated and personalized treatment taking into account the symptomatic and biological profile of each patient. In this context, radiotherapy is considered one of the most developed therapeutic areas due to the appearance of linear accelerators that combine the administration of high doses of radiation with the use of dedicated beam collimation and safety systems. However, the adoption of these systems implies the definition of safety standards and protocols in a procedure namely quality control able to test linear accelerators performance to complete the treatments for which they are designed. In this sense, quality control of linear accelerators is a crucial mark in the daily routine of radiotherapy physicists and technicians. The goal is to minimize the uncertainty in the irradiation of tumour volume by using quality control to obtain parameters related to the performance of components that individually compose the radiotherapy system.

Champalimaud Clinical Center (CCC) is an international reference focused on the innovation and new technologies. At the forefront of the treatments administered are radiotherapy treatments performed at the Department of Radiotherapy of the CCC. In this department quality control is performed according to the recommendations of the American Association of Physicians in Medicine (AAPM). Combined with technical recommendations specific to the linear accelerators used, such procedure culminates in a vast protocol, which implies a daily verification period of more than one hour. In fact, the quality control is based on a time-consuming and mostly manual process performed daily, causes errors in the measurement processes. In this context, the project developed within the scope of this dissertation is related to the discussion of the main limitations and in the optimization of the quality control protocol currently adopted in the clinic, making it more reliable and effective in order to relieve the clinical effort allowing the specialists to focus on other issues. Therefore, the automation of such procedures presents itself as an efficient solution to speed up the process of quality control and to reduce errors associated therewith.

Nowadays, the linear accelerators on the market tend to provide sophisticated imaging systems, such as the Electronic Portal Image Device (EPID), which detect the radiation coming from the beam and generate representations called portal images. In the beginning, such imaging systems were used for verifying the patient's position during treatments. Subsequently, the portal images were used for other purposes, in which the automation of quality control is highlighted. In particular, the use of portal images allows the extraction of performance metrics, based on the analysis of the intensity values of each pixel, that evaluate parameters related to the beam quality and to the geometry relative to other components of the accelerator, as an example, the collimator and the gantry.

Although some of the largest suppliers of linear accelerators had developed and integrated their own portal imaging analysis software, such as the Machine Performance Check (MPC) developed by Varian Medical Systems (Varian Medical Systems, Inc., Palo Alto, CA), many clinical units continue to approve the idea of creating their own solutions as alternative to the solutions proposed by linear accelerator suppliers. Even though the MPC was considered as an alternative during this project, the features presented by this software did not discarded the possibility to improve the analysis tool to better fitted the clinic requirements.

In this context, the process of optimization of the quality control protocol implemented in the CCC consisted in the development of a software, using Python language, that allows the storage of the data in SQL databases, which facilitates the data management and its visualization, as well as their future analyses. In addition, some modules for acquiring and analysing numeric parameters were also included in this software being them, the module dedicated to the manipulation of the electrometer, the device used in the dose values reading, and the module responsible to the verification of the positioning of the leaves of the multi-leaf collimator (MLC). To sum up, the developed software combines the data storage and management component of quality control tests. The faster control of the main commands of the electrometer (using a communication via RS232 connection) speed up the registration of the readings in digital format and the using of portal images acquired with the EPID to automatic extract the positioning of the leaves of the MLC reduces the uncertain related to the human error in these measurements.

The decision to include these two modules was based on the analysis of the quality control data and failures records files, and on the recommendations of the professionals responsible for conducting the quality control, who described the configuration of the electrometer and the MLC test as a time-consuming and ineffective process, respectively. The initial analysis of the data related to the parameters verified in the quality control during the year 2017 and the observation of the data concerning the failures, both from linear accelerator Edge®, revealed the occurrence of 28 failures related to the MLC component during this period, without prior detection during quality control. This result is in accordance with the statements of the professionals, describing the leaf positioning test as an inaccurate process, and validate the decision of start by develop a module dedicated to the analysis of the positioning of the leaves.

The results obtained using the dose reading module are found to be the same that those obtained by the manual method previously used with reduction of the time spent.

Regarding the results related to the leaves positioning module, the collimator inclination and the different distances between the leaves and the centre of rotation shown to have an impact in the final leaves positions. In addition, this study suggests an overexposure caused by the excessive opening of the leaves (about 1.2-1.4 mm in the considered situation). It is important to note that previous studies performed in this clinic confirm these results. However, the same studies, when a dynamic component is introduced in the movement of the leaves, reveal the opposite results, suggesting an closure of the leaves and, consequently, a tumour underexposure with respect to the contribution of this component.

In short, this project allowed to discuss and optimize the daily quality control of the CCC providing to the clinic a tool capable of increasing the protocol execution efficiency and, in this context, to easier the management of the resulting data. It should also be noted that the introduction of the leaves positioning analysis and the storage of dose readings modules could bring to the clinic new research projects based on data analysis techniques.

Key-words: radiotherapy; quality control; linear accelerator; portal images.

Contents

List of Figures

List of Tables

List of Abbreviations

3-D CRT Three-dimensional conformal radiation therapy

a-Si Amorphous silicon

AAPM American Association of Physicists in Medicine

CBCT cone beam computer tomography

CCC Champalimaud Clinic Centre

CT computed tomography

DNA deoxyribonucleic acid

EPID electronic portal image device

FFF flattening-free filter

IGRT image-guided radiation therapy

IMRT Intensity-modulate radiation therapy

IsoCal Isocenter Calibration

LINAC linear accelerator

MLC multileaf collimator

MPC Machine Performance Check

QA Quality assurance

QC quality control

SRS/SRT steriotatic radiosurgery/radiotherapy

VMAT volumetric modulate arc therapy

1 Introduction

Cancer is one of the leading causes of death, and can be defined as an abnormal and uncontrolled division of new cells empowered by changes in cell cycle. During their life, cells experience mitosis, where cell division takes place, and S phase, where deoxyribonucleic acid (DNA) synthesis occurs. The whole process is often controlled to assure that in case of flaws, the cell cycle is interrupted. Therefore, failures at control points during cell cycle can lead to an unchecked cell division [1]. Nowadays, ageing, ethnicity, estrogens overexposure, environmental factors, obesity, or radiation are factors associated with the development of cancer. Besides that, some patients present a genetic predisposition to develop this pathology since they can inherit the genes that codify the information to develop abnormal cells. All these factors contribute to the number of people affected worldwide.

In 2015, according to Portuguese Institute of Statistics, malignant tumours represented the second basic cause of death. They were responsible for 26 647 deaths, which corresponds to 24,5% of all mortality in this country in the same year [2]. These numbers show the importance of improving techniques involved in cancer treatments. Radiotherapy, chemotherapy, and surgery are the main therapies whose purpose is to remove or decelerate the division of cancer cells to extend average life expectancy.

Radiotherapy uses ionizing radiation like X-rays to irradiate malignant cells and damage their DNA strands. Currently, this technique is used in curative and palliative treatments. However, the use of a single therapy in the treatment of cancer may not be efficient enough in inactivating malignant cells. In this case, the option is to combine radiotherapy with other techniques as chemotherapy or surgery to improve treatment results. Depending on the situation of each patient a different radiotherapy treatment modality can be considered, external radiotherapy and brachytherapy are the two possible choices. In case of external radiotherapy, the tumour is irradiated using a beam of particles generated externally. For brachytherapy, the source of radiation is placed inside the body [1]. The present work is focused on external radiotherapy which uses linear accelerator (LINAC) as the mechanism to generate the beam and deliver the radiation to the patient. The last generations of these devices confer more accuracy in the delivery system leading to the practice of single sessions with the delivery of concentrated dose of radiation to the tumour. In this situation, since high doses of radiation are considered, the damages caused by a possible system failure can have serious consequences. To prevent some of these failures, linear accelerators are submitted to daily tests in order to verify machine performance, a process named daily quality control. Nowadays, a major issue is the clinical effort to perform machine daily tests since quality control can be time-consuming. Acquiring the results is not an automated process, but a mostly manual procedure that uses a large set of measuring instruments and phantoms to obtain a machine performance overview.

The current project was developed at Champalimaud Clinic Centre (CCC) in straight cooperation with the clinical team, a benefit that allowed better understand their needs and limitiations. The project has as main goal the implementation of a new tool based on an automated procedure capable of quickly performing the quality control of the linear accelerator. Reducing time spent, increasing the accuracy of the measurements and save the data in digital format are the three major concerns of this project which are achieved by an integrate solution that in sum is capable of speeding up dosimetry checks, storaging data and performing an analysis of collimator leaf positions. Actually, some linear accelerator

producers already develop their own tools to evaluate machine performance as Machine Performance Check (MPC) [3, 4, 5], a software developed by Varian Medical Systems capable of automate some quality control measurements based on portal image analysis. This software was investigated and used to inspire the design of the new solution.

The use of portal images in quality control is an alternative higly studied by others [6, 7] in past to evaluate the possibility of automate the process reducing the time spent and the number of instruments used while providing accurate results. In this work, most functionalities of the solution presented are based on the benefits of this technology.

The current dissertation follows the steps taken during the investigation. Therefore, we start by analysing the current situation and the norms imposed by the regulatory agencies. Then, the basic principals of operation of MPC were studied in order to consider this tool as a solution for the current protocol limitations. However, a new solution was developed and the suggestions for the new quality control protocol are finally presented.

2 Background

This chapter starts by present the essential concepts of external radiotherapy giving the reader an overview focused on the basic physics behind radiation used in cancer treatment and how ionizing radiation causes cellular damage. The main mechanisms related to linear accelerators and delivering the dose to the tumour are explained to introduce the quality control subject. Quality control of linear accelerators is the main concern of this project and all the general issues about that are covered in this section. A more detailed description related to tolerances levels adopted by CCC, the tests performed and authority recommendations are provided in the following subsections.

2.1 External Radiotherapy

External radiotherapy is one of the strands of cancer treatment that uses radiation to effectively treat the tumour with minimal exposure of healthy tissues. In this situation, an externally generated X-ray beam using a linear accelerator is considered. In Portugal, the number of patients admitted for radiotherapy treatments has increased. According to DGS statistics, an increase of 5% in the number of patients per year between 2009 and 2013 was estimated. In addition, the same institution refers an increase in the number of radiotherapy units from 18 in 2008 to 25 in 2015. These data validate the investment by the scientific community in the looking for new solutions that solve current problems that affect the progress of radiotherapy. Below will be explained the fundamentals of radiotherapy in order to better understand the importance of linear accelerator in the treatment of cancer.

2.1.1 Radiobiology

The interaction between radiation and organic tissues is the underlying principle to radiotherapy treatments. Depending on the energy and its effects on cells, it is possible to distinguish between ionizing and non-ionizing radiation. X-rays and gamma rays are examples of ionizing radiations and infra-red, microwaves and radio waves are examples of non-ionizing radiation. The radiation used in radiotherapy treatments is the ionizing radiation and become associated with higher frequencies that revealed the capacity to induce ionization of the atom whereas non-ionizing radiation leads only to the excitation of the electrons [8].

Considering the interaction between ionizing radiation and organic tissues, damage to DNA strands can occur through direct or indirect action. On the one hand, the radiation can have direct action upon the DNA and the atoms are ionized due to physical interactions which may result in biological damage, are examples electrons, alpha particles and heavy ions. On the other hand, for photons and neutrons the interaction can occur in an indirect way by radiation interaction with other molecules and atoms which leads to the production of electrons with high energy that can move through the tissue and generate free radicals. By diffusion these radicals can damage DNA strands breaking chemical bonds [9].

When the DNA strand of a malignant cell is destroyed, this cell is prevented from further dividing. In this order, the ionizing radiation is administered to the patient through a beam limited to the tumour region. By dividing the required total dose of radiation in daily doses administered over time is possible

to ensure the integrity of healthy tissues. The effectiveness of treatment depends not only on the amount of radiation administered but also, among other factors, the radio-sensitivity of tissues and their capacity to recover [1].

2.1.2 Planning Treatment

A cancer diagnosis supposes a clinical evaluation to define the treatment strategy (Figure 1). For external radiotherapy treatments, the therapy starts with an individual planning for each patient based on the prescribed requirements (Figure 2). A planning computed tomography (CT) image is acquired [8].

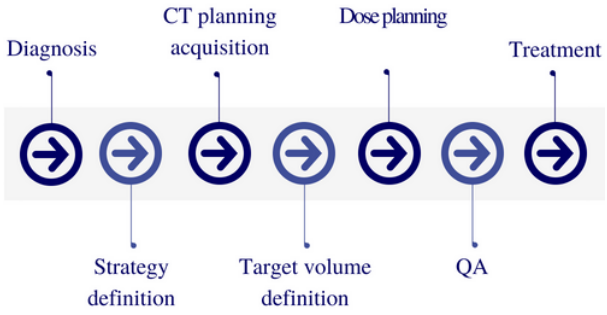

Figure 1: Main steps during external radiotherapy treatment.

A medical team in cooperation with physicists are able to develop the individual treatment plan using the previous image acquired. Diagnostic images can be obtained through other techniques such as positron emission tomography, magnetic resonance imaging or ultrasound imaging which will be an additional source of information. However, dose calculation is performed using CT where internal target volume, planning target volume, clinical target volume and the gross tumour volume as well as the organs at risk around are marked [10].

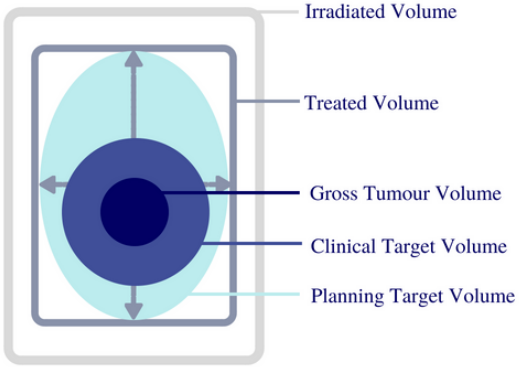

Figure 2: Definition of target volume. Target volume includes real tumour volume (gross tumour volume), real and suspect tumour volumes (clinical target volume), the margin for variations in tumour size or position (planning target volume), the volume which receives the dose for cure (treated volume) and the volume which receives the significant dose in relation to normal tissues (irradiated volume). Adapted from [10].

The following steps involves all the dosimetry measurements to start the treatment. In this situation, a specific software (Eclipse^{TM} - Treatment Planning System) [11] is used to calculate the dose in each volume involved. Once complete, the plan is tested using a phantom and treatment starts after plan approval. A cone beam computer tomography (CBCT) is acquired and compared with CT planning in

order to evaluate patient and tumour position, procedure named image-guided radiation therapy (IGRT). Finally, if structures position match in both images, the tumour volume is irradiated.

2.1.3 Linear Accelerator

The irradiation of the tumour volume is performed by a LINAC used in external radiotherapy treatments to generate a radiation beam that interacts with matter. This device consists of a gantry, which includes the collimator system, a gantry support, a modulator, a treatment couch and a control console [8].

During the treatments, the position used as reference for patient placement is the isocenter. This position corresponds to the location where the different components, gantry, collimator and couch rotation axis intercept each other as shown on Figure 3.

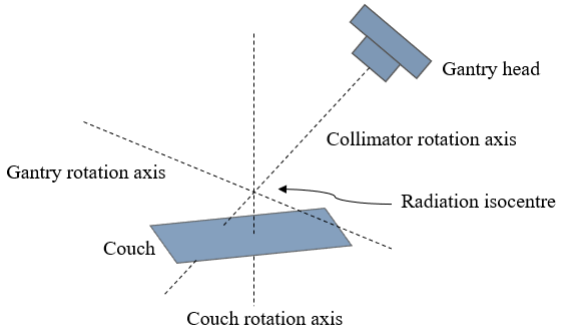

Figure 3: Illustration of linear accelerator radiation isocentre. Representation of the radiation isocentre position which corresponds to the place where gantry, collimator and couh rotation axis intercept each other.

The collimator rotation axis is also defined as the central axis of the treatment beam. The generation of the treatment beam in radiotherapy using a LINAC occurs with the production of radiofrequency waves in the magnetron or klystron depending if are low or high energy linear accelerators. At the same time, electrons are produced and subsequently injected in the electron gun by heating a tungsten filament. These electrons are accelerated by the action of the previous radiofrequency waves produced. The beam is created when the electrons hit and interact with the tungsten target. During its course, the electron beam is redirected with the aid of three magnets that lead to the curvature of the beam, directing it towards the target. By focusing on the tungsten target, electrons leads to megavoltage X-ray photons [1, 8] and the treatment beam is produced. The process is illustrated on Figure 4.

The photons forming the treatment beam are not uniformly distributed along the beam. Therefore, in order to obtain beam homogenization and to reduce the dose delivered, a specific filter, flattened filter, is introduced for each X-ray energy considered (Figure 5). The use of flattened filters will generate flat dose profiles which homogenize dose variation across the beam. These filters includes high Z materials and usually adopt a conical shape in order to flatten the peaked bremsstrahlung spectrum of megavoltage photons.[8].

The new advances in radiotherapy treatments lead to the administration of high doses to the tumour in order to increase the effectiveness of the treatments. Although the risk associated to this practice and what the irradiation using high doses can mean to the healthy tissues in case of failure, the vast list of benefits increase their popularity. In this situation, the treatments are performed without requiring the existing filter, a methodology known as flattening-free filter (FFF). Thus, high dose rates can be

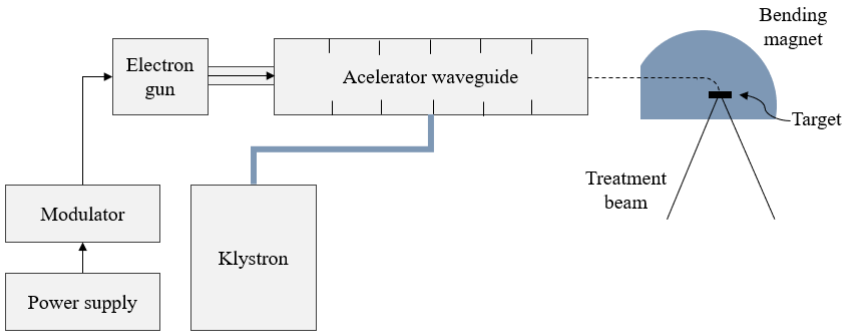

Figure 4: Illustration of linear accelerator used in external radiotherapy. Representation of the dose delivery system responsible for producing high X-rays. The klystron accelerate electrons inside the waveguide tube to produce microwaves. Then, the electrons are directed by a magnet in direction of the target in order to produce treatment beam.

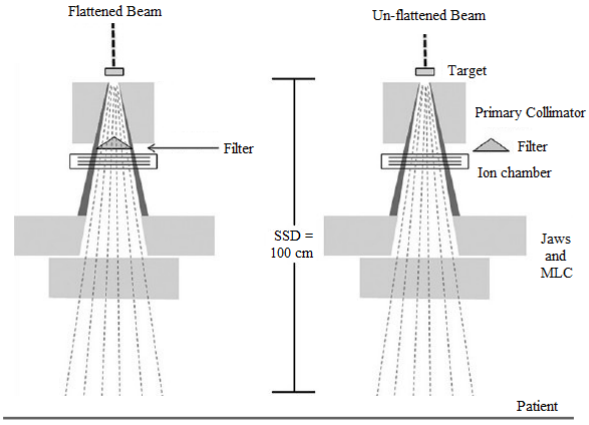

Figure 5: Illustration of differences between flattened and un-flattened beams used in external radiotherapy. Representation of the filtering systems and collimator system used to filter, set maximum aperture and re-shaped treatment beam. Adapted from beams.

administered in a shorter period of time which contribute to the decreasing of patient discomfort.

In addition, collimator system is responsible for reducing the dispersion, setting the maximum aperture of the beam and change beam shape. The primary collimator, jaws and multileaf collimator (MLC) are the components that form the collimator system, introduced to increase treatment accuracy.

Collimator system

The collimator system define the treatment radiation field delivered to the patient. As previously mentioned, this system include a fix component, the primary collimator, used to reduce the beam dispersion and to set the maximum aperture of the beam, and two movable components, the jaws and MLC, capable of adjust beam shape. Here only the movable components will be studied. While jaws consist of only four solid blocks that form only square or rectangular fields, the MLC has a configuration that allows the physicist to adjust the beam more accurately.

Therefore, MLC consists of a set of thin leaves divided into opposite banks, A and B (Figure 6). The independent movement of each leaf in one direction is used to match beam and tumour shape [1].

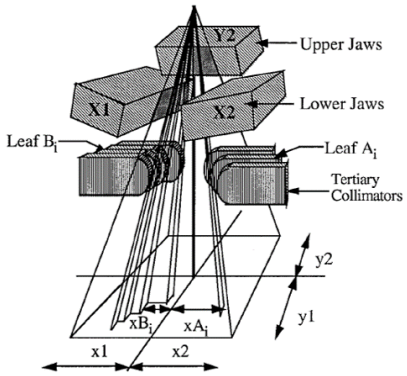

(a) Representation of general collimator system including upper and lower jaws and multileaf-collimator (in this scheme Y1 jaws has been omitted).

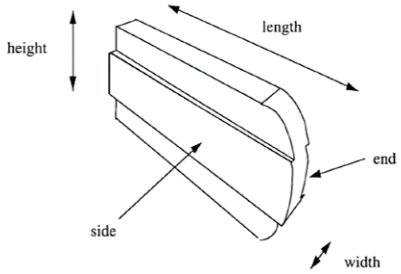

(b) Example of a curve end termination and a stepped side of a collimator leaf.

Figure 6: Schematic representation of a generic photon collimator system. Adapted from [12].

Considering the last LINACs generations, most of them contain 60 leaf per bank presenting widths of 5 mm or less. This configuration gives to this component the ability to adjust the treatment beam in such a way that single dose treatments start to be performed (see section 2.1.4).

2.1.4 Delivery Techniques

Associated with the technology improvement different dose delivery techniques emerge (Figure 7). Currently, dose delivery is performed using one of the following techniques:

3-D CRT – Three-dimensional conformal radiation therapy (3-D CRT) uses a set of beam positions to create an irradiated tumour volume with high dose distribution. In this case, for each position, the radiation beam is shaped to match the tumour volume. This is possible due to the patterns created for each beam moving the leaves of the collimator according to the three-dimensional information obtained previously. Nevertheless, the protection of surrounding tissues is not accurate enough to irradiate with high doses [13, 14].

IMRT – Intensity-modulate radiation therapy (IMRT) guarantees more accuracy than 3-D CRT. During irradiation and in addition to beam shaping, beam intensity can be modulate. For each beam position, the beam is subdivided into different intensity levels, improving treatment accuracy. The tumour irradiation can be performed in phases, the tumour is not irradiated between changes in MLC pattern or gantry rotations, or can be performed continuously, the tumour volume is always irradiated and during the treatment, the MLC will adjust the leaves to create the specific patterns [14, 15, 16].

VMAT – volumetric modulate arc therapy (VMAT) allows the continuously tumour irradiation during

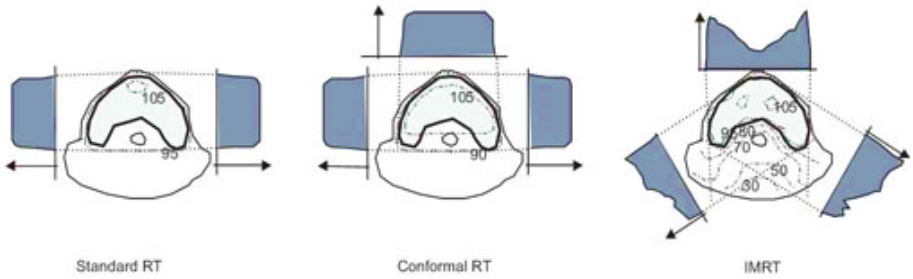

Figure 7: Ilustration of different techniques for tumour irradiation. Tumour irradiation using: 1) standard and conformal radiotherapy with uniform beams and 2) IMRT with intensity-modulated beams. Numbers correspond to a percentage of a prescribed dose. Adapted from [13].

gantry rotation and MLC motion. It is an advance of IMRT techniques since it is possible to change rotation velocity, dose rate and MLC shape simultaneously [17].

SRS – steriotatic radiosurgery/radiotherapy (SRS/SRT) is the most recent technique used in tumours in the brain or central nervous system. The increasing accuracy and precision related with this technique and with the imaging systems used makes possible to deliver a high dose of radiation most of the times in a single treatment session [14, 16].

2.2 Quality control in Radiotherapy

LINACs are subjected to daily tests to ensure the accuracy with which these devices deliver the required radiation doses. A set of procedures and tolerances should be considered based on guidelines suggested by regulatory authorities. Quality assurance (QA) can be defined in the context of radiotherapy as *"(...) the correct monitoring of the patient together with all the procedures that ensure compliance with dose prescribed, restricting the healthy tissues to the minimum dose and safeguarding the exposure of the technical team involved"* [1]. Initial acceptance and commissioning verification, periodic quality control (QC) and patient specific-QA are part of quality assurance. The current project is focused on QC protocol which consists in a daily review performed to verify if the stipulated requirements are fulfilled, adjusting and reviewing any faults.

2.2.1 Quality control program

The QC program of a LINAC must specify a set of indications as the parameters to be tested, the instruments required to perform the tests, a test description and its frenquency, the expected results and the actions to be taken when there is no agreement with established standards [1]. The challenge is to develop a protocol capable of cover all the previous indications without an increase of clinical effort. The QC verification can be divided according to different test categories responsible for evaluate machine performance:

- **Security**, ensuring the operation of all security systems which may include visual and audio interlocks, door closing safety, anti-collision systems and beam status indicator;
- **Geometric accuracy**, testing geometric precision in radiation delivering based on couch, gantry, collimator and jaws performance evaluation;

- **System stability**, comparing the measures with previous ones to evaluate long-term response;
- **Image quality**, evaluating the performance of image system devices used to treatment monitoring, usually the tests achieved mainly verify alignment with isocentre;
- **Integrity of infrastructure**, identifying damages on device and its components that can compromise the treatment;
- **Dosimetry**, verifying if the dose administered correspond to the dose measured using ion chambers.

The previous categories of tests are valid for daily, monthly and annual verifications. However, the number of tests included in the daily protocol is different from the number of testes included in a monthly or annual protocol. Daily quality control should be composed by a few set of quickly checks able to detect main problems responsible to prevent a safe dose delivery at the same time that can be included in the daily clinical tasks without disturb its routine. In addition, monthly and annual checks complement daily checks. These less frequent tests are more exhaustive in order to thoroughly evaluate the equipment performance.

Regarding the above categories of tests, it is important to note that not all clinics include all of the above categories of tests in their daily control routine. However, dosimetry tests are a practice imposed by major regulatory authorities, since they detect direct beam faults. These tests are performed using ion chambers, devices particularly sensitive to ambient conditions of temperature and pressure, connected to an electrometer.

Dosimetry test using ion chamber and electrometer

One of the main tests performed during quality control to check X-ray output is the daily monitoring of the dose values. During dose measurements the correct operation of linear accelerator is ensured by using an detector, in which interaction with the radiation occurs, and a measuring device, responsible to read the detector output and display dose values. Cylindrical ion chambers are usually used in radiation therapy environment as dosimeters to measure output dose when connected to an electrometer, a measuring device. These chambers are composed by a central electrode (anode), a coating (cathode) and a sensitive volume filled by a gas. The atoms in the sensitive volume are ionized by the action of the radiation when it interacts with the medium. The voltage applied between the cathode and the anode leads to the migration of the produced ions and the electrometer measures the electric current generated by the ion flux. Since ambient conditions as temperature and pressure can influence the dosimeter response in such way that a pressure increase or temperature decrease causes an increase in air density leading to a wrong dose value, a correction factor is introduced:

$$F = \frac{(273,15+T)P_0}{(273,15+T_0)P}, \tag{1}$$

where T and P are the ambient temperature and pressure, and T_0 and P_0 are the standard equal to 20°C and 1013.15 mbar respectively. In addition, relative humidity is also verified in order to examine if this parameters is within certain values (20%-80%). This physical quantity influences the number of joules of energy deposited in the gas per unit of charge released, $(W/e)_{air}$, and consequently the dose absorbed as shown on equation 2.

$$D = \frac{Q}{V\rho}\left(\frac{W}{e}\right), \tag{2}$$

where Q is the charge in the chamber, ρ the density of the gas and V the gas volume. As mentioned, relative humidity presenting measured output within 20-80% is accepted, to these values corresponds to a $(W/e)_{air}$ = 33.97 J/C approximately. During quality control, before the dose measurements are performed, the user must enter the high voltage, temperature and pressure values on the electrometer. By sending the previous information to the device, initial voltage used to bias ion chamber can be applied and the measurements can be corrected taking into account ambient conditions.

Until now, the technological advances and the emergence of other solutions do not replace ion chambers. These devices remaining the standard method to perform dose measurements due to its proved reliability. Therefore, based on the previous fact, one of the aims of this project was not to replace these devices in clinical routine but rather to reduce human error and decrease the time-spent by simplifying the communication between the user and the equipment.

2.2.2 AAPM recommended tolerances

The AAPM [18] suggests a brief daily check based on dosimetry, mechanical and security tests for each treatment modality as shown in Table 1.

Table 1: AAPM suggestion for the parameters to be analyzed and respective tolerances based on the external radiotherapy modality considered, NON-IMRT, IMRT and SRS/SBRT. Adapted from [18].

PROCEDURE	DESCRIPTION	NON-IMRT	IMRT	SRS/SBRT
	Dosimetry			
X-ray output	Dose delivered should be within 3% of the baseline value.	± 3%	± 3%	± 3%
	Mechanical/Geometry			
Laser localization	Verification of the laser alignment, system used to adjust patient or objects position.	± 2 mm	± 1.5 mm	± 1 mm
Distance indicator	Measurement of a fixed distance between the patient and the source of radiation (SSD).	± 2 mm	± 2 mm	± 2 mm
Collimator size indicator	Measurement of light field edges dimension.	± 2 mm	± 2 mm	± 1 mm
	Safety			
Door interlock	Ensure that the door opening means beam off.	Functional	Functional	Functional
Door closing safety	Ensure that the door proximity sensors avoids collisions.	Functional	Functional	Functional
Audio-visual monitor	Confirm that it is possible to hear and see the patient in the treatment room.	Functional	Functional	Functional
SRS interlocks	Additional recommended interlocks.	NA	NA	Functional
Radiation area monitor	Functional when the beam is on.	Functional	Functional	Functional
Beam on indicator	Functional when the beam is on.	Functional	Functional	Functional

Since imaging systems are used during the treatments, they should also be submitted to quality control

verifications. The Table 2 presents AAPM [18] suggestions for CBCT, planar kV and MV imaging systems.

Table 2: American Association of Physicists in Medicine (AAPM) suggestion for the imaging daily quality control based on the external radiotherapy modality considered, NON-SRS/SBRT and SRS/SBRT. Adapted from [18].

PROCEDURE	NON-SRS/SBRT	SRS/SBRT
Planar kV and MV (EPID) imaging		
Collision interlocks	Functional	Functional
Positioning/repositioning	± 2 mm	± 1 mm
Imaging and treatment coordinate coincidence	± 2 mm	±1 mm
Cone-beam Computed Tomography		
Collision interlocks	Functional	Functional
Positioning/repositioning	± 1 mm	± 1 mm
Imaging and treatment coordinate coincidence	± 2 mm	± 1 mm

2.3 Electronic portal imaging device

The most recent LINAC also include image acquisition systems such as electronic portal image device (EPID) that cooperate during radiation therapy treatment to improve measurements accuracy such as displacements in tumour position or evaluation of beam quality [1]. Nowadays, this device, also named flat-panel detector, composed by Amorphous silicon (a-Si) replace liquied-filled ionisation chamber and camera-based EPID [19]. The a-Si panel is used to acquire 2D portal images generated by action of the X-ray produced in the linear accelerator. This is possible once the flat-panel detector is positioned on the opposite side of the gantry head following the rotational movement.

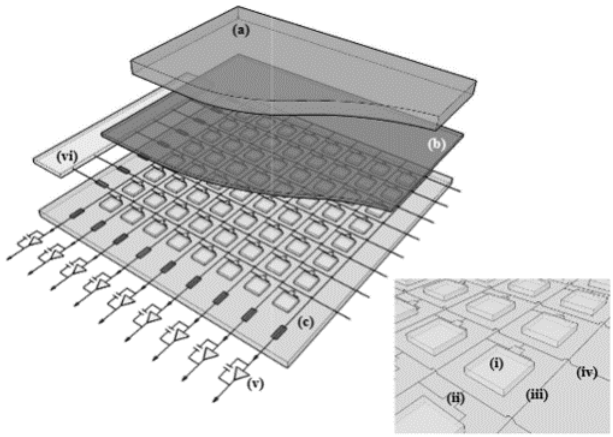

Figure 8: Illustration of a flat-panel image array. Representation of the main components: copper plane (a), scintillating phosphor (b), active matrix array (c) which includes, a-Si photodiode (i), TFT (ii), data line (iii) and gate control (iv), and external electronics (d) which includes, pre-amplifiers (v) and control gate circuity (vi). Adapted from [20].

The a-Si EPID consists of a copper plate, a phosphor screen and a light sensor composed by photodiodes and thin film transistors (TFT) as shown on Figure 8. During the detector irradiation, the X-ray photons interact with the phosphor screen (gadolinium) which in turn emits a new photon (light). The photons generated through this process are detected by the photodiodes and the signal produced is

proportional to the light that reaches each one. In addition, the TFT allow the control of the current between the photodiodes and the electrical components. Thus, the TFT which before irradiation was non-conductive, now allows current to flow between the photodiode and the amplifier. The signal is amplified and encoded in order to generate the 2D images [21].

This technology, initially emerged as a possible way to obtain valuable information about phantom or tumour displacement based on an intensity grayscale. Currently, this device can be also used to obtain beam information and, jaws and MLC leaves positioning based on the verification of the portal images produced.

According to [22] during 2012 in Portugal there were 41 LINACs, of which 30 are equipped with an image guidance system.

2.3.1 Clinical use of portal images

Portal imaging systems were introduced in the optimization of quality protocol [23]. The idea is to adapt the routine protocols used in the clinic to replace manual procedures by automatic image-based analysis. Initially, EPIDs were used to locate the tumour position, however, with the appearance of the a-Si EPID the image quality was improved and new uses were found for this technology [19]. Portal images has been study as a way to evaluate LINAC performance by geometric checks. The ease with how this information is acquired has made EPID a desired tool in the automation of QC since currently, in most cases, this technology is attached to the linear accelerator. The portal images can be acquired following one of the three arrangements shown in Figure 9.

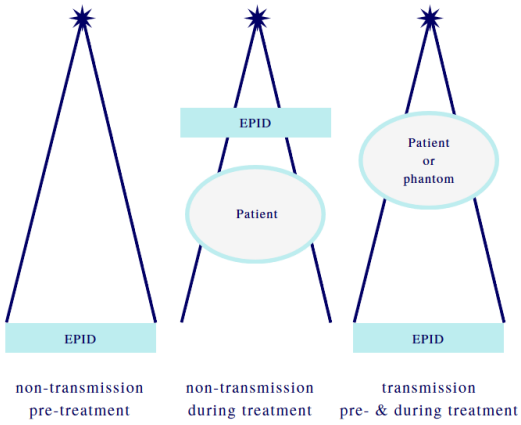

Figure 9: Illustration of the arrangements used in EPID dosimetry. Possible verified dose measurements at EPID level or inside the patient or the phantom are displayed. Adapted from [19].

Non-transmission pre-treatment method is used during automated quality control procedure to evaluate parameters as field size, collimator centre of rotation, leaf positioning, imaging system offset or beam quality since there is no object positioned between the source and the detector capable of influencing the measurements. Transmission pre-treatment method is usually used to verify phantom/patient positioning and dosimetry [19].

2.3.2 Physical aspects of portal image

In addition to the hardware problems like damages on the flat panel that can affect pixel intensity values, there are other factors which also may contribute to poor image quality. The current paragraph highlights the impact of X-ray scatter on the portal images. In addition, the following subsections also explains how beam quality and geometric parameters are measured on portal images

X-ray scatter

The scatter is a secondary effect of the interaction of primary photons with matter. During the interaction with the flat panel detector, primary photons suffer Compton effect, if the kinetic energy of the incident photon is too high, scattered photons (non-primary photons) can be produced. These photons, like the primary photons, contribute to the intensity values that compose the portal image. Therefore, the effect caused on the portal image is a reduction of contrast between open regions and collimator region and this contribution increase with the increase of field size. The dependence of field size is explained by the fact that the larger the field size, the larger the surface of the collimator available for scattering.

2.3.3 Verification image

Literature reports portal image systems as important tools to obtain accurate measurements of field size [6], MLC field leaves position [24], and dosimetry evaluations of beam symmetry and beam flatness [6, 7]. Many of these parameters are verified daily during quality control using different instruments which requires extra labour effort. The use of EPID can reduce the number of instruments used as well as the time spend during QC. Previous studies [25, 26] developed their own algorithms and interfaces to analyse portal images and most of these algorithms are based on pixel intensity converted to a greyscale space. In the following paragraphs, will be explained how pixel intensity values are used to measure important parameters related to machine performance.

2.3.3.1 Image correction

According with [6, 7] some corrections can be performed before measurements. Damages on the flat panel can affect pixel signal and reproduce wrong intensity values. Dark-field image ($I_{dark-field}$) is obtained with the beam off whereas flood-field ($I_{flood-field}$) is acquired with the beam on. A set of images for each type are acquired and the average image is used to effect corrections. Therefore, the analysed image (I_{raw}) must be submitted to the procedure traduced in Equation 3 adopted to smooth pixel differences.

$$I_{corrected} = \frac{I_{raw} - EPID_{flood-field}}{I_{dark-field} - I_{flood-field}} \tag{3}$$

After image correction, beam profiles can be extracted, and measurements can be performed. The beam profile for in/cross plane is obtained from open field image centre. In both cases [6, 7] adjacent profiles were extracted and averaged to create a single beam profile for each plane direction.

2.3.3.2 Flatness, symmetry and penumbra

Beam flatness and beam symmetry are important characteristics of beam uniformity and they are obtained for beam profile in in/cross plane. Beam flatness is defined considering the maximum, D_{Max}, and the minimum, D_{Min}, intensity values within flattened area, which is the segment that corresponds to 80% of total beam profile width. The beam symmetry is obtained considering the intensity values between two symmetric points, D_{left} and D_{right}, within flattened area. Literature references [1, 6, 7] report different ways to assess these characteristics. Regardless of the equation chosen, it is important to ensure constancy when the measurements are compared with a baseline, i.e., current measurements and reference values must be calculated with the same equation. According with [7] flatness and symmetry can be assessed as:

$$Flatness = \frac{|\, D_{Max} - D_{Min} \,|}{(D_{Max} + D_{Min})} \times 100 \tag{4}$$

$$Symmetry = \left(\frac{|\, D_{left} - D_{right} \,|}{D_{centre}} \right)_{max} \times 100 \tag{5}$$

Penumbra can be defined as the region of the beam profile where dose rate changes quickly as function of distance from central axis. Physical penumbra is usually founded using the distance between 20% and 80% isodose lines.

2.3.3.3 Field Size

Field size corresponds to the projection in a plane perpendicular to the beam axis when the leaves of the collimator are completely open being defined by jaws position. It is measured using a light source centered with the radiation source. According to [6], dosimetrical or physical field size can be obtained extracting the beam profile for both planes. For each beam profile, a central axis is considered, and from this point the first pixel position whose intensity decreases to 50%, comparative to the central axis, is searched in both directions. Then, the field size in each direction (in/cross plane) is defined by the difference between the two field edge pixels (first pixel with less 50%) in the same profile multiplied by pixel size.

2.3.3.4 Multileaf collimator positioning accuracy

The use of a multileaf collimator improves the precision with which the dose is delivered to tissues. Imprecision of MLC position may be the result of a degradation of the mechanical and electronic components performance and can lead to an increase of the dose delivered to the patient. This information is usually evaluated using a visual test that does not provide the necessary accuracy. In this situation, a different MLC pattern is reproduced in each day in order to visual confirm the compliance between the shadow projection and the calibrated pattern (Figure 10).

In order to solve these problem, EPID-based algorithms to determine leaves positioning using the previous MLC patterns have been developed [27]. The rectangular MLC pattern and the picket fence pattern are the simplest standard used by these algorithms to obtain leaves positions. Picket fence test has been widely used to test MLC accuracy since this pattern places the leaves at different distances from

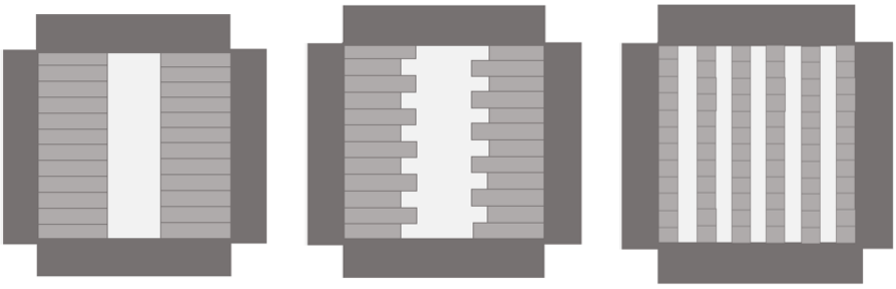

Figure 10: Illustration of the MLC patterns most used to perform positioning tests. Representation of rectangular, picket fence and garden fence MLC pattern (left-to-right).

the centre. In addition, more complete tests such as garden test are also used to evaluate leaves positions accuracy. The garden fence test consists of a narrow bandwidth spaced at equal intervals. This test is one of the most complete tests since it allows to check leaf transmission and leaf separation.

2.4 State of the Art

2.4.1 Machine Performance Check

Based on the exhaustive market demand for a solution to quality control automation, some linear accelerator producers develop their own software based on portal images to complete daily tests. Varian Medical Systems creates MPC, an application capable of performing a parameter analysis during QC routine. The procedure is performed through data automatically extracted from portal images which are acquired with or without a specified phantom, Isocenter Calibration (IsoCal), depending on the parameters to analyse. A screenshot of MPC using IsoCal phanton for isocenter calibration is shown on Figure 11.

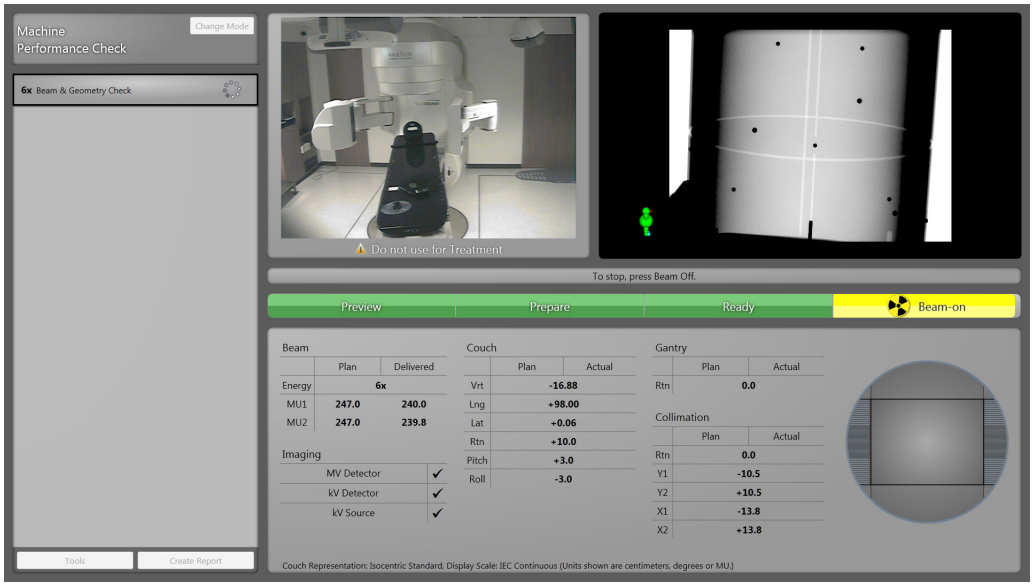

Figure 11: Illustration of MPC software using IsoCal phanton to measure the offset in isocenter position. Adapted from [28].

MPC software avoids manual measurements and a large set of extra measuring instruments. Due to

its practical nature, investigators from Radiotherapy and Radiosurgery Departments have been focusing on evaluating the possibility of used MPC in their routines [3, 4, 5]. MPC uses data from imaging portal systems as kV and MV imaging systems to guarantee geometric accuracy and beam output agreement with the previous baseline defined. This is possible since the MPC measures the offset values from the baseline image and evaluates beam performance similar to the methods described above. After images acquisition and analysis, a final report with the values of quality control parameters is provided.

Nowadays, the literature to support the accuracy of MPC is slight and summarizing in three studies performed in [3, 4, 5]. The main goal of these studies was to compare the information obtained using MPC imaging system and their quality control routine protocols to understand if the new method is accurate enough and useful to reduce time spent. In [3] a sample (N=10) obtained using MPC and routine protocol were acquired during two consecutive periods of 3 weeks for flattened and unflattened beams, the mean and standard deviation was calculated to comparation between two methods reveling the similary of the results obteined. However, in this article there was no information about MPC sensitivity being this proved only in [4] by introducing changes in the system and verifying MPC response. In [4, 5] (N=95) mechanical and geometric performance were evaluated during 4 months. Therefore, it is important to note that beam constancy is only reported in [3]. All the three studies were performed using a Varian TrueBeam 2.0 linear accelerator.

3 Materials and Methods

As explained earlier, this project is focused on optimizing LINAC's daily quality control procedures. In order to introduce the work developed and the studies performed, this chapter starts with a description of the overall project, which includes a problem statement, a proposed solution, and its validation. The idea is to give the user an overview of events before presenting a more detailed explanation.

3.1 General description

This project was divided into four phases depending on the chronological evolution of the project as shown on Figure 12.

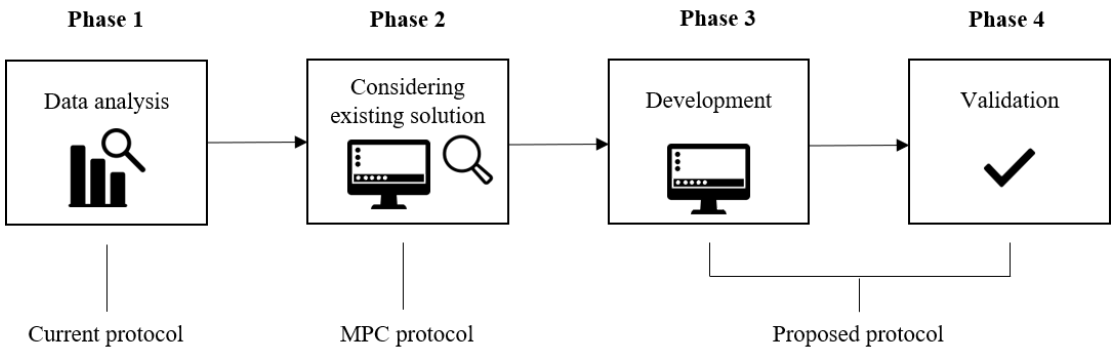

Figure 12: Overview of the project design.

The first phase consisted of the evaluation of the current procedure based on the analysis of previous quality control records of Edge radiosurgery system, performed during the year 2017. The previous records were used to evaluate the current situation, taken into account the compliance with regulatory standards and the number of failures registered, and establish the requirements to the solution design. In presenting these data, we intended to prove the limited effectiveness of the current QC protocol in some aspects. At the same time, with the analysis of the previous information, it is expected that the critical points on which future developments are focused will be defined. As will be further explained, with the analysis of these data it was possible to identify the MLC leaf positioning test and the time spent in the configuration of the electrometer as the major contributors to the increase of the low accuracy of results and to the time required to perform all tests, respectively.

Based on the previous evidence, the tests included in dosimetry and geometry categories were the goal of this project. Machine Performance Check (MPC) software created by Varian was investigated in a second phase of the project in order to inspect its capability to perform such tests. The Figure 13 shows a scheme of the software's principals of operation, a more detailed explanation of MPC is provided later (see 3.3.2.1). However, it will be possible to realize in the following sections that the possibility of developing our own solution is not excluded by MPC.

Therefore, reducing the time spent in the electrometer and increasing the accuracy of the MLC tests were achieved by developing a new solution on the third phase of this project. This new solution is

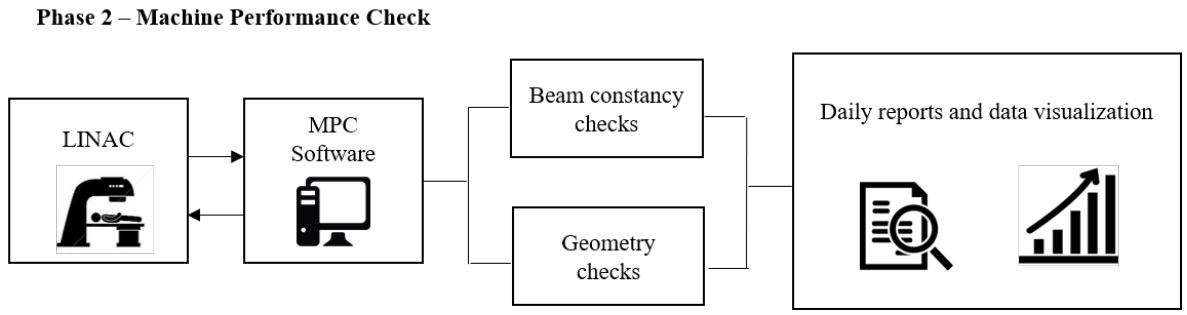

Figure 13: Overview of the Machine Performance Check software design.

capable of integrating the current quality control protocol by automating of dose reading and leaves positioning analysis. A graphical user interface (GUI) used to easy the communication between the user and the measuring device was designed. The desired solution must include control of temperature, pressure and high voltage values, increment time, start of acquisition and storage of data. In addition, a second module capable to receive portal images files and verify leaf positioning was also designed. While the first described functionality is only used as a way to send the user's instructions and save the measurements performed externally, the second module, dedicated to the determination of leaves positioning, works as an analysis tool. These two software modules were included in a global solution able to communicate with SQL databases saving the data introduced by the user or resulting from its own analysis.

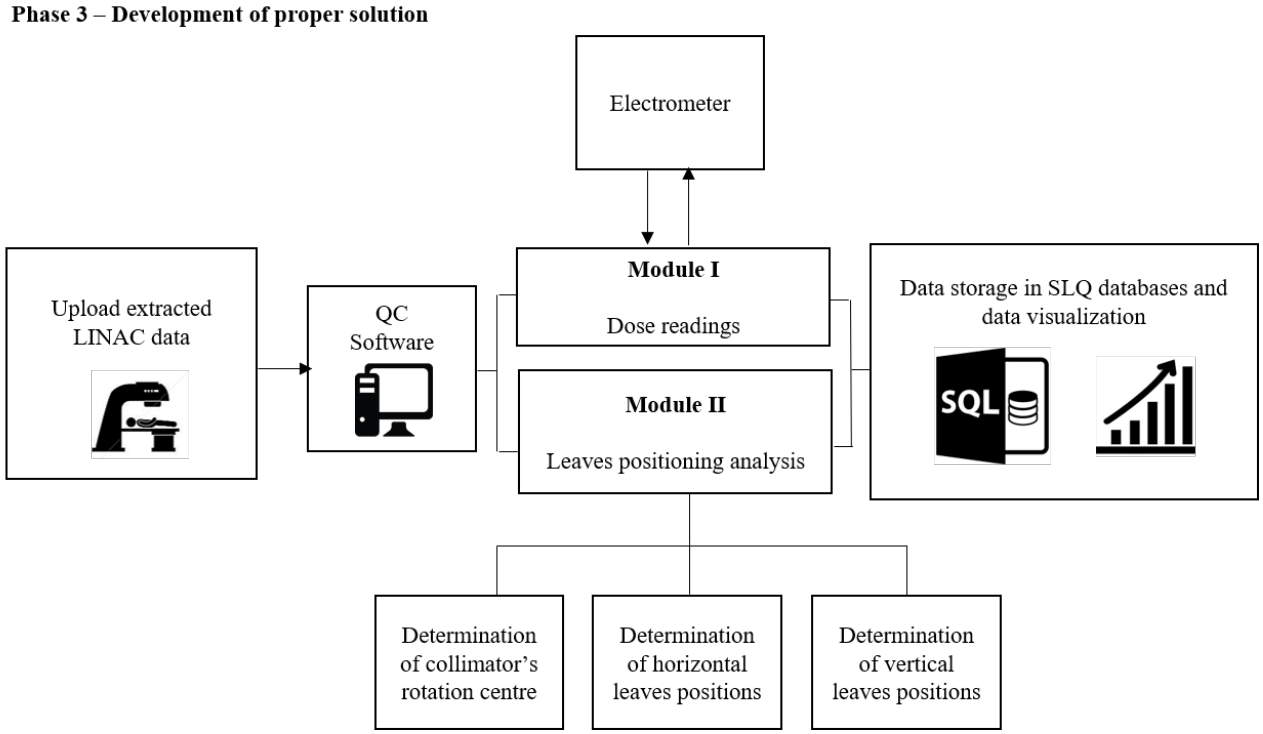

Figure 14: Overview of the software design adopted.

Once developed, in the last phase of this project each module included in the solution was submitted to a set of tests in order to validated the developed software (Figure 15). To guarantee the reliability of the results obtained for dose reading module, the results obtained were compared with the results obtained by the manual process. Regarding leaves positioning module, the evaluation process was divided into tests of the performance of the algorithm and tests to identify the different factors that can influence the

analysis on which leaf positioning determination are based.

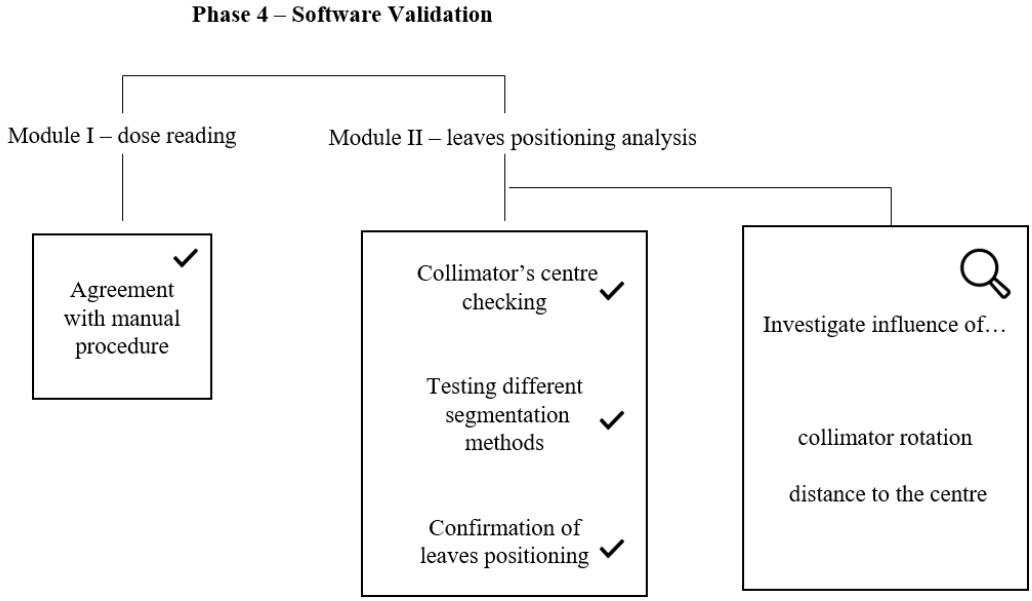

Figure 15: Schematic representation of the tests performed during solution validation phase. Specification of the main steps given in order to test the algorithm performance and to identify the influence of some factors (collimator rotation and distance to the centre) on the results obtained.

The tests to evaluate software performance includes evaluation of collimator determination algorithm, test to different segmentation methods and evaluation of leaves positioning prediction. In addition, collimator slope and leaf tip distance to the centre were investigated in order to study the influence of such factors in the results obtained. The validation process aims to adjust the protocol for a more reliable analysis identifying trends resulted from systematic errors of the algorithm and estimating the associate errors.

3.2 Current QC protocol implemented at Champalimaud Clinical Centre

A brief explanation of the current quality control implemented at CCC is presented in the following sub-chapter. This protocol was created based on both the AAPM standards and the manufacturer's recommendations and assumes the verification of a large parameter list. This set of daily tests is performed to ensure the basic security and precision during linear accelerator operation by detecting any inaccuracies or failures before treatments take effect.

3.2.1 Protocol description, recommendations, tolerances and uncertainties

The current protocol is the result of the requirements expressed in Portuguese Decree-Law Nº.180/2002 of August 8, American Association of Physicists in Medicine (AAPM) [18], Report 398 from International Anatomic Energy Agency (IAEA) [29] recommendations, and department experience. However, creating a full protocol considering all previous entities can lead to a exhaustive and extensive procedure requiring extra effort.

In fact, QC is not a rigid process since each department can adapt their own protocol following the country statements. Therefore, the parameters verified for different machines can be slightly different

depending on the LINAC model and the treatments performed in each day. Currently the linear accelerators operational at the CCC are a TrueBeam® system and a Edge® radiosurgery system both from Varian (Varian Medical Systems, Inc., Palo Alto, CA). Therefore, Varian suggests a set of performance specifications that should be verified to ensure the correct operation of their linear accelerators as shown in Table 3.

Table 3: Parameters and respective tolerances related to performance specifications of Varian Medical Systems linear accelerators.

PARAMETER	TOLERANCE
Performance Specifications	
X-ray output	3%
Gantry rotational accuracy	$\leq 0.3^{\circ}$
Target to gantry axis distance	$\pm$ 0.2 cm
MLC leaf end position accuracy at all leaf positions relative to the collimator axis	$\pm$ 1 mm
Pitch and roll	$\pm 0.25^{\circ}$

Therefore, for each LINAC, a set of tests related with operating conditions, geometry, security, dosimetry and imaging devices are part of the quality control protocol. Table 4 describes which are the components evaluated for each category of tests and respective tolerances accepted.

By comparing both protocols described on Table 1 and Table 4 it is possible to conclude that the CCC protocol is more exhaustive than AAPM protocol. In this situation additional tests are included, the department extended the AAPM protocol and introduced a daily analysis related to operating conditions based on physicists recommendations. Moreover, the department also adds couch, gantry, collimator and MLC position verification into category of geometry tests based on Varian suggestions shown on Table 3. Since the treatments performed on each equipment differ in terms of energies used, the main differences between TrueBeam and Edge quality control protocol are observed in the category of dosimetry. Table 5 shows the set of energies tested for each equipment.

The dosimetry checks are performed using a field size 10 x 10 or using wedges represented in Table 5 using varian wedge code (type-angle-orientation).

In dosimetry, the accepted dose ranges correspond to $\pm$3% of the pre-set values, measured under reference conditions for each energy, as suggested by the AAPM. The energy used in each treatment is related to the location of the tumour to be irradiated. Currently, a large set of energies is evaluated daily for TrueBeam linear accelerator. Nevertheless, only 6MV, 6FFF MV and 10FFF MV are used in breast, head and abdomen treatments respectively. The remaining energies present on Table 5 are currently not used but they still being verified daily in order to ensure a general overview of LINAC behaviour. In the case of the Edge, all the three energies tested are used being the energy of 10FFF MV the most required and used in the treatments of lung and ballon prostate.

Regarding the tests performed during the QC, operating conditions is an extra category of tests included by Radiotherapy Department to evaluate LINAC performance, with the exception of air conditioning, hand controller and treatment room conditions, all the remaining parameters of this category of tests are accessed using a specific tool of ARIA platform available on workstation computers. This tool provides an overview of the correct operation of the linear accelerator. These computers also provide information about monitor chambers (MU1 and MU2). These values are later compared with the values read from console display LCD. Treatment room conditions, which includes atmospheric pressure, temperature and

Table 4: Description of the parameters and respective tolerances related to operating conditions, geometry and security categories, evaluated during quality control at Champalimaud Clinical Centre.

PARAMETER	DESCRIPTION	TOLERANCE
Operating Conditions		
Water temperature	System cooling.	(39-41) °C
SF_6 gas pressure	The waveguide is pressurized with sulphurhexafluoride (SF_6) which acts as an electric isolator.	(29-35) psi
Flow sensor and temperature facility supply	System cooling.	$\geq$ 2 gmp (7-15) °C
Motors voltage	The voltage necessary to restart couch initial position.	$\geq$ 24 V and $\geq$ 27 V
Hand controller	Component that allows to control the movement of all the equipment.	-
Air conditioning	Ensures greater patient comfort.	-
LINAC room conditions	Room conditions that influence the dose calibration factor.	(15-35) °C; (30-70) %; (700-1100) mbar
Dosimetry		
X-ray output	Dose readings	$\pm$3%
Geometry		
Pitch and roll couch	Couch rotation movements that adjust patient position.	$\pm$ 0.25
SSD 100cm	Distance between source and irradiated surface.	$\pm$ 1 mm
Field size	Evaluate the precision in the positioning of jaws.	$\pm$ 2 mm
MLC	Evaluate the precision in the positioning of leaves.	$\pm$ 1 mm
Lasers	Laser system to guide the positioning of the patient/phantoms.	$\pm$ 1 mm
Gantry angulation	Evaluate the precision in the positioning of gantry.	$\pm$ 0.5°
Collimator angulation	Evaluate the precision in the positioning of collimator.	$\pm$ 0.5°
Safety		
Anti-collision MV/kV devices	Detection sensors system that prevents collision with other objects.	-
Door security	Sensor that prevents closing during the passage of a person.	-
Sound indicator	Audible warning during the irradiation period.	-
Visual indicator	Set of lights associated with beam on/off states.	-
Beam off button	Button capable of interrupting the irradiation.	-
MU1 and MU2 counters	Dose delivered expressed in motor units (MU) and measured by monitorchambers, which are ionization chambers attached to gantry head.	-
Display LCD	Display of the dose delivered in motor units (MU).	-

Table 5: Description of the energies considered with respective field size used and tolerances accepted for each linear accelerator model at Champalimaud Clinical Centre.

ENERGY	FIELD SIZE
TrueBeam	
6 MV	10 x 10
10 MV	10 x 10
15 MV	10 x 10
6 FFF MV	10 x 10
10 FFF MV	10 x 10
6 MV	EDW60IN
10 MV	EDW10OUT
15 MV	EDW45IN
6 MV	EDW20OUT
10 MV	EDW30IN
Edge	
6 MV	10 x 10
6 FFF MV	10 x 10
10 FFF MV	10 x 10

relative humidity, are measured using independent sensors. These variables contribute to ion chamber calibration and correct operation.

Geometry tests evaluate the correct mechanical operation of some important components involved in dose delivery. Couch, gantry, collimator and laser are the components which may interfere with the dose received by the patient. In order to measure surface slope of couch, gantry and collimator a slope indicator is used. As couch allows rotations according to different axes, it is evaluated in both axes, pitch and roll, while gantry and collimator have only one axis of rotation. For all rotation movements of each component, a different angle is considered for each day. The source-surface-distance (SSD) is also considered in geometry checks. A pointer with a 100 cm mark as shown on Figure 16 is attached to the gantry head in order to verify the agreement between this measure and the linear accelerator incorporated scale.

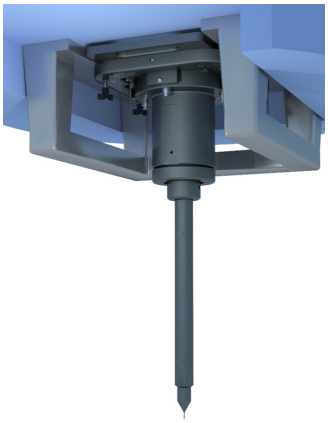

Figure 16: Illustration of front pointer test used to measure SSD. The device represented was developed by AKTINA Medical® for Siemens® linear accelerators.

Geometry tests also include verification of collimator jaws and leaves position accuracy. The field size

defined by jaws is evaluated using a light source aligned with the treatment source. The light reproduces the shadow defined by the boundaries of the jaws. The distance between these boundaries is defined as field size and measured using millimetre paper. The position of the different leaves in the MLC is evaluated using the same light source aligned with the treatment source and a paper sheet with a specific MLC pattern. The leaves are positioned to match with the pattern in the sheet and using the shadow reproduced it is possible a visual inspection as illustrated on Figure 17.

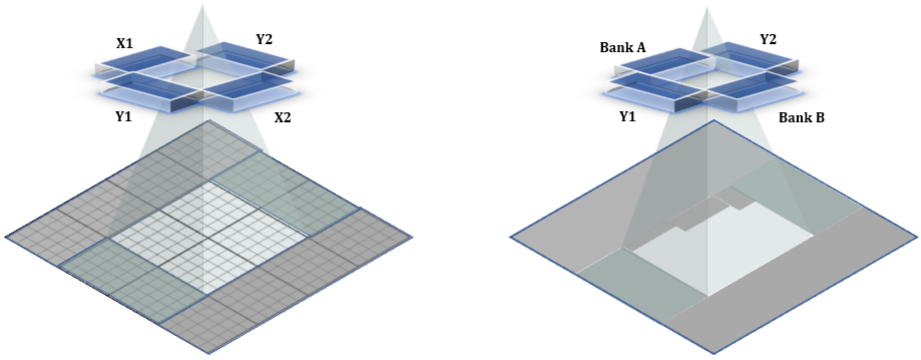

Figure 17: Illustration of quality control geometry test used to evaluate jaws and multileaf collimator accuracy.

Finally, the set of geometric test finishes with the evaluation of the laser system. The two lasers, used to align patient or phantom position, are fixed on the opposite sides of the room in order to match with isocenter position. A visual inspection using a sheet of paper verifies the match between of both lasers in coronal and sagittal plans.

The operation of the hand controller device is indirectly evaluated during the movement of the LINAC components. Furthermore, it is also guaranteed that the air conditioning is on to ensure patient comfort and stabilize the atmospheric conditions of the room. The remaining checks related to security mechanisms certify that, in case of failure the system is able to alert the user. Before recording dose values, console buttons operation, MU counters and display LCD agreement are tested during the warm-up phase.

After this, the beam output is measured for a set of energies described on Table 5 using a ion chamber and a electrometer as previously described. Once a week, dose measurements are performed using a matrix detector (Star Track + Energy Verification) produced by IBA Dosimetry (IBA Dosimetry GmbH, Bahnhofstrasse, Schwarzenbruck, Germany) which will make it possible to record 2D information [19] such as measurements of symmetry and flatness. In addition to the non-practical use, this device has few detector points demonstrating low spatial resolution when compared with EPID.

Quality control of the imaging systems is performed using a specific phantom, Penta-Guide. A CBCT image is acquired each day considering translation and rotation+translation movements. This image is then compared with an CT baseline image in order to verify if vertical, longitudinal and latitude displacements are out of the bounds ($\pm$ 2mm). The anti-collision mechanisms of the imaging system are also evaluated. According with AAPM [18] suggestions presented on Table 2, image quality control should evaluate CBCT imaging but also planar kV and MV imaging systems.

Therefore, Varian linear accelerators QC presupposes the verification of two other image systems, the Calypso® system (Calypso® Extracranial Real-Time Tracking) and OSMS (Optical Surface Monitor-

ing System Intracranial Real-Time Tracking). Calypso, is an image system capable of detecting internal or external Beacon® transponders used to detect slight movements and improve the treatment accuracy [30]. OSMS, uses video cameras to produce 3D surface data in order to detect patient surface movements. The quality control of these two components is performed using respective phantoms and imaging analysis systems which detect variations in the position of the phantom.

3.2.2 Edge® radiosurgery system and imaging systems

The LINAC used in the current project was an Edge® radiosurgery system (Figure 18). This device includes a High-Definition 120 Multileaf Collimator (HD 120 MLC) with central high resolution leaves width of 2.5 mm and outboard leaves width of 5 mm as well as a MV imaging system used to acquire portal images. The main features of LINAC's MV imaging system are shown on Table 6.

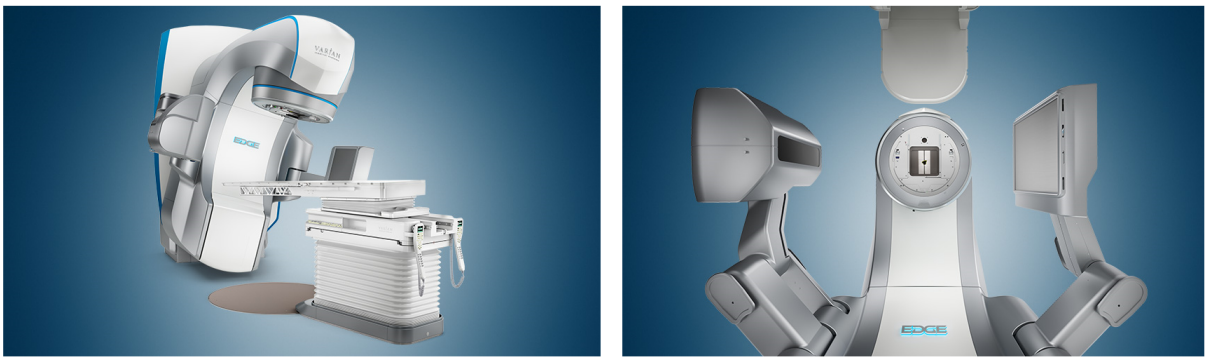

Figure 18: Representation of the Edge® radiosurgery system. Adapted from [16].

Table 6: Specification of the MV imaging system characteristics of TrueBeam and Edge radiosurgery system from Varian Medical Systems.

Parameter	Edge^{TM}	TrueBeam^{TM}
MV Imaging Descriptive Specifications		
Receptor model	aS1200	aS1000
Active imaging area	43.0 x 43.0 cm	30 X 40 cm
Pixel matrix	1280 x 1280 px	1024 x 1024 px
Pixel size	0.34 x 0.34 mm	0.39 x 0.39 mm

3.2.3 PTW® Unidos electrometer

During the current procedure, a Unidos^{Webline} electrometer from PTW (PTW, Freiburg, Germany) was used for dose measurements (Figure 19). This device enables computer communication by a serial port, connected by a RS232 cable dual 9 pin, used to send instructions to the device and receive its dose measurement results.

Figure 19: Representation of the PTW® Unidos^{Webline} electrometer used in the dosimetry mesurements at the CCC. Adapted from [31].

In summary, the process described above is time-consuming and includes a visual test of one of the major accelerator components, the collimator leaves, which does not provide the desired accuracy. Nevertheless, the equipment used, the linear accelerator and the electrometer, allow the optimization of quality control protocol through the automation of some procedures.

3.3 Machine Performance Check

Some researchers have devoted their time to studying alternatives to the current methods, the use of portal images to perform LINAC quality control testes has been widely regarded. Due to this scientific work, technological progress has brought new tools capable of replacing current procedures while ensuring compliance with all requirements. MPC was designed by Varian to be used in their own LINACs as an additional tool to the existing QA hospital program.

3.3.1 IsoCal phantom

MPC uses IsoCal (Isocenter Calibration) phantom to perform some of the geometric evaluations related to isocentre determination and couch positioning accuracy. This phantom is a hollow cylinder with 23 cm of diameter and length and contains 16 tungsten-carbide small balls with 4 mm of diameter that work as reference points (Figure 20). The checks using this phantom are performed by detecting the change of position of these points in images acquired on different days.

3.3.2 Software description

The software is available on ARIA Oncology System Platform accessible on the workstation at the Radiotherapy Department. MPC receives portal images to measure beam constancy and geometry related to LINACs performance. All the information regarding MPC operations in order to converting portal images information into machine performance evaluation metrics was obtained from [32]. It should be noted that before using MPC on daily routine, its configuration is mandatory:

- Definition of users privileges;

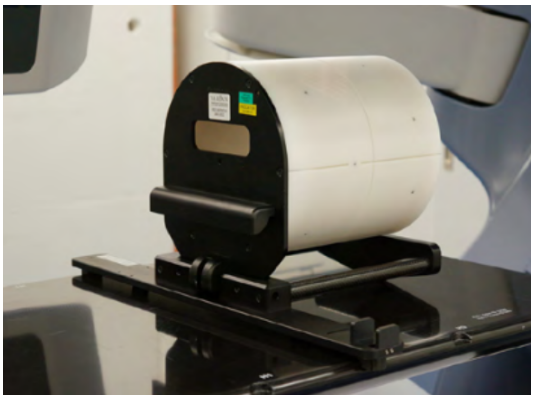

Figure 20: IsoCal phantom, from Varian Medical Systems, used in isocenter calibration. Phantom required to perform Machine Performance Check tests.

- Acquisition of couch position reference;
- Definition of baselines.

Once successfully finished, MPC is able to acquire daily measurements. To the whole set of parameters that can be obtained using MPC, this project focus on dosimetry output changes and leaf positioning. Since the dose/output value is the major aspect in a daily quality control protocol, the focus on output change is required. In addition, there is currently no external tool capable of evaluate leaf positions with MPC detail, so, for this reason our study was focused also in this parameter in order to developed a new method based on MPC and capable of ensure the correct position of the leaves when a baseline image is acquired. Bellow will be introduced the algorithms that were adopted in MPC to perform quality control of output changes and leaves positioning. Although the IsoCal phantom is part of the solution presented by Varian, it is not used in the tests specified.

3.3.2.1 Output change analysis

MPC is designed to receive portal images and transform pixel intensity values into geometric information. For each energy tested, an open-field image is acquired using MV imaging system and compared with a baseline image previously defined. Therefore, a ratio image is calculated using the image acquired and a baseline, both with 18 cm x 18 cm, uncorrected and acquired with gantry at 0° (Figure 21). Each pixel in the ratio image represents the intensity change between the two correspondent pixel of each image. To reduce jaw-collimator effect on the boundaries, the software sets a Region of Interst (ROI) of 13.3 cm x 13.3 cm by default. The average of all the intensity pixel values at the ROI is calculated and this value corresponds to the mean value of the percentage of intensity change between the two images. Below is shown an example of the image of the check and ratio image. These images are acquired using MV imaging system from Edge^{TM} and analyzed using MPC in order to determine output change.

As the output change is influenced by beam changes, it represents an useful metric in the detection of beam abnormalities. However, since dose measures are not performed, this solution do not replace dosimetry measures using ion chamber and electrometer.

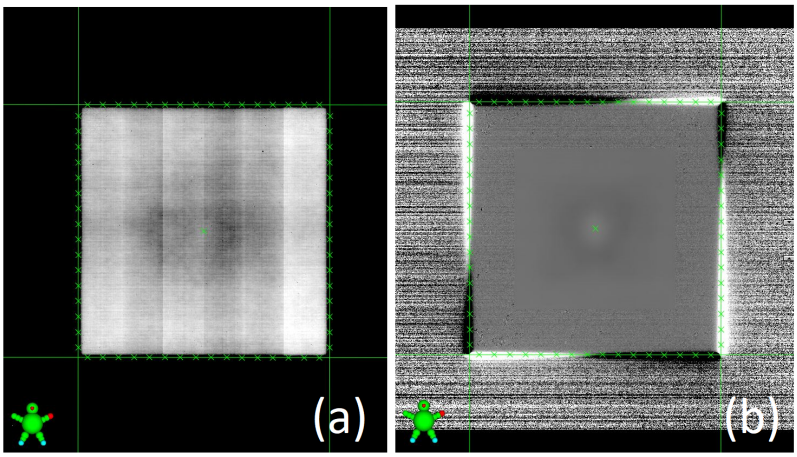

Figure 21: Check image (a) used to obtain centre shift and ratio image (b) used to obtain output change and uniformity change (resolution: 18 cm x 18 cm; gantry angle: 0°; collimator angle: 270°; both acquired using MV imaging system from Edge^{TM} and processed using Machine Performance Check analysis software developed by Varian Medical Systems, Inc.).

3.3.2.2 Leaf positioning analysis

Leaf positioning determination by MPC starts with the detection of collimator rotation centre, which is achieved by extracting the edges in the boundaries between open and close regions. Finally, the position of each leaf is calculated as the distance between leaf tip and the central edge passing in the rotation centre.

Edge detection

Edge detection routine is based on inflection point detection. The algorithm starts by defining the probe lines perpendicularly to the direction of the edges to be detected. Once inflection points are found, by measuring intensity change along these probe lines, edges are fitted accordingly to the final inflection points distribution (Figure 22).

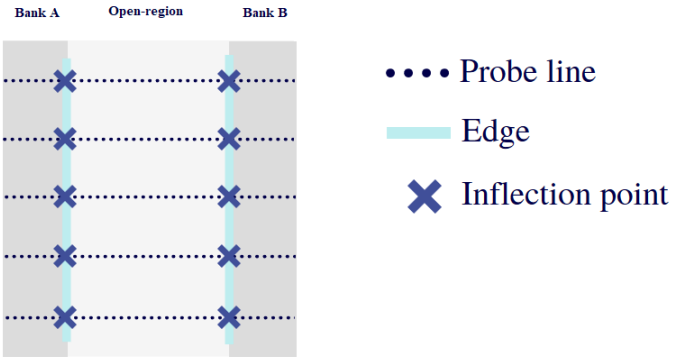

Figure 22: Illustration of edge detection method implemented in MPC software. Edge detection mechanism is based on the determination of inflection points and consequent definition of probe lines.

It should be noted that edges detection is the starting point to obtain the rotation centre and hence, leaves positioning. Given that, the process used to get the rotation centre will be now explored. Considering 5 collimator angles (45, 90, 270, 305 and 360)°, an image associated with each rotation angle is acquired allowing the extraction of the collimator's edges for each image. However, only one edge of

each image is required for the following calculations.

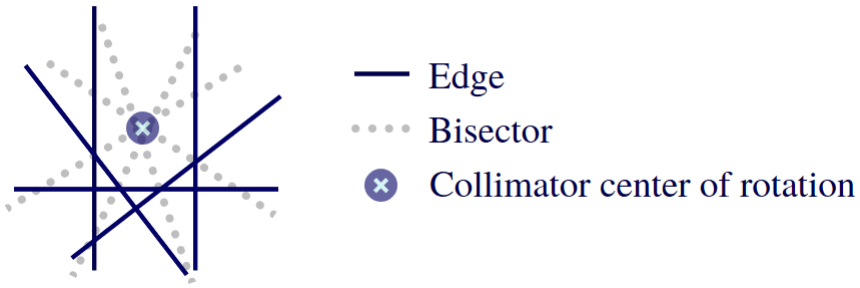

Figure 23: Illustration of the method for determination of collimator rotation center implemented MPC software. Determination of collimator centre is achieved by detecting the same edge represented for each one of the five consecutive shots acquired considering different collimator angle positions (45, 90, 270, 305 and 360)°.

Finally, the set of edge images is subdivided in pairs, given by successive angles, and for each pair the corresponding bisector is determined. Once computed all the bisectors, the rotation centre directly corresponds to the geometrical centre of the minimum circle that includes all the pair intersection points as shown on Figure 23.

MLC positioning

As previously reported, MLC leaf positioning is done relatively to a baseline image. A static picket fence pattern (Figure 24) for a field size of (22 x 7) cm is used to determine individual leaves positioning accuracy. However, the use of a unique MLC pattern for this end is a limitation of MPC.

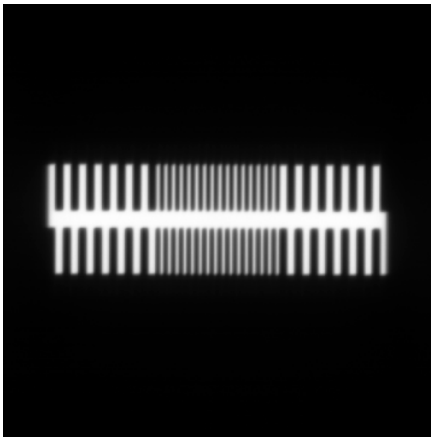

Figure 24: MLC picket fence pattern used by MPC to determine relative leaves position. Images acquired using EPID imaging system from Edge® radiosurgery system. A field size of 22 cm x 7 cm was considered, such as a gantry angle of 0° and a collimator angle of 270°. Image file exported using Machine Performance Check software.

For each leaf pair (formed by two opposite leaves of distinct banks) a beam profile is defined along the leaf moving direction and the central axis is find using collimator centre of rotation and image boundaries. Leaf tip is marked as the point where there is a steepest gradient. Then, for each leaf, the distance between leaf tip and central axis is calculated and compared with the distance obtained for the same pair in the baseline image. This measure corresponds to the individual leaf offset so that for a positive value, leaf is

further from the central axis comparing to the baseline image [3]. MPC also provides information about maximum and mean offset for each leaf bank.

Jaws positioning

A similar evaluation is perform to obtain jaws positioning, the test makes use of a comparison between the acquired image and the baseline one. For each shot, the four edges (X_1, X_2, Y_1 and Y_2) are detected and a central axis is defined as previously described. The distance between each edge and the central axis is calculated and compared with the values obtained for the baseline.

Briefly, MPC uses relative measures to evaluate geometry parameters. Therefore, the precision of such results is strongly dependent of the previously defined baseline. If optimal conditions are not guaranteed during the baseline acquisition, daily acquisitions may misrepresented. Defining a baseline for beam constancy checks can be achieved since ion chambers are a reliable method for comparison. However, a precise evaluation of jaws and leaves positioning cannot be performed since the current method do not offer the necessary accuracy to ensure they correct operation.

3.4 Proposed QC protocol

Based on the previous evidences, a new tool was developed in order to contribute to the future inclusion of MPC in clinical routine and to overcome its limitations in relation to the requirements of the clinic. The software was developed using Python® 3.4.0 py. As previously introduced the software is divide in two modules, module I, responsible to establish communication with the measuring device, and module II, dedicated to the analysis of portal images to find leaves positions (see Figure 14).

3.4.1 Python programming language

As previously mentioned, the programming language chosen for software development was Python® 3.4.0 [33]. The main reason for choosing this programming language for the development of this solution was due to the fact that this is a high-level programming language with a high number of packages already developed and important to achieve the aim of this project. A high-level language is a programming language closer to human language as opposed to low-level programming languages that are closer to the language of the machine. The advantage of using high-level languages is that the development process is facilitated and accelerated. As mentioned, a large number of packages available (such as the *numpy* package, which facilitates data manipulation, or the *serial* package, which allows communication with RS-232 ports) also contributed to the choice of Python. Finally, as Python allows the use of Qt [34], a framework multi-platform used to develop applications, it was also chosen to develop the software interface.

Pylinac

In addition to MPC, *Python* also has a library entirely dedicated to the analysis of scanned film or EPID images. This package was create to provide the user the tools needed to automate TG-142 quality assurance (QA). In this situation, the *starshot()* function that allows the determination of a rotation center is highlighted. This module analyses a starshot image made of radiation beam with the gantry, collimator or treatment couch. Since the number of startshot influences the precision required in the obtained results, a greater number will lead to greater precision in determining the center (see Figure 25).

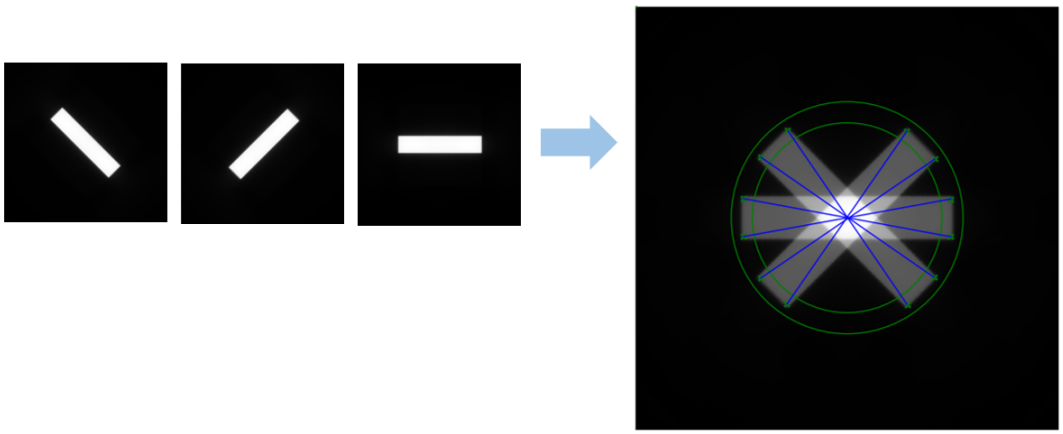

Figure 25: Representation of the method implemented by the *Starshot()* function of the *Pylinac* package to determine the colimator's center of rotation. The method is based on the analysis of a set of portal images acquired, in this example, considering a collimator angle of -45°, 45° and 90° and a gantry angle of 180°. Images acquired using EPID imaging system from Edge® radiosurgery system positioned at the isocentre.

The idea will be to later evaluate the performance of the method developed by comparison with the presented module.

3.4.2 Automatic leaf positioning analysis

3.4.2.1 Data sets

To study the performance of leaf positioning, a set of different images stored in the XIM format is used (see A). The files were decompressed using a Python open-source function (see B) and passed as input to the different functions included in the developed tool. All images show radiation fields formed with by MLC leaves considering different angles of the collimator. They were acquired with the flat panel positioned in the isocenter and with the gantry angle at 0°. The choice of the angle of the collimator used it is dependent on the intended function. All the specifications are summarized on Table 7.

In this context, an image set is composed of 4 images received by the algorithm to determine leaf positioning accuracy as shown on Figure 26.

Table 7: Specification of device configuration for acquisition of the images to be submitted to the method of analysis of leaves positioning developed in the present work.

IMAGE	GANTRY ANGLE	COLLIMATOR ANGLE	LOCATION
Set rotation centre (first image)	0°	-45°	Isocentre
Set rotation centre (second image)	0°	45°	Isocentre
Calculate horizontal leaf position	0°	90° or 270°	Isocentre
Calculate vertical leaf position	0°	90° or 270°	Isocentre

3.4.2.2 Image processing

In the first place, the software receives the image set and read the files in .XIM format to convert each image in a matrix of pixel intensity values. Since the images contain information about the leaves, they

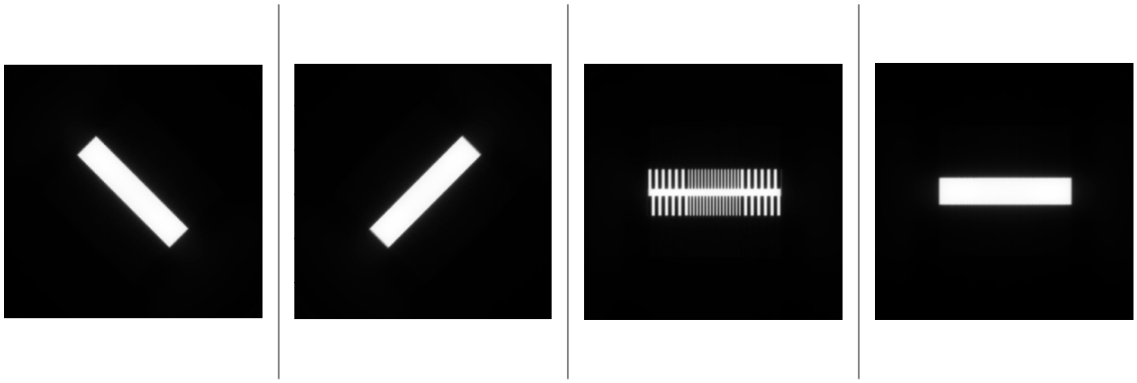

Figure 26: Representation of the set of images used by the developed software to determine leaves positioning. Images acquired using EPID imaging system from Edge® radiosurgery system positioned at the isocentre. From left to right: the first image was acquired with a collimator angle of -45° and a strip width of 2 cm from the centre; the second image was acquired with a collimator angle of +45° and a strip width of 2 cm from the centre; the third image was acquired considering a collimator angle of 90° and a picket fence MLC pattern with leaves positions alternating between 3,5 cm and 0,5 cm; and, finally, the last image was acquired considering a collimator angle of 90° and a strip width of 2 cm also from the centre.

may be submitted to processing techniques for the extraction of important spatial properties. For an accurate leaf positioning analysis, image segmentation preprocessing is crucial. Given that, the choice of the best method to discriminate irradiated (open regions) and non-irradiated zones (closed regions) using an EPID image plays a central role and therefore, three different methods, currently used in image segmentation and previously reported in other studies, were compared (Figure 27). Accordingly to the processing applied, the tested methods can be divided into boundary-based or region-based methods. Otsu thresholding represents a region-based method, whereas Canny algorithm represents a boundary-based method [25, 35]. In addition, some studies [26, 27] describe other method based on maximum intensity level found for each leaf profile. In the following, an explanation of the basic principles of each method is given.

Canny edge detection

Canny method converts the matrix of the intensity values in a binary matrix. The function used to performed Canny edge detector algorithm is available in OpenCv as *Canny()* py. The convolution between image matrix and a gaussian filter 5x5 is initially performed in order to smooth pixel data before line detection. After image smoothing, image gradient is found by applying the Sobel Operator to the image matrix in both, vertical and horizontal, directions. The first derivative is the result, G_x and G_y, and it is used to obtain the magnitude (equation 6) and the direction of the gradient (equation 7) for each pixel.

$$G = \sqrt{{G_x}^2 + {G_y}^2} \tag{6}$$

$$\Theta = tan^{-1}\left(\frac{G_y}{G_x}\right) \tag{7}$$

Therefore, equation 7 allows obtaining edge direction given its perpendicularity to the gradient direction previously calculated. The algorithm rounds the angles obtained to one of the four values which represent vertical, horizontal and the two diagonal directions. After edge detection, two additional steps are performed in order to thin edges and reduce the number of false positives. Firstly, each pixel is eval-

uated in the direction of the gradient as the possibility of being a maximum in its neighbourhood, if this possibility is not confirmed the pixel value is put to zero. Then, an upper and lower limit is set. The aim is to accept the pixels which present values above the upper limit and reject the ones which show values below the lower limit, values placed between limits are accepted only if they are connected with accepted pixels.

Otsu thresholding

The Otsu method is used to create binary images from gray-level images. The function used to performed Otsu algorithm is available in *skimage* package as *threshold_otsu()* py. Given the bimodal nature of the images used in this study, the Otsu method was considered as a solution in order to discover the boundary between the two regions. These images with a bimodal histogram are characterised by presenting a higher incidence of image pixels in two regions of the grayscale. In this situation, this effect is verified since there are two distinct regions, the region of incidence of the radiation and the region covered by the collimator leaves. Intuitively, in the present situation, each peak in a bimodal histogram corresponds to irradiated and non-irradiated zones. Mathematically, this method finds the value which maximizes inter-class variance. Once this limit is found, it is possible to transform the image into a binary image with values below this limit being 0 and values above the limit being 1. This binary image can now be used to find the boundaries between the two regions.

Half-maximum intensity value

This is the most accepted method by scientific community to establish the limit between open and close regions. Accordingly to [27], the physical position of each leaf is found on the position of pixel presenting 50% of the maximum grayscale intensity value (corresponding to the 50% dose level) for each profile. Since Canny and Otsu thresholding convert data to a binary matrix, only the method based on the half-maximum intensity value is able to implement precise sub-pixel techniques. Therefore, linear interpolation was used to find leaf positioning when the current method was implemented.

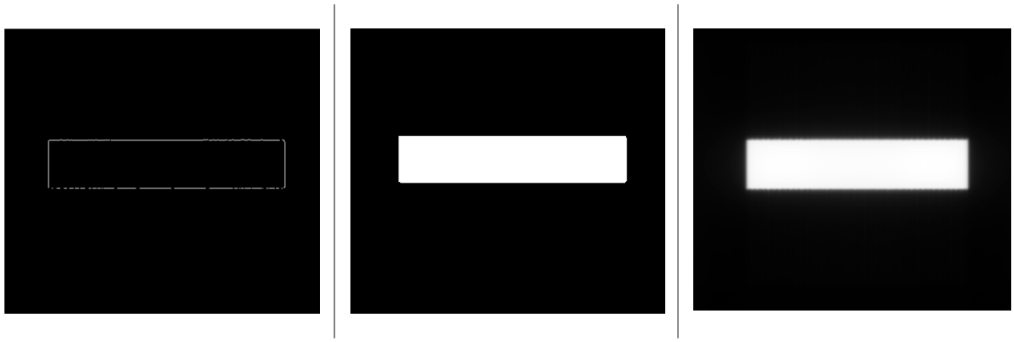

Figure 27: Representation of a set of portal images subjected to different segmentation algorithms. From left to right: Canny Edge Detector, Otsu Thresholding and Half-Maximum Intensity Method. Images acquired using EPID imaging system from Edge® radiosurgery system positioned at the isocentre. A rectangular MLC pattern is presented to arrange MLC leaves positioning. Images acquired considering a gantry angle of 0° and a collimator angle of 90°.

3.4.2.3 Collimator rotation centre

As previously explained, the proposed software computes leaf positioning relatively to the collimator's rotation centre. Then, after image processing, the next step is find the rotation centre, a process achieved by using two of the four images acquired with EPID. In this situation, the flat panel is placed at the isocentre with gantry at 0° and images are acquired for collimator angles of -45° and +45°.

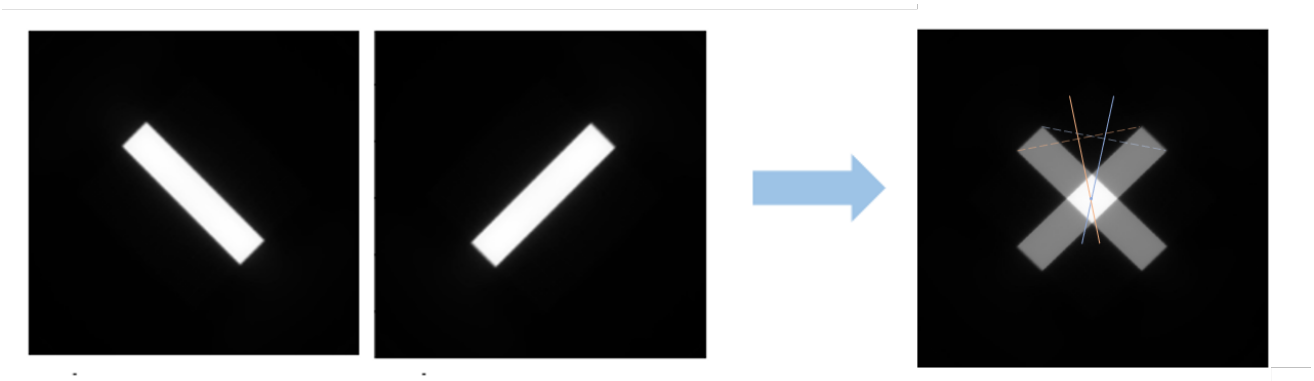

Figure 28: Schematic representation of the methodology implemented by the software developed to determine collimator rotation centre. Representation of the both images used, acquired considering a collimator angle of -45° and (b)+45° (left-to-right) and a gantry angle of 0°. A rectangular MLC pattern was used considering a strip width of 2 cm from the centre. Images acquired using EPID imaging system from Edge® radiosurgery system positioned at the isocentre. Representation of the integrated image formed, where an example of the points and the bissectors used to determine the centre position are shown.

Considering the image acquired at +45°, the algorithm finds the vertices coordinates of the rectangle that best fits the shape of the collimator in this image. Then, the process is replicated for the other image, acquired with the collimator at -45°. Given a pair of points defined on each image, a line is defined between each point and its correspondent on the other image, resulting on two lines. Finally, the perpendicular bisector of each line is then computed, and the rotation centre directly corresponds to the intersection between these both bisectors (Figure 28).

3.4.2.4 Horizontal leaf position

Once is the prior processing finished, the proposed software is used to compute leaf positioning for any MLC pattern even if acquired with the collimator at 90° or 270°. Considering the horizontal direction as the perpendicular direction of leaf movement, the horizontal central positions of each leaf are found based on the intensity profile.

One horizontal intensity profile is used to obtain individual central leaf position. First, the gradient of this profile is calculated using the *np.gradient()* function of *Python*. Then, each horizontal leaf position is found based on the detection of gradient peaks (Figure 29).

3.4.2.5 Vertical leaf position

Considering the example of a unique leaf, after found the horizontal pixel coordinate where central leaf position is located, a 1D profile along vertical direction is extracted.

In this context, two different ways to obtain leaf pairs position can be considered based on the segmentation method implemented. If the Canny edge detector or Otsu thresholding method are used, the

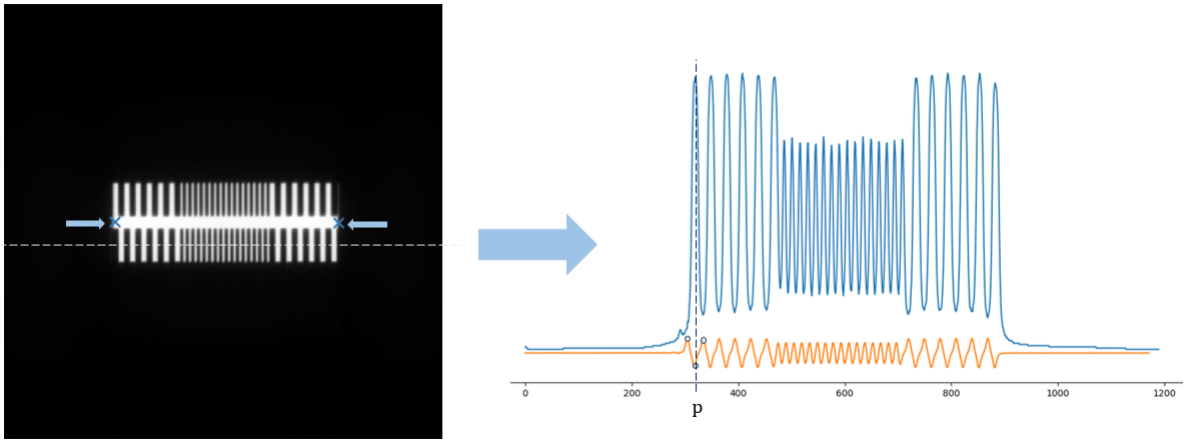

Figure 29: Illustration of the proposed method for determining the central position of the collimator leaves. Exemplification of the determination of position *p* of leaf number 2. The correspondent pixel to leaf position is found based on the analysis of a portal image of a *picket fence* pattern acquired considering the EPID placed at the isocenter, a collimator angle of 90° and a gantry angle of 0°. The blue profile represent the original intensity values whereas the orange profile represent the gradient. *Picket fence* MLC image was acquired using an EPID imaging system from Edge® radiosurgery system.

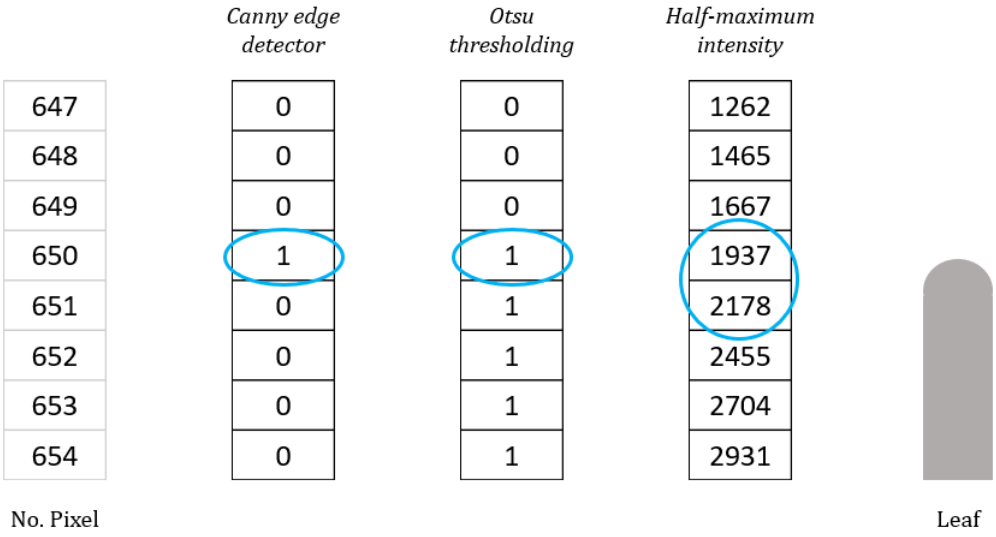

Figure 30: Illustration of the arrays used by each segmentation method considered to detect leaf positioning. The arrays illustrated show the original intensity values, used by Half-Maximum Intensity Method to detect leaf positioning, and the binary values, resulted from a prior segmentation based on Edge Canny Detector and Otsu Thresholding for further leaf positioning detection.

leaf position is obtained by finding the '1' in the extracted profile since the boundaries are signed as the changes from 0 to 1 in both cases (Figure 30). The results obtained by using this methodology are discrete with a step equal to the pixel size. However, the semi-maximum intensity method can apply interpolation techniques used to estimate the mean values, yielding (Figure 31).

For all leaves, the distance between the collimator rotation centre and the leaves tips must be, then, computed. Considering each leaf, this offset corresponds to the difference between the location of the centre and the leaf tip location multiplied by the pixel size.

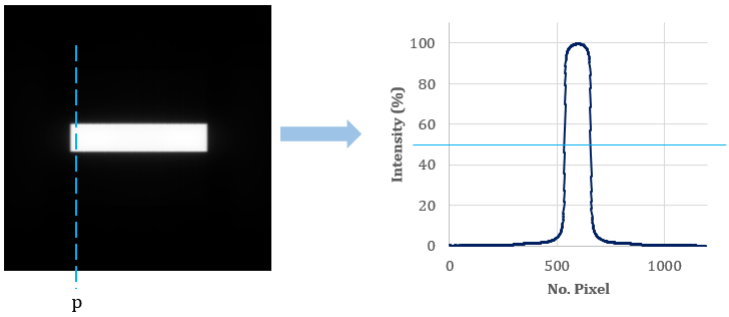

Figure 31: Representation of the proposed method for discrimination between open region and leaf region based on half of the maximum intensity value find in a profile obtained along central leaf position. Illustration of the a leaf position calculation using a rectangular MLC pattern and sub-pixel interpolation. The beam profile presented was acquired in the direction of the leaves movement. Images acquired using EPID imaging system from Edge® radiosurgery system positioned at the isocentre and considering a collimator angle of 90° and a gantry of 0°.

3.4.3 Automatic electrometer readout

Nowadays, dose measurements are performed using an ion chamber connected with an electrometer, able to provide dose readouts calibrated for temperature and pressure. As previously reported, the electrometer used at CCC is a PTW Unidos^{Webline} optimized to communicate via RS232 with a computer. The proposed solution includes a serial terminal receiving user instructions provided by a graphical user interface (GUI) developed to this end and sending the commands to the electrometer. In this situation, the PTW electrometer is considered a DCE (data communication equipment) transmitting and receiving the data to the computer, a DTE (data terminal type), on pins 2 and 3 respectively. Data transmission between devices is enabled by an instruction, passed to the electrometer from the computer in ASCII code. The PTW Unidos^{Webline} provides a list of commands, so that users can send this commands using specific serial terminals to communicate with the device. The electrometer response is given as a voltage level that is encoded in binary, and is then converted to a more user-friendly notation. In the developed solution only a few set of basic commands are considered as shown on Table 8.

Table 8: List of ASCII comands used in the communication between PTW Unidos^{Webline} electrometer and computer.

Command	Instruction
NUL	Start background acquisition.
INT	Start the dose acquisition during a range of time previously set.
STA	Start a dose or charge measurement.
RES	End a dose or charge measurement and reset the measured values.
MV	Send the last dose value measured.
DUV	Set the value of a user settings parameter.

The serial interface of the PTW Unidos^{Webline} electrometer operates on a large scale of baud rate values (1200, 2400, 4800, 9600, 14400, 19200, 38400, 57600 or 115200) that can be set by the user. In addition, 8 data bits, no parity and one stop bit are considered.

Python®, was also used to simulate the terminal using *serial* package. As previously reported, the script created to simulate the terminal was later incorporated into the developed global solution, a graphical user interface (GUI) capable of communicate with the electrometer and save the data measured in a proper database.

4 Results and Discussion

In the present section the current QC protocol is discussed and new alternatives are presented. A software application, in which the proposed protocol and QC data analysis capabilities were implemented is suggested. As explained earlier, the current limitations of time spent on the configuration of the electrometer and low accuracy of the leaves positioning tests were solved by developing a set of tools also included in the software developed. The results for the validation tests of such tools will also be presented in this section. Lastly, the leaves positioning results, obtained using the above mentioned application, are discussed.

4.1 Optimization of protocol design

General QC results

The proposed protocol emerges as an optimization of the previous protocol (see Table 4). The current protocol, the protocol suggested by the AAPM (see Table 1), and the protocol suggested by Varian (see Table 3), were compared in order to understand which variables are the most important and which are missing in the current protocol.

By observing the Table 9, it can be concluded that there is no complete agreement between the parameters verified by the CCC protocol and the requirements established by the AAPM and Varian. Such situation is due to the fact that the protocol implemented in the CCC results is an aggregation of AAPM and physicists' recommendations. The tests included in operating conditions and safety categories result from internally adopted rules, thus not included in the AAPM or Varian recommendations directly.

The exclusion of geometry tests only because they are not recommended by AAPM is not an option bearing in mind the most recent advances in radiotherapy and the arising of single dose based treatments. For this reason, it is imperative to test the performance of the above-mentioned geometric parameters, given their relevance for ensuring the accuracy of the dose delivery.

Regarding security tests, the number of checks is also considerable given the complexity of the LINACs used.

Only the imaging systems category of AAPM recommendations encloses tests that are not performed in the daily CCC protocol. The verification of kV and MV planar imaging systems is recommended by the AAPM and currently is not included in the current QC performed in the CCC since such imaging modalities are not adopted in daily treatments. However, since portal images are acquired using this MV planar imaging system, EPID checks should be included in the quality control protocol.

Bringing the MPC to the clinic will allow rapid analysis of a large number of currently verified parameters and the inclusion of new parameters in the existing protocol. However, such a tool does not allow analysis of parameters related to LINAC operating conditions or safety mechanisms. In this way, we studied the importance of the permanence of such parameters in the current protocol. The study was also extended to the remaining parameters.

Therefore, we evaluate the current tests with respect to the severity of the damages that a fault can induce (S), the number of occurrences registered (O) and the number of times that each fault is detected

Table 9: Comparison between the parameters included in daily linear accelerator control of Champalimaud Clinical Centre (CCC) and quality control suggested by American Association of Physicists in Medicine (AAPM) and Varian Medical Systems, Inc.

PARAMETER	AAPM	CCC	VARIAN
Operating conditions			
Temperature (exit - cooling system)	-	x	-
SF6 gas pressure	-	x	-
Flow rate (enter - cooling system)	-	x	-
Temperature (enter - cooling system)	-	x	-
Motor voltage	-	x	-
Hand controller	-	x	-
Air conditioning	-	x	-
Room air conditions	-	x	-
Geometry			
Lasers	x	x	-
SSD	x	x	x
Jaws	x	x	-
Couch (pitch/roll)	-	x	x
MLC	-	x	x
Gantry (angle)	-	x	x
Collimator (angle)	-	x	-
Dosimetry			
X-ray output	x	x	x
Imaging systems			
CBCT	x	x	-
Calypso	-	x	x
OSMS	-	x	x
Planar kV and MV	x	-	-
Security			
Door security	x	x	-
Audio-visual monitor	x	x	-
SRSR interlocks	x	x	-
Radiation monitor area	x	x	-
Beam on indicator	-	x	-
Anti-collision MV and kV	x	x	-
MU1 and MU2 counters	-	x	-
Display LCD	-	x	-

during QC (D). Table 10 summarizes possible failures detected during current QC and the respective data was registered during the year of 2017 and regards Edge®. It is important to note that failures can be classified as ”minor effect” (stress work department), ”moderate effect” (delay in treatment), ”serious effect” (slight damage not caused by radiation) and ”injury” (over/under dosage), depending on the potential damage caused. This classification was then crossed with the number of occurrences of each fault in order to estimate which are the main parameters that should be verified in daily routine. Therefore, the results shown in the Table 10 demonstrate the relevance of the tests performed due to the high number of failures they detect but also the severity of the failures they prevent.

MLC leaves related failures

It is also possible to identify on Table 10 the number of failures of some parameters without prior detection during QC. The leaves positioning of MLC with 28 failures occurred during one year is the parameter that presents the greatest number of failures which were not prevented by QC. According to the QC records acquired during the year 2017, these leaves were never outside the tolerance parameters. There are several factors that can contribute to the fact of collimator leaves failing and triggering interlocks, which are not identified during quality control: the wear caused by the exhaustive movement, the elapsed time between failure occurred and quality control and the low accuracy of the control test. The poor quality of the visual test performed to evaluate leaves position accuracy demonstrates a real need to develop a new automatic tool aimed to increase the accuracy of such checks and probably reduce the number of failures.

Based on this evidence, MLC-related failures were investigated more closely aiming to understand whether high occurrence is related to a specific leaf or set of leaves and if exists predominance in one of the banks. Figure 32 shows the percentage of failures occurred per leaf and per bank on Edge® during a year.

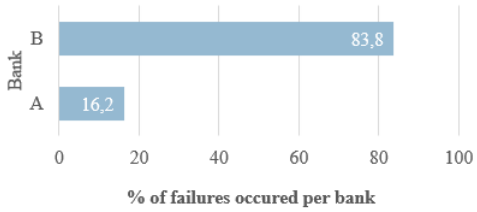

(a) Percentage of MLC failure occurrence per bank.

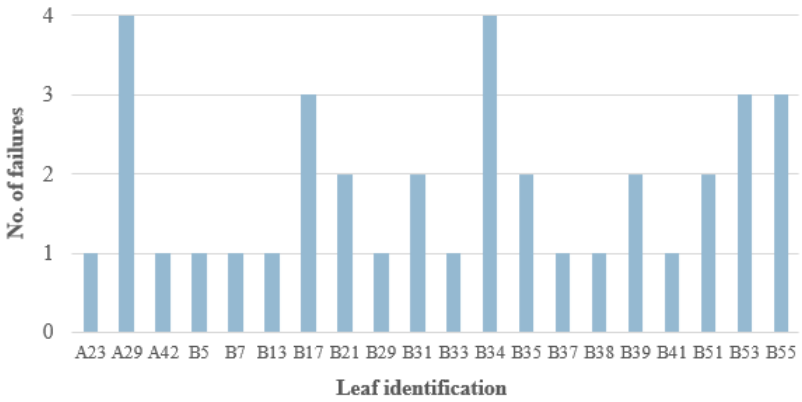

(b) Number of MLC failure occurrence per leaf.

Figure 32: Multi-leaf collimator failure occurrence. The data was related to the Edge® linear accelerator at CCC acquired during the year of 2017.

This analysis was used to discover whether failures occur in a random or systematic way. The results show the high predominance of failures occurred in bank B accounting for 83,8% of occurrences (31 occurrences) against 16,2% of occurrences (6 occurrences) in bank A. Also, leaves A29 and B34 show a greater number of occurrences (4 occurrences) when comparing with the remaining leaves. This results suggest systematic problems on the underlying mechanisms of control of these components.

Based on these results, QC must then be more focused on geometry issues in order to improve MLC positioning checks. The increase in the accuracy with which the daily control of the leaves positioning

Table 10: Analysis of the effects caused by the failures to be detected during the quality control performed by the physicists at Champalimaud Clinical Centre (CCC). In this table is presented for each parameter the number of occurrences registered (O), the number of times that each fault is detected during QC (D) and the category of severity in which it is included (S).

FUNCTION	FAILURE	POTENTIAL EFFECTS OF FAILURE	O	D	S
Delivery of the correct radiation dose to the tumour during treatment with minimal exposure of the surrounding tissues and the medical/technical team involved.	Water temperature fluctuations (exiting the cooling system)	Late or non-detection of overheating or overcooling of the system.	2	2	Moderate effect
	Gas pressure fluctuations	Abnormal conduction of the RF waves in the waveguide.	24	22	Moderate effect
	Water temperature fluctuations (entering the cooling system)	Late or non-detection of overheating or overcooling of the system.	39	39	Moderate effect
	Flow rate fluctuations (exiting the cooling system)	Late or non-detection of overheating or overcooling of the system.	-	-	Moderate effect
	Low couch motors voltage	Unable couch movement during power failure.	-	-	Minor effect
	Hand controller malfunction	Prevent device movements using hand control.	10	10	Minor effect
	Air conditioning malfunction	Increase patient discomfort and reduce the control of room temperature.	-	-	Minor effect
	Dose readout uncorrected for temperature and pressure	Radiation overexposure.	1	1	Injury
	Relative humidity fluctuations	Radiation overexposure.	16	16	Injury
	Inaccurate couch positioning	Radiation overexposure.	16	16	Injury
	Inaccurate SSD positioning	Radiation overexposure.	-	-	Injury
	Inaccurate jaws positioning	Radiation overexposure.	4	-	Injury
	Inaccurate MLC positioning	Radiation overexposure.	28	-	Injury
	Inaccurate laser positioning	Radiation overexposure.	6	6	Injury
	Inaccurate gantry positioning	Radiation overexposure.	-	-	Injury
	Inaccurate collimator positioning	Radiation overexposure.	-	-	Injury
	Anti-collision MV/kV systems	Collision.	-	-	Serious effect
	Door security	Collision.	-	-	Serious effect
	Sound indicator	Lack of alert system.	-	-	Moderate effect
	Visual indicator	Lack of alert system.	-	-	Moderate effect
	Beam off	Radiation overexposure.	-	-	Injury
	MU1 and MU2 counters	No compliance between ion chambers.	-	-	Injury
	Display LCD	No information about dose delivered.	-	-	Injury

is performed, can lead to the identification of systematic failures and even their prevention.

Proposed protocol design

Performing validation tests on MPC it is a necessary task to the future adoption of the suggested quality control protocol. Due to its commercialization on the market, the MPC is expected to comply with the measurement accuracy indicated. In this way, two proposals are presented in this section, including and not including MPC checks.

On the one hand, reducing the time spent can be achieved by bringing MPC to the clinic routine. This is a practice to be adopted after MPC validation. As already mentioned, in this project, only the viability

of the software was evaluated to perform the quality control and the failures were solved by developing external tools capable of not only validating some of the MPC (leaves positioning) measurements but also storing the data that are not acquired by this tool but which are essential to the protocol. In this way, it is suggested that MPC be used daily after its validation. Dose measurements should continue to be performed using ionization chambers and the electrometer that can be managed using the developed software. This software should also be used to store the data resulting from the tests belonging to the categories not included in the MPC, namely operating and safety conditions.

On the other hand, with the non-use of MPC, quality control is performed using the same instruments used in the current protocol. However, the test for the analysis of leaves positioning is replaced by the analysis tool included in the developed software. Dose measurements are performed as described above. The results are stored in the software developed in the fields created for this purpose.

For both situations, regarding dosimetry evaluations, 6 MV, 6FFF MV and 10FFF MV energies are the ones used during the current treatments, so the daily tests must be reduced by discarding tests with wedge filters.

Although the first protocol suggestion lacks validation of the software, this is the method that offers a greater reduction of the time spent, from 1h to approximately 30 min. As such it is expected that more tests will be developed in order to bring MPC to the clinic. However, the second protocol was the intermediate solution found until complete validation of MPC. This solution is not only capable of increasing the accuracy of some measurements in the current protocol, but also of storing the data in digital format. Briefly, by adopting the above mentioned recommendations the clinic would be equipped with a more efficient protocol given the tests daily performed and the execution time.

4.2 General solution presentation

This section includes a brief explanation of the quality control tool developed and prepared to be used with Varian linear accelerators and PTW Unidos Webline electrometers. A more detail explanation how to install, run and used the software is provided in C.

This software makes use of SQL technology for storing information resulted from quality control procedures. The databases were created exclusively through Python using the *sqlite3* package tools [33]. The database used to storage this data is composed by five different tables responsible for storing the data grouped into the following categories: sign in information, imaging systems, general parameters, dosimetry, collimator leaves and geometry parameters as shown on Figure 33.

All tables have in common a single parameter, the date. In this situation, the date is the primary key, which means that each date only corresponds to a single value for each parameter. The existence of a unique key parameter is a requirement of SQL tables. Date was chosen as key parameter in order to avoid ambiguities in the information collected, as the existence of several values associated with the same instant.

The quality control workflow starts by registering user and time so that this data can be later accessed for management purposes. Thus, after the user typing his name in (1) and the date on which the procedure starts in (2). A new database can be created in (3) or, alternatively, the selection of an existing one in (4). Subsequently, once the information necessary for the start is filled in, the data is authenticated in (5), a procedure in which the system verifies the information inserted, is a mandatory requirement to proceed. If this condition is met, the software prevents an overwrite of the information. After checking

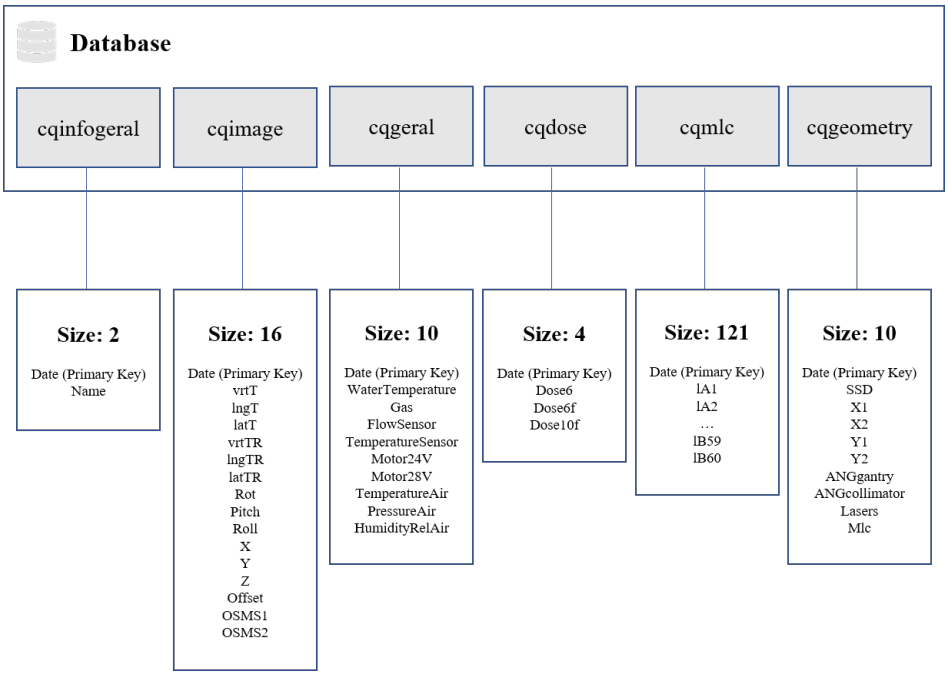

Figure 33: Database structure and design adopted to save quality control data.

all the fields, the user can advance to the main menu in (6). In order to minimize the data loss related to accidental program closing, this feature is locked in the top bar and is only available in the last menu. The main menu gives to the user access to the form for data storage, perform their own measurements and access to the data visualization tool (Figure 34).

Data resulting from measurements obtained using the current daily protocol which means the measurements obtained using external instruments can be stored in (1, 2 and 5). The user should complete a set of forms adjusted to the different categories of tests that will be presented later. However, the software provides an analysis tool to determine the collimator's leaf positions and replace the current daily visual test. The quality control images can be obtained using the XML code presented in Appendix 1 A. These images are then uploaded to (4) in order to be analysed. For this procedure, four images are required. The software also establishes a connection to external devices, the electrometer. This device can be connected with the software in (3).

The features included in this software are intended to provide the user with a tool for digitizing data and having the data in a digital format can easier future analyses. In this software, time trends can be accessed in (6) (Figure 35).

The electrometer must be connected to the computer using RS-232 communication cable. The interaction between the software and the electrometer starts in Settings. After choosing the COM port, (1), the connection must be effective in (2), an action that will activate the features available in Measurements. After the communication between the devices is established, the user can guarantee dose correction by filling the fields in (3). Subsequently, the user has the possibility to opt for a manual acquisition method in (4) or by an automatic method, whose time interval is defined in (5). These configurations are applied in (6). The user should start the measurement process by defining background in (7). Considering the available energies, the software is prepared to store information related to 6 MV, 6FFF MV and 10FFF MV. To start the measurements the user should click on (8). In this situation, if the user has chosen the manual method the process will end after clicking on (9). Then, the user must select the corresponding

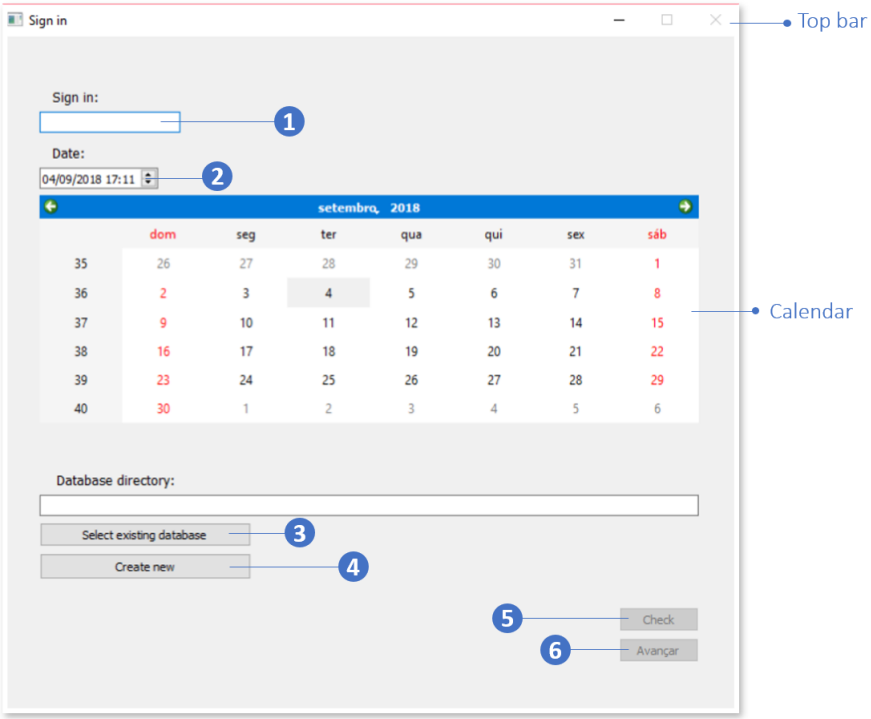

(a) Sign in interface.

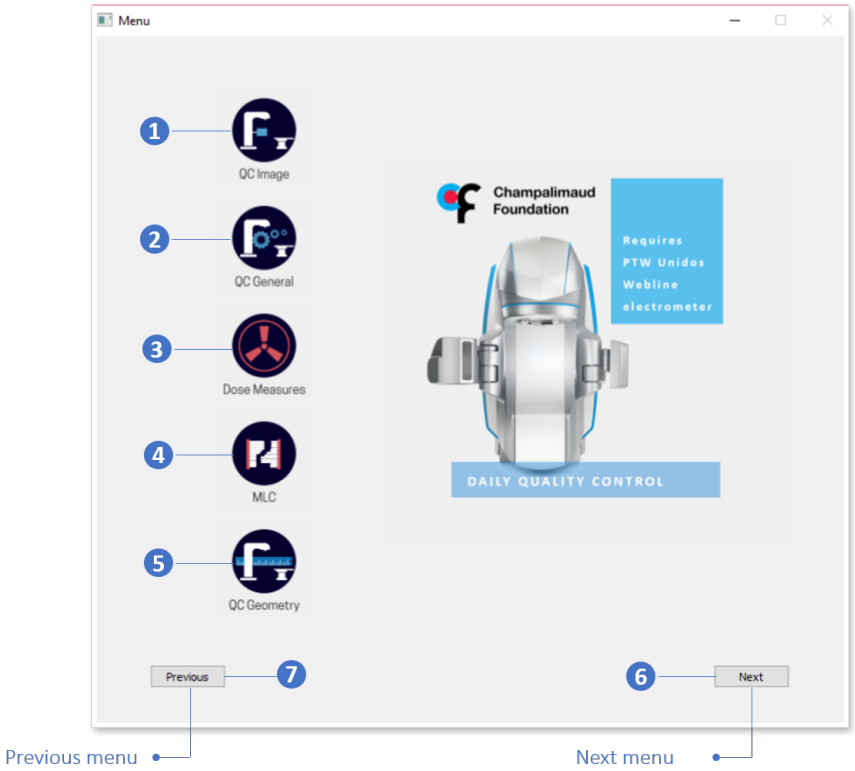

(b) Main menu interface.

Figure 34: Representation of the sign in interface used in the software developed to identify the user and the database and representation of main menu interface used to access to the main functionalities.

energy field in (10) and after all, measurements are saved in (11) (Figure 36).

The main menu also allows access to the EPID image analysis tool to determine the collimator leaves

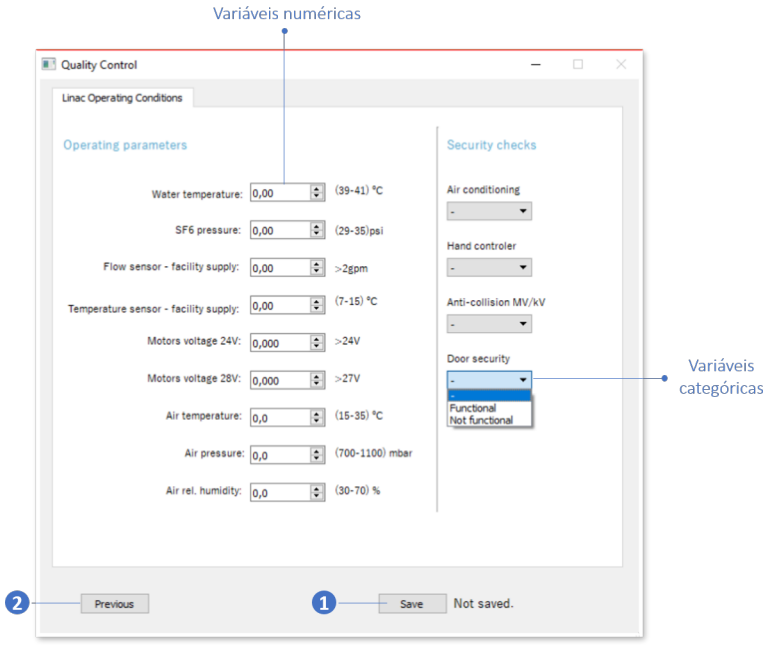

(a) Completed form.

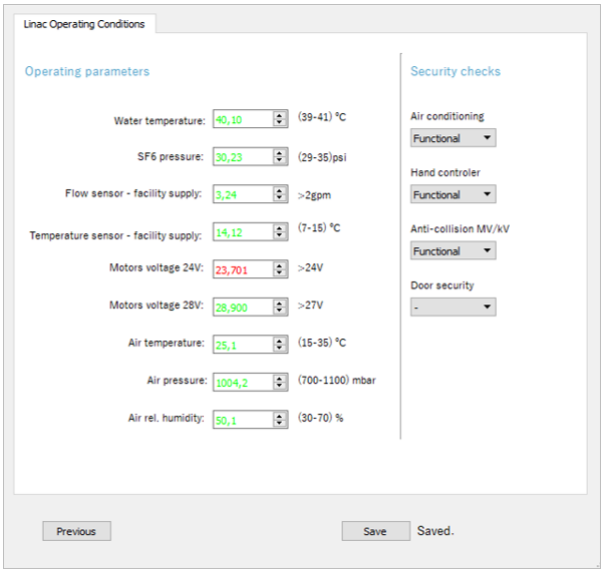

(b) Form after data storage and evaluation.

Figure 35: Representation of the form used to store the data related to the operating conditions of the linear accelerator and included in the software developed.

positioning accuracy. The software is designed to receive images acquired with the EPID positioned in the isocenter. The text boxs in (1) are filed with the correspondent image directory whose specifications are described in the legend above the field. A preview of the images is generated in (2). After the user confirms the choice of the images, the determination of leaf positions is done in (3). Since the process is finished, the results can be consulted in (4) (Figure 37).

Finally all the results saved on the databases can be also visualized. The user should select the table and the variable to be accessed, as presented in (1) and (2). The visualization of the time trend is generated by clicking (3). The dashboard is composed by a graph showing the time variation of the chosen variable and a general overview of all the variables that compose the table chosen (Figure 38).The user can exit in (4).

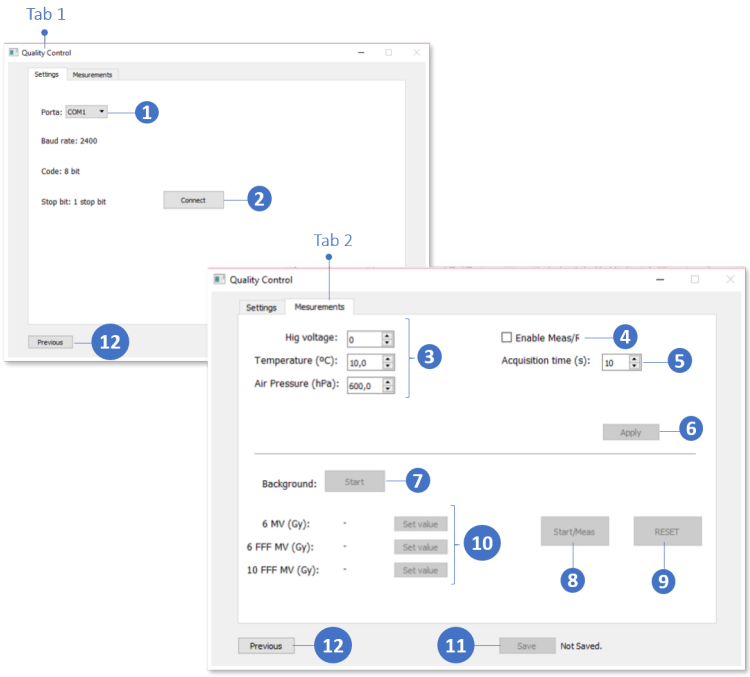

Figure 36: Representation of the interfaces used to manage the electrometer commands and to store dose measurements. A solution included in the software developed.

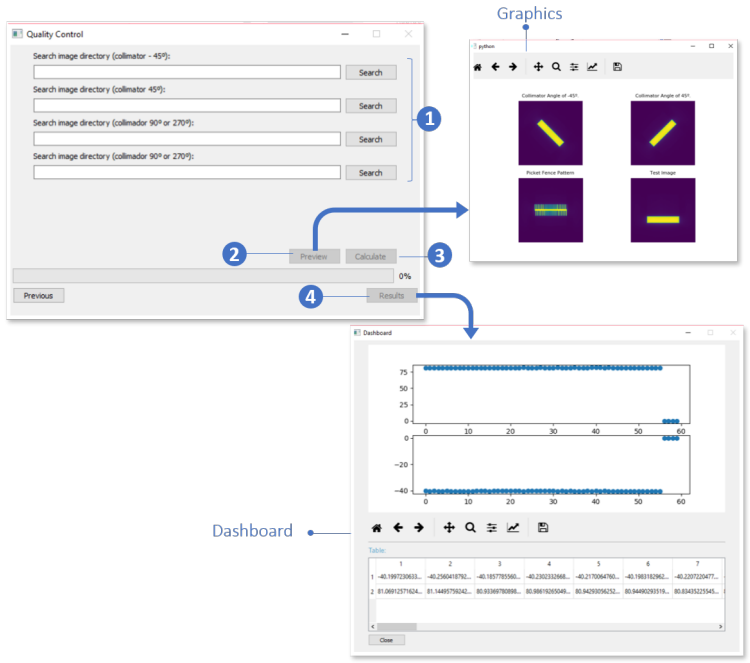

Figure 37: Representation of the interfaces used to receive portal images and perform image analysis in order to calculate MLC leaves positions.

4.3 Performance analysis

MLC leaf positioning errors lead to differences between planned and real treatment dose delivery. This fact makes the verification of each leaf positioning crucial for daily control in order to avoid an radiation overexposure or underexposure. Hence, a weekly visual test considering a maximum offset between the measured and the expected leaf positioning of 1 mm as recommended by AAPM, may not be small enough considering the size of the treated segments. In this context, potential errors in MLC

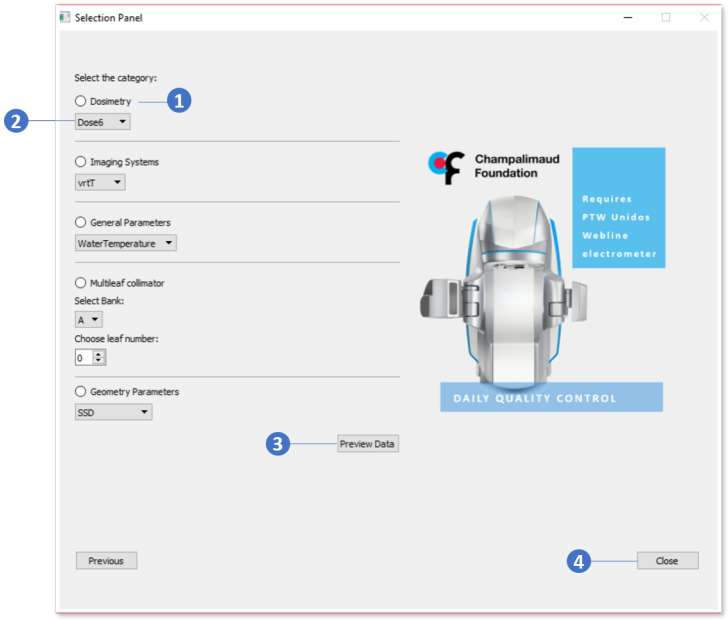

Figure 38: Representation of the interfaces used to select the variable in order to preview time trends.

leaves positioning can lead to serious damage in healthy tissues. Therefore, the solution suggested in the present work aims to improve the current analysis of MLC leaves positioning and to contribute to a safe treatment in order to accurately and automatically detect differences smaller than 1 mm.

Next, a performance evaluation of the solution developed is presented. The rotation centre location estimated by the algorithm, and the result obtained with the *Pylinac* built-in method were compared. Then, different segmentation methods were tested and finally, the absolute leaves positioning results using the developed application are benchmarked.

4.3.1 Evaluation of collimator determination

The Table 11 shows the results obtained for the estimation of the error associated to the determination of collimator's rotation centre based on the comparison of two algorithms, the in-house software and Pylinac tool (see section 3.4.1). In both cases, three images acquired with the collimator at -45, 45 and 90 were used as shown in the Figure 25. The measurements were performed for each of the cases, Pylinac and developed software, with images acquired on three different days. Table 11 shows the resulting average values corresponding to collimator's centre coordinates X and Y obtained for each one of the two methods.

Table 11: Average of the positions obtained in pixels for collimator's rotation centre used in the estimation of the error associated to this measure based on the comparison of the in-house software and Pylinac tool.

METHOD	X (pixel)	Y (pixel)	TIME [s]
Pylinac	592.2	594.9	12.7
In-house solution	593.0	594.0	7.9

Table 12 shows the differences in the centre coordinates between both methods, Pylinac and developed tool, in milimeters for each one of the directions, X and Y.

The differences between the two algorithms for the presented case are approximately -0.3 mm to

Table 12: Error associated to the collimator's rotation centre measurement based on the comparison of the in-house software and Pylinac tool.

X (pixel)	Y (pixel)
0.3 ± 0.1	-0.3 ± 0.1

the Y-direction and 0.3 mm to the X-direction. Since the Y-direction corresponds to the direction of leaves movement, it is used to estimate the agreement between both algorithms, in-house software and *Pylinac tool*. However, it is important to note that in this analysis X-direction, which corresponds to the direction perpendicular to leaves movement, was not discarded since its provides an general overview of the method performance. In this situation, the differences of +0.3 mm and -0.3 mm correspond to the average of the differences obtained between the two methods on different days. The standard deviation is the deviation of these differences from the average value.

Once the position of the leaves was calculated in relation to the center of rotation, this result means that by choosing the method developed, an absolute difference of 0.31 mm in the position of the leaves is introduced when compared with the position obtained using *Pylinac*. However, the time spent by the developed algorithm is approximately half the time spent by the *Pylinac* which is an important advantage. Therefore, taking into account the time reduction and the fact of the differences presented are acceptable (less than 1 mm) the solution developed was considered to determine rotation centre.

4.3.2 Test of different segmentation methods

Once evaluated the method used to determine collimator rotation centre, the study focused on the image segmentation process. In this context, Edge Canny Detector, Otsu Thresholding and Half-Maximum Intensity Value were the methods considered in order to find the one that best defines the threshold between the open region and the regions of the leaves. To this end, a set of images, also described on Table 7, were acquired on 4 different days and used to determine leaves positioning. Considering the daily mechanical wear of this component, small deflections in the position of the leaves are expected even if all have been positioned at the same distance from the center of rotation. In this situation, the leaves were positioned at a distance of 2 cm from the centre as shown on Figure 39.

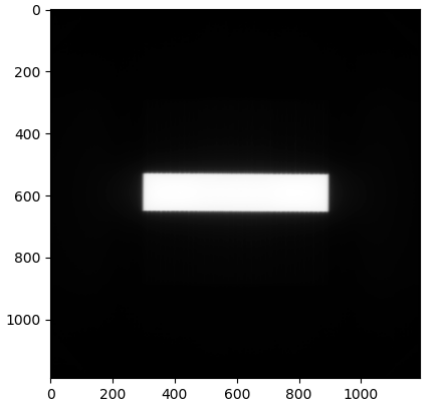

Figure 39: Representation of a portal image showing a rectangular MLC pattern used to obtain leaf positioning. Portal image acquired using EPID imaging system from Edge® radiosurgery system positioned at the isocentre. A collimator angle of 90° and a gantry angle of 0° were considered.

First, the mean position of each leaf was obtained. As a result, to each leaf corresponds a mean value which represents the mean of the 4 positions recorded during the 4 days. Figure 40 shows the boxplot of the mean values and its distribution for each one of the previous mentioned methods.

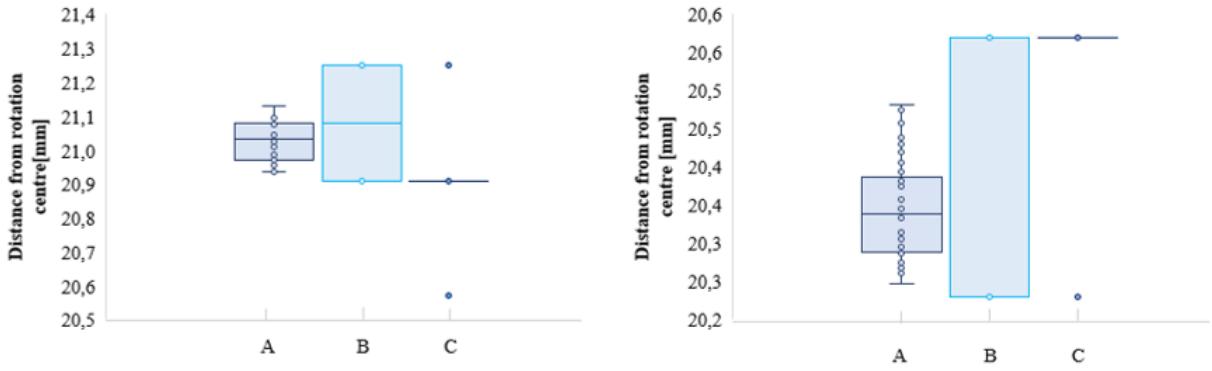

(a) Bank A. **(b)** Bank B.

Figure 40: Boxplot of the mean distance that each leaf presents in relation to the rotation centre, evaluated at 224 observations (56 leaves x 4 days) along each bank A and B over 4 days and considering three different image segmentation techniques. Half-Maximum Intensity Value (A), Otsu Thresholding (B) and Edge Canny Detector (C) were the segmentation techniques evaluated.

The method based on the Canny Edge Detector showed lowest variability of the data. This mean that Edge Canny Detector, in this situation, is the least sensitive method to detect slight variations of the leaves. On the other hand, while in the previous case the leaves position are estimated as presenting practically the same distance to the centre, in Otsu Thresholding method, the distribution of the points oscillates between two possible distances. This means that the sensitivity to detect slight variations can be increased, however, only differences larger than the pixel size (0,34 mm) can be found. According to the obtained results, the analysis suggest leaves perfectly aligned in the first situation and misaligned presenting systematic errors of 0.34 mm in the second case. In this situation and based on the previous evidences, edge-based (Edge Canny Detector) and region-based (Otsu Thresholding) segmentation techniques prove to be not sensitive enough to perform portal image segmentation. In this way, a new approach was considered, the leaf detection was performed based on intensity values whose value represents half of the maximum intensity in the profile considered. This approach allowed the inclusion of linear interpolation which led to leaves positioning results closer to the expected values and independent of the pixel size.

4.3.3 Confirm leaf positioning prediction

In the previous section, 4 portal images were used to determine the segmentation method to be implemented in the following studies. The same results obtained for Half-Maximum Intensity Value were here used to test their veracity in respect of leaves position prediction. As mentioned previously, these results corresponds to the mean value of each leaf position for each bank measured during the 4 days. In the present section, these data was used to measure the distance between leaf pairs in order to find the mean aperture of the banks. The Figure 41 shows the boxplot of the distance between leaf pairs. The main informations are summarized on the Table 13.

Based on the analysis of the graph it is possible to conclude that the algorithm suggests an excess

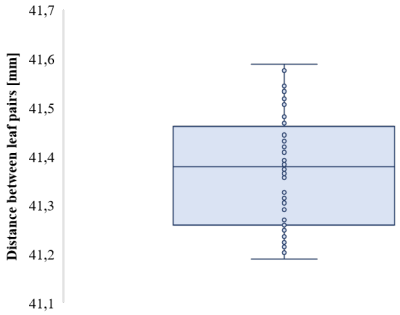

Figure 41: Boxplot of the mean distance between leaf pairs evaluated at 28 distances over 4 days.

Table 13: Results obtained for the mean distance between leaf pairs evaluated at 28 distances over 4 days. Mean, mean of the standard deviation, maximum and minimum value of the leaf pairs distances are presented.

PARAMETER	VALUE (mm)
Mean	41.4
Mean standard deviation	0.1
Maximum	41.6
Minimum	41.2

mean aperture of the collimator leaves of about 1.4 mm. To evaluate this result, images integrated over the delivery were acquired. The MLC leaf pairs sweep across the field, irradiating a 20 mm gap every 20 mm. Figure 42 shows the portal images resulting from the *garden fence test* (see 2.3.3.4). During this test, increments in positioning errors of $\pm$ 0.4 mm were entered on all stripes. Finally, an open field image is acquired in order to compare with the MLC patterns generated and in order to estimate the leaf transmission percentage.

An average profile, over all leaves, were extracted per image along in-plane direction (in the direction of movement of the leaves). Figure 43 shows the profiles obtained.

When the profile of the open field and the set of profiles of the integrate images were compared, we conclude that the baseline presenting values of intensity higher than the baseline of the open field. This evidence shows that even if the collimator leaves are closed, they do not totally prevent the transmission of radiation. As the data presented are the result of an image integration over the delivery, to discover the percentage of radiation transmitted, the mean baseline value is divided by the number of acquisitions. In this way, a rough estimation of 1% of average leaf transmission. This value of 1% represents the increase in relation to the baseline value measured in the open field image.

Then, by comparing the results obtained for larger apertures of the stripes (+0.4 mm and +0.8 mm) with the results obtained for smaller apertures (-0.4 mm and -0.8 mm), we observed a reduction in peak amplitude in the last situation comparing to the first one. This evidence means that by reducing the aperture of the leaves we are reducing the overlap between the strips, and the result obtained is more closer to the open field image which is the aim of this test.

Therefore, the beam profile extracted from the corrected integrated image estimate by reducing strip width in approximately 0.6 mm was the profile identified as the more closer to the open field profile. The value of 1.2 mm (resulted from 2 x 0.6 mm, for each bank) was then compared with the value of + 1.4 mm previous estimated by the algorithm for the same day. The result obtained is close enough to the expected precision (approximately 0.1 mm). However, it is important to note that there are several

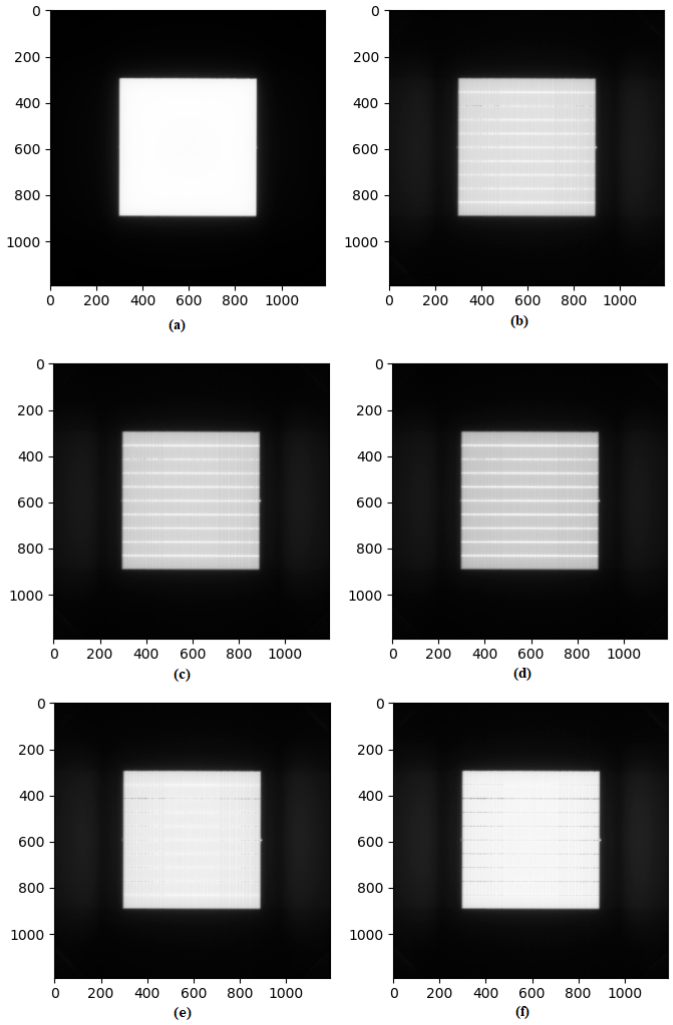

Figure 42: Representation of the set of portal images obtained during the *garden fence test* execution. Representation of open field image (a), original integrate image over the delivery (b), integrate image including systematic errors of 0.4 mm increasing strip aperture (c), integrate image including systematic errors of 0.8 mm increasing strip aperture (d), integrate image including systematic errors of 0.4 mm decreasing strip aperture (e) and integrate image including systematic errors of 0.8 mm decreasing strip aperture (f).

factors that can unbalance collimator leaves arrangement between image acquisitions, such as oscillations in gantry positioning, collimator tilt or even the leaves movement itself can leaf to small discrepancies on the results.

In sum, it is important to note that the differences found with respect to the planned values, both, the developed tool and the garden test, identify an opening of the collimator leaves. This fact can mean a subtle overexposure of the tumour during the treatments. However, considering small fields, small error in leaves positioning can be traduced in considerable percentages of error in the dose delivered.

4.4 Evaluation of independent factors influence on portal images

Next, the influence of independent factors in the determination of leaves positioning was studied. The influence of collimator rotation, distance to the centre and leaf width were considered.

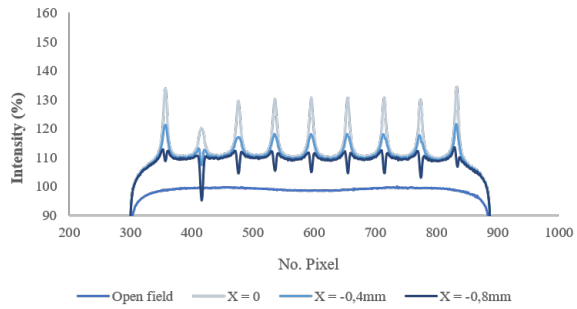

(a) Average profile acquired from original image, original integrate image over the delivery and integrate image including systematic errors decreasing strip aperture.

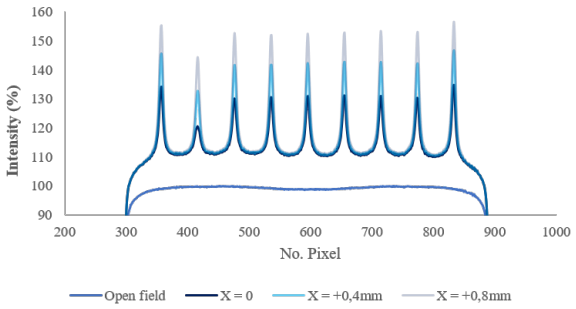

(b) Average profile acquired from original image, original integrate image over the delivery and integrate image including systematic errors increasing strip aperture..

Figure 43: Representation of the different profiles acquired for portal images of open field and resulting from the *garden fence test*. The *garden fence test* was performed considering a strip width and a strip centre spacing both of 20 mm. Systematic errors of 0.4 mm and 0.8 mm were included in both direction (increasing and decreasing strip width).

4.4.1 Collimator angle measurement

The influence that a potential angular misalignment between the collimator and the image detector can have on the calculation of the position of the leaves was evaluated. In order to determine the slope of the collimator, the X-Jaws were used at a distance of 2 cm from the rotation center. Since X-Jaws are massive blocks without irregularities, it is assumed that by acquiring a set of profiles along their entire length, the position determined does not present greatly changes. A change in the position of the X-jaws, can be explained by a deviation in the angle of the collimator. Figure 44 shows the position of the X-Jaws before and after the collimator correction.

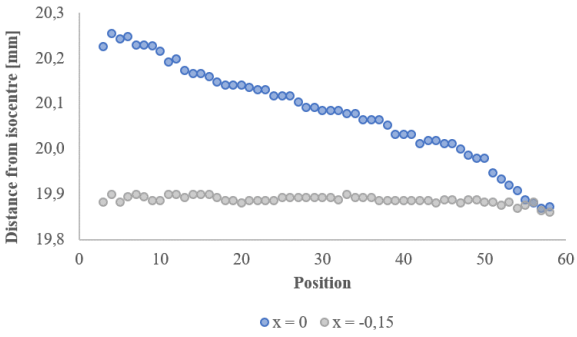

(a) Jaw X1.

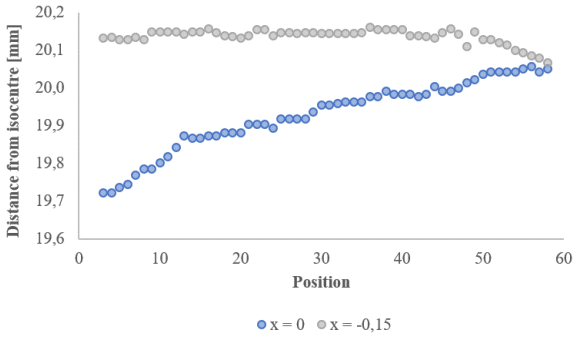

(b) Jaw X2.

Figure 44: Distance to the rotation center evaluated at 56 points along the jaws before and after the correction of -0.15° of the collimator angle considering the collimator at 90°.

In this situation, a deviation of approximately -0.15° was found, considering the collimator at 90°. This preliminary study using X-Jaws prove that collimator misalignment can influence boundaries detection. Therefore, the same process was reproduced now considering MLC component, MLC leaves were positioned at 2 cm from the rotation centre. The Figure 45 shows the leaves position for different angles of collimator.

In this case, three different situations are presented: the original leaves positioning, the position observed after a correction of -0.05° and the position observed after a correction of -0.15°. The choice

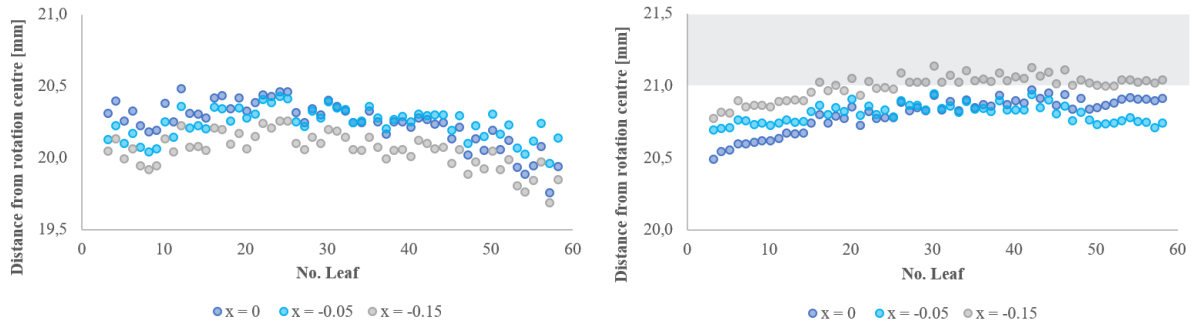

(a) Bank A. **(b)** Bank B.

Figure 45: Distance to the rotation center evaluated at 56 leaves distributed along the MLC before and after the correction of -0.05° and -0.15° of the collimator angle considering the collimator at 90°.

by the 0.05° angle was achieved due to the boxplot analysis (Figure 46), which shows the distribution of the distance to the center for the leaves of each bank according to the different situations (uncorrected, corrected to 0.05 and corrected to 0.15).

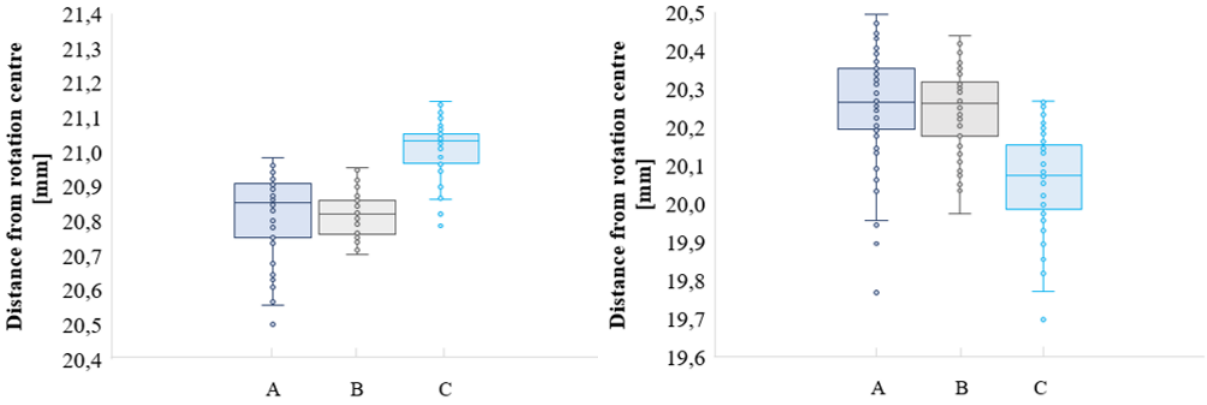

(a) Bank A. **(b)** Bank B.

Figure 46: Boxplot of the distance to the center for the leaves of each bank considering collimator at 90° according to three different situations: uncorrected (A), corrected to 0.05° (B) and corrected to 0.15° (C).

Thus, the angle chosen should reduce the amplitude of the boxplot and consequently the variation of the data. As mentioned previously, in this situation, the value -0.05° was the value found for the deviation of the position of the MLC, considering the collimator at 90°.

4.4.2 Off-axis accuracy

Finally, we studied the influence of the distance to the center presented by the leaves on the error associated to their positions. Such an effect was initially expected since there are subtle differences in the beam profiles acquired along the in-plane direction and can be explained by the error introduced by the component itself during its movement. In order to study this effect, new portal images were acquired. In this situation three different distances from the center of rotation were considered as shown in Figure 47.

The leaves positions were obtained for each bank with the leaves placed at different distances from the centre. The Table 14 shows the results obtained.

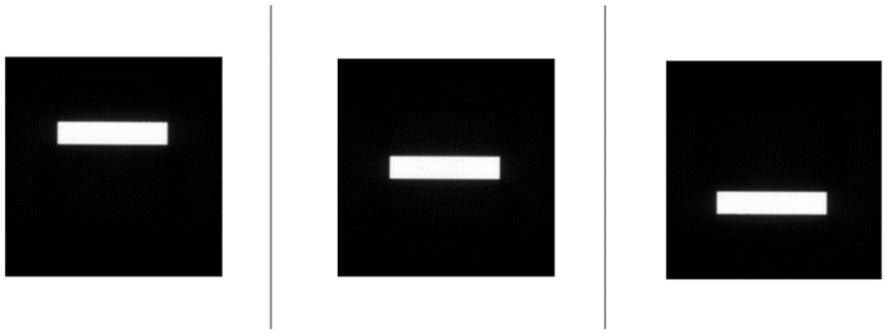

Figure 47: Portal images used to study the influence of different leaf positions in the error associated to the leaves positioning. The images were acquired using EPID imaging system from Edge® radiosurgery system positioned at the isocentre. A gantry angle of 0°, a collimator angle of 90° and MLC aperture of 4 cm were considered.

Table 14: Results obtained for the mean positions of collimator leaves acquired at different distances from the centre. Representation of leaf position measured.

Bank	**A**			**B**		
Distance	**-4 cm**	**2 cm**	**8 cm**	**-4 cm**	**2 cm**	**8 cm**
Average leaf position	-40.41 ± 0.06	20.06 ± 0.09	80.03 ± 0.09	-39.79 ± 0.06	21.01 ± 0.07	81.44 ± 0.10

These results shows that the error in leaves positions changes with the distance to the centre. The distances between pairs of leaves for each of the three analysed images were also calculated. Figure 48 shows the boxplot with the distribution of the distance values obtained for the three situations.

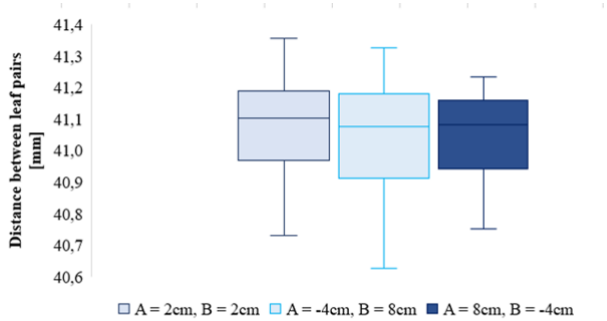

Figure 48: Boxplot of the distances between pairs of leaves for different positions relative to the collimator rotation centre.

By observing the boxplots, we conclude that the leaves positioning differ when the three situations are compared. In sum, in clinical terms it is important to note that, despite its almost negligible effect, a leaf presents variable errors taking into account the distance to the center of rotation considered.

5 Future Work

This project led us to reflect on the procedures that have been used to verify linear accelerators. Although the developed solution met the main requirements of the clinic, many limitations remain and several new questions have emerged with this work. This section briefly explains the main topics that should lead to further research in order to reduce the limitations of this process.

Additional software developments

As future work, it will be necessary to design and execute more performance tests in order to validate the developed application for leaves positioning determination. In fact, the suggested method present promising results when compared to the current one. However, more features, such as an automatic collimator tilt detection and gantry angle measurement, must be implemented in the developed solution. Regarding the automatic method strictly developed to manage the electrometer commands, at this moment the software allows the control of all the main commands used in the daily routine. However, it would be important to prepare it to manage a larger commands list to facilitate the optimization of not only QC but also routines related to calibration of the ionization chambers or LINAC commissioning.

Briging MPC to clinic routine

As suggested in this project, the MPC which present some limitations in relation to the requirements of the clinic and requires validation, should be considered as an additional tool in the quality control. The developed tool for leaf positioning analysis can be used to define a proper baseline in order to introduce MPC in clinic routine. This possibility will require validation studies on MPC not only related to the leaves position accuracy but in relation to the all parameters that can be obtained using this software.

Studing of quality control paramenters' trends

Considering the data storage in digital format, it will be possible to study the behaviour of quality control parameters identifying trends or dependencies between variables. This data is useful for future failure prediction analysis.

Developement of dynamic MLC test

The tools of analysis of the positioning of the leaves in static situations as the case of the MPC and the solution developed are very useful in clinic routine. However, these tools do not recreate the original situation in which the leaves are moving during the treatments. On the one hand, as already mentioned, results obtained in other studies performed in this clinic suggest the closure of the collimator leaves and as such an underexposure of the irradiated area. On the other hand, the results of this study show the opposite situation. For this reason, we suggested the development of an automatic leaves position analysis tool capable of detect leaves position in dynamic situations and that can be included in the quality control.

6 Conclusion

Since EPID has been discarded for verification of patient placement purposes, the use of this device for other clinical practices has been considered. In the last years, the CCC was looking for new and more efficient methodologies to perform quality control without neglecting accuracy. Given its importance to ensure that all scheduled treatments are carried out with maximum safety, quality control routines imply daily tasks to be exhaustively performed, including not only standard security evaluations but also analysis of specific parameters related to LINAC performance.

The present project focused on the optimization of LINAC-related parameters verification and on the adoption of EPID to facilitate clinical routine. The improve of the quality control protocol was achieved by taking into account two aspects: a proper storage of the generated data and the optimization of some tests. This strategy was materialized by implementing a software application that simplifies quality control data storage.

For tests optimization purposes, dose readouts and MLC leaves positioning were considered. On the one hand, the choice of these two tests resulted from recommendations of the physicists responsible for the conduction of quality control, which claim electrometer configuration as a time-consuming process and reported low accuracy of the MLC test. On the other hand, such decision resulted from the analysis of linear accelerator Edge's quality data acquired during the year 2017 that revealed a relevant number of failures directly related to the MLC positioning test.

The initial analysis of the quality control data allows to conclude that the current quality control protocol includes tests on parameters presenting low failure occurrence and low risk associated, such as couch motors voltage or hands controller. These verifications contribute to the high execution time that characterizes the current protocol and to the volume of stored data. We proposed a weekly test for such variables avoiding its daily evaluation. This approach aims to minimize work load without exposing professional staff to a total change of quality control routine.

Regarding, the above mentioned analysis of data related to the quality control of the Edge linear accelerator, a higher number of failures in the leaves of bank B was identified compared to the leaves of bank A. Subsequently, the analysis of the portal images, making use of the developed software, allowed to verify that bank B leaves present the greatest deviation, relatively to a given baseline. Given that most of the failures are followed by technical interventions (for example to replace control boards) that usually lead to leaves positioning re-calibration, both facts suggest a correlation between failures count and leaves positioning offset. However, the magnitude of such causal relationship need to be confirmed and properly quantified and the daily use of the developed toll acts on this direction, given that the determination of leaves positioning, in addition to the failure records, contributes to create a robust database that enables the detection of hidden patterns.

For performance purposes, the results derived from portal image analysis using the developed application were then evaluated. To this end, the method used to determine the center of rotation was firstly compared to *starshot()* function of the *Pylinac* package. Such comparison revealed similar efficiency (with a deviation between both methods of approximately 0.32 mm) and a reduction of approximately 40% of the computation time. Next, the most accurate method to be used in determining the boundary

between the leaves and the open region was investigated. Canny Edge Detector, Otsu Thresholding and Half-Maximum Intensity were the segmentation methods included in such study, that revealed the best results for Half-Maximum Intensity in terms of greater proximity to the expected value and possibility of inclusion sub-pixel precision.

Finally, the results for the distance between pairs of leaves, using the developed application, were compared with the garden test results. The inclusion of systematic errors in the positioning of the collimator leaves in the garden test allowed to identify a deviation bias between banks A and B of approximately 1.2 mm, compared to an error of approximately 1.4 mm suggested by the implemented algorithm for a standard bank aperture of 2 cm.

We propose the use of the developed tool to optimize quality control. This tool can be use to validate and include MPC in the clinic routine or in alternative case mantain the same instruments used in the current protocol. However, in last case we suggest the replacement of the visual test for the analysis of leaves positioning by the analysis tool included in the developed software. In both situations, dose measurements should continue to be performed using ionization chambers and the electrometer that can be now managed using the developed software. The results are stored in proper databases.

In short, this project allowed to provide a tool able to increase QC efficiency and facilitate its data management. In addition, the module aimed to analyse leaves positioning will allow CCC team to design and put in practice new research projects dedicated to further study some of the perspectives previously pointed in this thesis as well as deepen the operational details of the MLC component.

References

[1] I. Rosenberg, *Radiation Oncology Physics: A Handbook for Teachers and Students*. International Anatomic Energy Agency, 2005.

[2] INE. Statistics portugal. Accessed: 2017/10/13. [Online]. Available: https://www.ine.pt

[3] A. Clivio et al., "Evaluation of the machine performance check application for truebeam linac," *Radiation Oncology*, vol. 10, no. 1, p. 97, 2015.

[4] M. P. Barnes and P. B. Greer, "Evaluation of the truebeam machine performance check (mpc) geometric checks for daily igrt geometric accuracy quality assurance," *Journal of Applied Clinical Medical Physics*, vol. 18, no. 3, pp. 200–206, 2017.

[5] ——, "Evaluation of the truebeam machine performance check (mpc): Mechanical and collimation checks," *Journal of Applied Clinical Medical Physics*, vol. 18, no. 3, pp. 56–66, 2017.

[6] G. J. Budgell, R. Zhang, and R. I. Mackay, "Daily monitoring of linear accelerator beam parameters using an amorphous silicon epid." *Physics in Medicine and Biology*, vol. 52, no. 6, pp. 1721–1733, 2007.

[7] B. Sun et al., "Daily qa of linear accelerators using only epid and obi," *Medical Physics*, vol. 42, no. 10, pp. 5584–5594, 2015.

[8] A. H. Vitoria, M. C. L. Arroyo, and C. P. Olmos, Eds., *Fundamentos de Física Médica, Vol.3, Radioterapia externa I. Bases físicas, equipos, determinación de la dosis absorbida y programa de garantía de calidad*. ADI Servicos Editorales, 2012.

[9] Y. Lemoigne and A. Caner, Eds., *Radiation Protection in Medical Physics*. Taylor Francis Group, 2009.

[10] A. K. Berthelsen et al., "What's new in target volume definition for radiologists in icru report 71? how can the icru volume definitions be integrated in clinical practice?" *Cancer Imaging*, vol. 7, no. 1, pp. 104–116, 2007.

[11] I. Varian Medical Systems. Eclipse treatment planning system. Accessed: 2017/10/15. [Online]. Available: https://www.varian.com/oncology/products/software/treatment-planning

[12] A. Boyer et al., "Task group 72 report: Basic applications of multileaf collimators," *Medical Physics*, 2001.

[13] L. Cozzi and A. Fogliata, "Imrt in the treatment of head and neck cancer: is the present already the future?" *Expert Review of Anticancer Therapy*, vol. 2, no. 3, pp. 297–309, 2002.

[14] P. Mayles, A. Nahum, and J. C. Rosenwald, Eds., *Handbook of Radiotherapy Physics Theory and Practice*. Springer, 2007.

[15] A. Taylor and M. E. B. Powell, "Intensity-modulated radiotherapy - what is it?" *Cancer Imaging*, vol. 4, no. 2, pp. 68–73, 2004.

[16] I. Varian Medical Systems. External beam radiation therapy treatments. Accessed: 2017/11/15. [Online]. Available: https://www.varian.com/oncology/treatment-techniques/external-beam-radiation.

[17] S. Rana, "Intensity modulated radiation therapy versus volumetric intensity modulated arc therapy," *Journal of Medical Radiation Sciences*, vol. 60, no. 3, pp. 81–83, 2013.

[18] E. E. Klein et al., "Task group 142 report: Quality assurance of medical accelerators," *Medical Physics*, vol. 36, no. 9, pp. 4197–4212, 2009.

[19] W. van Elmpt et al., "A literature review of electronic portal imaging for radiotherapy dosimetry," *Radiotherapy and Oncology*, vol. 88, no. 3, pp. 289–309, 2008.

[20] F. M. G. de Moura, "Amorphous silicon detector panel damage: correlating physical parameters to clinical usability," *Ph.D. dissertation*, 2008.

[21] Wikipedia. Flat panel detector. Accessed: 2017/11/16. [Online]. Available: https://en.wikipedia.org/wiki/Flat_panel_detector.

[22] C. Grau et al., "Radiotherapy equipment and departments in the european countries: Final results from the estro-hero survey," *Radiotherapy and Oncology*, vol. 112, no. 2, pp. 155–164, 2014.

[23] M. C. Kirby and P. C. Williams, "Measurement possibilities using an electronic portal imaging device," *Radiotherapy and Oncology*, vol. 29, no. 2, pp. 237–43, 1993.

[24] A. Agnew, C. E. Agnew, M. W. D. Grattan, A. R. Hounsell, and C. K. McGarry, "Monitoring daily mlc positional errors using trajectory log files and epid measurements for imrt and vmat deliveries," *Physics in Medicine and Biology*, vol. 59, no. 9, pp. 49–63, 2014.

[25] T. Eckhause et al., "Automating linear accelerator quality assurance," *Medical Physics*, vol. 42, no. 10, pp. 6074–6083, 2015.

[26] S. J. K. Baker, G. J. Budgell, and R. I. MacKay, "Use of an amorphous silicon electronic portal imaging device for multileaf collimator quality control and calibration," *Physics in Medicine and Biology*, vol. 50, no. 7, pp. 1377–1392, 2005.

[27] S. C. Vieira, R. A. Bolt, M. L. P. Dirkx, A. G. Visser, and B. J. M. Heijmen, "Fast, daily linac verification for segmented imrt using electronic portal imaging," *Radiotherapy and Oncology*, vol. 80, no. 1, p. 86–92, 2006.

[28] K. H. V. Medical Physics, Institute of Radiooncology. Machine performance check - a useful tool for machine qa? Accessed: 2018/09/18. [Online]. Available: http://www.wienkav.at

[29] P. Andreo et al., *Absorbed dose determination in External Beam Radiotherapy: An International Code of Pratice for Dosimetry based on Standards of Absorbed Dose to Water*, ser. 398. International Anatomic Energy Agency, 2000.

[30] I. Varian Medical Systems. Calypso surface beacon transponder external real-time motion tracking. Accessed: 2017/11/13. [Online]. Available: https://www.varian.com/oncology/products/real-time-tracking-motion-management/calypso-extracranial-tracking

[31] PTW. Universal dosemeter. Accessed: 2018/07/10. [Online]. Available: http://www.ptw.de/unidos_webline_dosemeter_rt0.html

[32] V. M. Systems, *Machine Performance Check Reference Guide V1.0.* Varian Associates Inc. Oncology Systems, Palo Alto, CA, 2013.

[33] P. S. Foundation. Python. Accessed: 2018/09/18. [Online]. Available: http://www.python.org

[34] ——. Pyqt. Accessed: 2018/09/18. [Online]. Available: https://pypi.org/project/PyQt5/

[35] P. Rowshanfarzad, M. Sabet, M. P. Barnes, D. J. O'Connor, and P. B. Greer, "Epid-based verification of the mlc performance for dynamic imrt and vmat," *Medical Physics*, vol. 39, no. 10, 2012.

Appendices

A Appendice 1

XML code used to acquired the portal images required to MLC leaves positioning analysis.

```
<VarianResearchBeam SchemaVersion="1.0">
    <SetBeam>
        <Id>1</Id>
        <MLCModel>NDS120HD</MLCModel>
        <Accs/>
        <ControlPoints>
            <Cp>    <!-- nr0 -->
                <Energy>6x</Energy>
                <Mu>0.00</Mu>
                <DRate>600.0</DRate>
                <GantryRtn>180.0</GantryRtn>
                <CollRtn>90.0</CollRtn>
                <CouchVrt>100.0</CouchVrt>
                <CouchLat>100.0</CouchLat>
                <CouchLng>17.0</CouchLng>
                <CouchRtn>180.0</CouchRtn>
                <CouchPit>0</CouchPit>
                <CouchRol>0</CouchRol>
                <Y1>10.00</Y1>
                <Y2>10.00</Y2>
                <X1>10.00</X1>
                <X2>10.00</X2>
                <Mlc>
                    <ID>1</ID>
                    <B>2.00 2.00 2.00 2.00 2.00 2.00 2.00 2.00
                       2.00 2.00 2.00 2.00 2.00 2.00 2.00 2.00
                       2.00 2.00 2.00 2.00 2.00 2.00 2.00 2.00
                       2.00 2.00 2.00 2.00 2.00 2.00 2.00 2.00
                       2.00 2.00 2.00 2.00 2.00 2.00 2.00 2.00
                       2.00 2.00 2.00 2.00 2.00 2.00 2.00 2.00
                       2.00 2.00 2.00 2.00 2.00 2.00 2.00 2.00
                       2.00 2.00 2.00 2.00</B>
                    <A>2.00 2.00 2.00 2.00 2.00 2.00 2.00 2.00
                       2.00 2.00 2.00 2.00 2.00 2.00 2.00 2.00
                       2.00 2.00 2.00 2.00 2.00 2.00 2.00 2.00
                       2.00 2.00 2.00 2.00 2.00 2.00 2.00 2.00
```

```
            2.00 2.00 2.00 2.00 2.00 2.00 2.00 2.00
            2.00 2.00 2.00 2.00 2.00 2.00 2.00 2.00
            2.00 2.00 2.00 2.00 2.00 2.00 2.00 2.00
            2.00 2.00 2.00 2.00</A>
    </Mlc>
</Cp>
<Cp>    <!-- nr1 -->
    <Mu>100.00</Mu>
    <GantryRtn>180.0</GantryRtn>
    <CollRtn>89.95</CollRtn>
    <Y1>10.00</Y1>
    <Y2>10.00</Y2>
    <X1>10.00</X1>
    <X2>10.00</X2>
    <Mlc>
        <ID>1</ID>
        <B>2.00 2.00 2.00 2.00 2.00 2.00 2.00 2.00
           2.00 2.00 2.00 2.00 2.00 2.00 2.00 2.00
           2.00 2.00 2.00 2.00 2.00 2.00 2.00 2.00
           2.00 2.00 2.00 2.00 2.00 2.00 2.00 2.00
           2.00 2.00 2.00 2.00 2.00 2.00 2.00 2.00
           2.00 2.00 2.00 2.00 2.00 2.00 2.00 2.00
           2.00 2.00 2.00 2.00 2.00 2.00 2.00 2.00
           2.00 2.00 2.00 2.00</B>
        <A>2.00 2.00 2.00 2.00 2.00 2.00 2.00 2.00
           2.00 2.00 2.00 2.00 2.00 2.00 2.00 2.00
           2.00 2.00 2.00 2.00 2.00 2.00 2.00 2.00
           2.00 2.00 2.00 2.00 2.00 2.00 2.00 2.00
           2.00 2.00 2.00 2.00 2.00 2.00 2.00 2.00
           2.00 2.00 2.00 2.00 2.00 2.00 2.00 2.00
           2.00 2.00 2.00 2.00 2.00 2.00 2.00 2.00
           2.00 2.00 2.00 2.00</A>
    </Mlc>
</Cp>
<Cp>    <!-- nr3 -->
    <CouchLat>105.0</CouchLat>
</Cp>
<Cp>    <!-- nr4 -->
    <CouchLat>95.0</CouchLat>
</Cp>
<Cp>    <!-- nr5 -->
    <CouchLat>100.0</CouchLat>
</Cp>
<Cp>    <!-- nr5 -->
    <Mu>100.00</Mu>
```

```
        <GantryRtn>180.0</GantryRtn>
        <CollRtn>135.0</CollRtn>
        <Y1>10.00</Y1>
        <Y2>10.00</Y2>
        <X1>10.00</X1>
        <X2>10.00</X2>
        <Mlc>
            <ID>1</ID>
            <B>2.00 2.00 2.00 2.00 2.00 2.00 2.00 2.00
               2.00 2.00 2.00 2.00 2.00 2.00 2.00 2.00
               2.00 2.00 2.00 2.00 2.00 2.00 2.00 2.00
               2.00 2.00 2.00 2.00 2.00 2.00 2.00 2.00
               2.00 2.00 2.00 2.00 2.00 2.00 2.00 2.00
               2.00 2.00 2.00 2.00 2.00 2.00 2.00 2.00
               2.00 2.00 2.00 2.00 2.00 2.00 2.00 2.00
               2.00 2.00 2.00 2.00</B>
            <A>2.00 2.00 2.00 2.00 2.00 2.00 2.00 2.00
               2.00 2.00 2.00 2.00 2.00 2.00 2.00 2.00
               2.00 2.00 2.00 2.00 2.00 2.00 2.00 2.00
               2.00 2.00 2.00 2.00 2.00 2.00 2.00 2.00
               2.00 2.00 2.00 2.00 2.00 2.00 2.00 2.00
               2.00 2.00 2.00 2.00 2.00 2.00 2.00 2.00
               2.00 2.00 2.00 2.00 2.00 2.00 2.00 2.00
               2.00 2.00 2.00 2.00</A>
        </Mlc>
    </Cp>
    <Cp>    <!-- nr6 -->
        <Mu>200.00</Mu>
        <GantryRtn>180.0</GantryRtn>
        <CollRtn>135.0</CollRtn>
        <Y1>10.00</Y1>
        <Y2>10.00</Y2>
        <X1>10.00</X1>
        <X2>10.00</X2>
        <Mlc>
            <ID>1</ID>
            <B>2.00 2.00 2.00 2.00 2.00 2.00 2.00 2.00
               2.00 2.00 2.00 2.00 2.00 2.00 2.00 2.00
               2.00 2.00 2.00 2.00 2.00 2.00 2.00 2.00
               2.00 2.00 2.00 2.00 2.00 2.00 2.00 2.00
               2.00 2.00 2.00 2.00 2.00 2.00 2.00 2.00
               2.00 2.00 2.00 2.00 2.00 2.00 2.00 2.00
               2.00 2.00 2.00 2.00 2.00 2.00 2.00 2.00
               2.00 2.00 2.00 2.00</B>
```

```
            <A>2.00 2.00 2.00 2.00 2.00 2.00 2.00 2.00
               2.00 2.00 2.00 2.00 2.00 2.00 2.00 2.00
               2.00 2.00 2.00 2.00 2.00 2.00 2.00 2.00
               2.00 2.00 2.00 2.00 2.00 2.00 2.00 2.00
               2.00 2.00 2.00 2.00 2.00 2.00 2.00 2.00
               2.00 2.00 2.00 2.00 2.00 2.00 2.00 2.00
               2.00 2.00 2.00 2.00 2.00 2.00 2.00 2.00
               2.00 2.00 2.00 2.00</A>
        </Mlc>
    </Cp>
    <Cp>    <!-- nr8 -->
        <CouchLat>105.0</CouchLat>
    </Cp>
    <Cp>    <!-- nr9 -->
        <CouchLat>95.0</CouchLat>
    </Cp>
    <Cp>    <!-- nr10 -->
        <CouchLat>100.0</CouchLat>
    </Cp>
    <Cp>    <!-- nr10 -->
        <Mu>200.00</Mu>
        <GantryRtn>180.0</GantryRtn>
        <CollRtn>225.0</CollRtn>
        <Y1>10.00</Y1>
        <Y2>10.00</Y2>
        <X1>10.00</X1>
        <X2>10.00</X2>
        <Mlc>
            <ID>1</ID>
            <B>2.00 2.00 2.00 2.00 2.00 2.00 2.00 2.00
               2.00 2.00 2.00 2.00 2.00 2.00 2.00 2.00
               2.00 2.00 2.00 2.00 2.00 2.00 2.00 2.00
               2.00 2.00 2.00 2.00 2.00 2.00 2.00 2.00
               2.00 2.00 2.00 2.00 2.00 2.00 2.00 2.00
               2.00 2.00 2.00 2.00 2.00 2.00 2.00 2.00
               2.00 2.00 2.00 2.00 2.00 2.00 2.00 2.00
               2.00 2.00 2.00 2.00</B>
            <A>2.00 2.00 2.00 2.00 2.00 2.00 2.00 2.00
               2.00 2.00 2.00 2.00 2.00 2.00 2.00 2.00
               2.00 2.00 2.00 2.00 2.00 2.00 2.00 2.00
               2.00 2.00 2.00 2.00 2.00 2.00 2.00 2.00
               2.00 2.00 2.00 2.00 2.00 2.00 2.00 2.00
               2.00 2.00 2.00 2.00 2.00 2.00 2.00 2.00
               2.00 2.00 2.00 2.00 2.00 2.00 2.00 2.00
               2.00 2.00 2.00 2.00</A>
```

```
    </Mlc>
</Cp>
<Cp>    <!-- nr11 -->
    <Mu>300.00</Mu>
    <GantryRtn>180.0</GantryRtn>
    <CollRtn>225.0</CollRtn>
    <Y1>10.00</Y1>
    <Y2>10.00</Y2>
    <X1>10.00</X1>
    <X2>10.00</X2>
    <Mlc>
        <ID>1</ID>
        <B>2.00 2.00 2.00 2.00 2.00 2.00 2.00 2.00
           2.00 2.00 2.00 2.00 2.00 2.00 2.00 2.00
           2.00 2.00 2.00 2.00 2.00 2.00 2.00 2.00
           2.00 2.00 2.00 2.00 2.00 2.00 2.00 2.00
           2.00 2.00 2.00 2.00 2.00 2.00 2.00 2.00
           2.00 2.00 2.00 2.00 2.00 2.00 2.00 2.00
           2.00 2.00 2.00 2.00 2.00 2.00 2.00 2.00
           2.00 2.00 2.00 2.00</B>
        <A>2.00 2.00 2.00 2.00 2.00 2.00 2.00 2.00
           2.00 2.00 2.00 2.00 2.00 2.00 2.00 2.00
           2.00 2.00 2.00 2.00 2.00 2.00 2.00 2.00
           2.00 2.00 2.00 2.00 2.00 2.00 2.00 2.00
           2.00 2.00 2.00 2.00 2.00 2.00 2.00 2.00
           2.00 2.00 2.00 2.00 2.00 2.00 2.00 2.00
           2.00 2.00 2.00 2.00 2.00 2.00 2.00 2.00
           2.00 2.00 2.00 2.00</A>
    </Mlc>
</Cp>
<Cp>    <!-- nr13 -->
    <CouchLat>105.0</CouchLat>
</Cp>
<Cp>    <!-- nr14 -->
    <CouchLat>95.0</CouchLat>
</Cp>
<Cp>    <!-- nr15 -->
    <CouchLat>100.0</CouchLat>
</Cp>
<Cp>    <!-- nr15 -->
    <Mu>300.00</Mu>
    <GantryRtn>180.0</GantryRtn>
    <CollRtn>90.0</CollRtn>
    <Y1>10.00</Y1>
    <Y2>10.00</Y2>
```

```
        <X1>10.00</X1>
        <X2>10.00</X2>
        <Mlc>
            <ID>1</ID>
            <B>3.5 0.5 3.5 0.5 3.5 0.5 3.5 0.5 3.5 0.5
               3.5 0.5 3.5 0.5 3.5 0.5 3.5 0.5 3.5 0.5 3.5
                0.5 3.5 0.5 3.5 0.5 3.5 0.5 3.5 0.5 3.5
               0.5 3.5 0.5 3.5 0.5 3.5 0.5 3.5 0.5 3.5 0.5
                3.5 0.5 3.5 0.5 3.5 0.5 3.5 0.5 3.5 0.5
               3.5 0.5 3.5 0.5 3.5 0.5 3.5 0.5</B>
                                <A>0.5 3.5 0.5 3.5 0.5
                                   3.5 0.5 3.5 0.5 3.5 0.5
                                    3.5 0.5 3.5 0.5 3.5
                                   0.5 3.5 0.5 3.5 0.5 3.5
                                    0.5 3.5 0.5 3.5 0.5
                                   3.5 0.5 3.5 0.5 3.5 0.5
                                    3.5 0.5 3.5 0.5 3.5
                                   0.5 3.5 0.5 3.5 0.5 3.5
                                    0.5 3.5 0.5 3.5 0.5
                                   3.5 0.5 3.5 0.5 3.5 0.5
                                    3.5 0.5 3.5 0.5 3.5</A
                                   >
        </Mlc>
    </Cp>
    <Cp>    <!-- nr16 -->
        <Mu>400.00</Mu>
        <GantryRtn>180.0</GantryRtn>
        <CollRtn>90.0</CollRtn>
        <Y1>10.00</Y1>
        <Y2>10.00</Y2>
        <X1>10.00</X1>
        <X2>10.00</X2>
        <Mlc>
            <ID>1</ID>
            <B>3.5 0.5 3.5 0.5 3.5 0.5 3.5 0.5 3.5 0.5
               3.5 0.5 3.5 0.5 3.5 0.5 3.5 0.5 3.5 0.5 3.5
                0.5 3.5 0.5 3.5 0.5 3.5 0.5 3.5 0.5 3.5
               0.5 3.5 0.5 3.5 0.5 3.5 0.5 3.5 0.5 3.5 0.5
                3.5 0.5 3.5 0.5 3.5 0.5 3.5 0.5 3.5 0.5
               3.5 0.5 3.5 0.5 3.5 0.5 3.5 0.5</B>
                                <A>0.5 3.5 0.5 3.5 0.5
                                   3.5 0.5 3.5 0.5 3.5 0.5
                                    3.5 0.5 3.5 0.5 3.5
                                   0.5 3.5 0.5 3.5 0.5 3.5
                                    0.5 3.5 0.5 3.5 0.5
```

```
                                        3.5 0.5 3.5 0.5 3.5 0.5
                                         3.5 0.5 3.5 0.5 3.5
                                        0.5 3.5 0.5 3.5 0.5 3.5
                                         0.5 3.5 0.5 3.5 0.5
                                        3.5 0.5 3.5 0.5 3.5 0.5
                                         3.5 0.5 3.5 0.5 3.5</A
                                        >
            </Mlc>
        </Cp>
        <Cp>    <!-- nr18 -->
            <CouchLat>105.0</CouchLat>
        </Cp>
        <Cp>    <!-- nr19 -->
            <CouchLat>95.0</CouchLat>
        </Cp>
        <Cp>    <!-- nr20 -->
            <CouchLat>100.0</CouchLat>
        </Cp>
    </ControlPoints>
    <ImagingParameters>
        <DuringTreatment/>
        <LatchBEL>true</LatchBEL>
        <LatchKVBEL>true</LatchKVBEL>
        <ImagingPoints>
            <ImagingPoint>
                <Cp>0.0</Cp>
                <AcquisitionStart>
                    <AcquisitionId>1</AcquisitionId>
                    <AcquisitionSpecs/>
                    <AcquisitionParameters>
                        <ImageMode id="Dosimetry"/>
                        <CalibrationSet>
                           DefaultCalibrationSetId</
                           CalibrationSet>
                        <MV/>
                    </AcquisitionParameters>
                </AcquisitionStart>
                <Mvd>
                    <Positions>
                        <Lat>0.0</Lat>
                        <Lng>0.0</Lng>
                        <Vrt>0.0</Vrt>
                        <Pitch>0.0</Pitch>
                    </Positions>
                </Mvd>
```

```
</ImagingPoint>
<ImagingPoint>
    <Cp>1.0</Cp>
    <AcquisitionStop>
         <AcquisitionId>1</AcquisitionId>
         <AcquisitionSpecs/>
    </AcquisitionStop>
</ImagingPoint>
<ImagingPoint>
    <Cp>5.0</Cp>
    <AcquisitionStart>
         <AcquisitionId>3</AcquisitionId>
         <AcquisitionSpecs/>
         <AcquisitionParameters>
             <ImageMode id="Dosimetry"/>
             <CalibrationSet>
                DefaultCalibrationSetId</
                CalibrationSet>
             <MV/>
         </AcquisitionParameters>
    </AcquisitionStart>
    <Mvd>
         <Positions>
             <Lat>0.0</Lat>
             <Lng>0.0</Lng>
             <Vrt>0.0</Vrt>
             <Pitch>0.0</Pitch>
         </Positions>
    </Mvd>
</ImagingPoint>
<ImagingPoint>
    <Cp>6.0</Cp>
    <AcquisitionStop>
         <AcquisitionId>3</AcquisitionId>
         <AcquisitionSpecs/>
    </AcquisitionStop>
</ImagingPoint>
<ImagingPoint>
    <Cp>10.0</Cp>
    <AcquisitionStart>
         <AcquisitionId>5</AcquisitionId>
         <AcquisitionSpecs/>
         <AcquisitionParameters>
             <ImageMode id="Dosimetry"/>
```

```
                <CalibrationSet>
                    DefaultCalibrationSetId</
                    CalibrationSet>
                <MV/>
            </AcquisitionParameters>
        </AcquisitionStart>
        <Mvd>
            <Positions>
                <Lat>0.0</Lat>
                <Lng>0.0</Lng>
                <Vrt>0.0</Vrt>
                <Pitch>0.0</Pitch>
            </Positions>
        </Mvd>
    </ImagingPoint>
    <ImagingPoint>
        <Cp>11.0</Cp>
        <AcquisitionStop>
            <AcquisitionId>5</AcquisitionId>
            <AcquisitionSpecs/>
        </AcquisitionStop>
    </ImagingPoint>
    <ImagingPoint>
        <Cp>15.0</Cp>
        <AcquisitionStart>
            <AcquisitionId>7</AcquisitionId>
            <AcquisitionSpecs/>
            <AcquisitionParameters>
                <ImageMode id="Dosimetry"/>
                <CalibrationSet>
                    DefaultCalibrationSetId</
                    CalibrationSet>
                <MV/>
            </AcquisitionParameters>
        </AcquisitionStart>
        <Mvd>
            <Positions>
                <Lat>0.0</Lat>
                <Lng>0.0</Lng>
                <Vrt>0.0</Vrt>
                <Pitch>0.0</Pitch>
            </Positions>
        </Mvd>
    </ImagingPoint>
    <ImagingPoint>
```

```
                    <Cp>16.0</Cp>
                    <AcquisitionStop>
                        <AcquisitionId>7</AcquisitionId>
                        <AcquisitionSpecs/>
                    </AcquisitionStop>
                </ImagingPoint>
                <ImagingPoint>
                    <Cp>20.0</Cp>
                    <AcquisitionStart>
                        <AcquisitionId>9</AcquisitionId>
                        <AcquisitionSpecs/>
                        <AcquisitionParameters>
                            <ImageMode id="Dosimetry"/>
                            <CalibrationSet>
                               DefaultCalibrationSetId</
                               CalibrationSet>
                            <MV/>
                        </AcquisitionParameters>
                    </AcquisitionStart>
                    <Mvd>
                        <Positions>
                            <Lat>0.0</Lat>
                            <Lng>0.0</Lng>
                            <Vrt>0.0</Vrt>
                            <Pitch>0.0</Pitch>
                        </Positions>
                    </Mvd>
                </ImagingPoint>
                <ImagingPoint>
                    <Cp>21.0</Cp>
                    <AcquisitionStop>
                        <AcquisitionId>9</AcquisitionId>
                        <AcquisitionSpecs/>
                    </AcquisitionStop>
                </ImagingPoint>
            </ImagingPoints>
            <ImagingTolerances/>
        </ImagingParameters>
    </SetBeam>
</VarianResearchBeam>
```

B Appendice 2

ximReader code developed by Varian Medical Systems, Inc. to read XIM files.

```
from __future__ import absolute_import, division, print_function
# might make this work on py2
from builtins import *

# Copyright (c) 2014, Varian Medical Systems, Inc. (VMS)
# All rights reserved.
#
# ximReader is an open source tool for reading .xim file (both
   compressed and uncompressed)
# HND compression algorithm is used to compress xim files. For a
   brief description of  HND
# compression algorithm please refer to the xim_readme.txt file.
#
# ximReader is licensed under the VarianVeritas License.
# You may obtain a copy of the License at:
#
#       website: http://radiotherapyresearchtools.com/license/
#
# For questions, please send us an email at:
   TrueBeamDeveloper@varian.com
#
# Developer Mode is intended for non-clinical use only and is NOT
    cleared for use on humans.
#
# Created on: 12:04:06 PM, Sept. 26, 2014
# Authors: Pankaj Mishra and Thanos Etmektzoglou
#
# Modified on : 10:58:045 AM, Jul. 24, 2015
# Modified by Nilesh Gorle

import textwrap
import os
import struct, sys, numpy as np
from matplotlib import pyplot as plt
from argparse import ArgumentParser
from pprint import pprint

LINE_SPACE = 150
XIMREADER_FILENAME = "XimReaderData.txt"
XIMREADER_IMG_NAME = "XimReaderImage.png"
```

```
class XimFileInfo(object):
    '''
    XimFileInfo is the main class to store header data, histogram
       data
    and property data in text format and saving the plot image.
    '''

    def __init__(self, **kwargs):
        '''
        XimFileInfo Constructor
        '''
        self.headerDataDict = kwargs.get('headerDataDict')
        self.histogramDataDict = kwargs.get('histogramDataDict')
        self.propertyDataList = kwargs.get('propertyDataList')

        self.outputFolder = os.path.join(os.path.dirname(__file__
           ), 'XimData')

        if not os.path.exists(self.outputFolder):
            os.mkdir(self.outputFolder)

        outputPath = os.path.join(self.outputFolder,
           XIMREADER_FILENAME)
        print ("%s is created on %s" % (XIMREADER_FILENAME, self.
           outputFolder))

        # Open file to write data.
        self.ximFile = open(outputPath, "w")

        # Flushing all contents from existing text file and
           appending new contents
        self.ximFile.seek(0)
        self.ximFile.truncate()

    def saveHeaderInfo(self):
        '''
        saving header information
        '''
        title = "Header Data".center(LINE_SPACE)

        self.ximFile.writelines("="*LINE_SPACE + "\n" + title + "
           \n" + "="*LINE_SPACE + "\n")
```

```
        thead = "FormatIdentifier".center(20), "|", "
           FormatVersion".center(20), \
                "|", "Width".center(10), "|", "Height".center(10)
                   , "|", \
                "BitsPerPixel".center(20), "|", "BytesPerPixel".
                   center(20), "|", \
                "CompressionIndicator".center(20)
        thead = "".join(thead)
        self.ximFile.writelines(thead + "\n" + "="*LINE_SPACE)

        FormatIdentifier = (self.headerDataDict["FormatIdentifier
           "]).replace("\x00", "")
        tbody = FormatIdentifier.center(20), "|", \
                str(self.headerDataDict.get("FormatVersion")).
                   center(20), "|", \
                str(self.headerDataDict.get("Width")).center(10),
                    "|", \
                str(self.headerDataDict.get("Height")).center(10)
                   , "|", \
                str(self.headerDataDict.get("BitsPerPixel")).
                   center(20), "|", \
                str(self.headerDataDict.get("BytesPerPixel")).
                   center(20), "|", \
                str(self.headerDataDict.get("CompressionIndicator
                   ")).center(20)
        tbody = "".join(tbody)
        self.ximFile.writelines("\n" + tbody + "\n" + "="*
           LINE_SPACE)
        print ("Header␣data␣stored␣into␣file␣successfully.")

    def saveHistogramInfo(self):
        '''
␣␣␣␣␣␣␣␣saving␣histogram␣information
␣␣␣␣␣␣␣␣'''
        title = "Histogram␣Data".center(LINE_SPACE)
        self.ximFile.writelines("\n"*4 + "="*LINE_SPACE + "\n" +
           title + "\n" + "="*LINE_SPACE + "\n")
        thead = "NumberOfBins".center(20), "|", \
                "Value".center(20)

        thead = "".join(thead)
        self.ximFile.writelines(thead + "\n" + "="*LINE_SPACE + "
           \n")
```

```
        valList = textwrap.wrap(str(self.histogramDataDict.get("
           Value")), width=130)


        tbody = str(self.histogramDataDict.get("NumberOfBins")).
           center(20) + "|\n"

        for i in range(len(valList)):
            tbody += ("␣"*20 + "|␣␣" + (valList[i]).center(20) +
               "\n")

        tbody = "".join(tbody)
        self.ximFile.writelines(tbody + "\n" + "="*LINE_SPACE)
        print ("Histogram␣data␣stored␣into␣file␣successfully.")

    def savePropertyInfo(self):
        '''
␣␣␣␣␣␣␣␣saving␣property␣information
␣␣␣␣␣␣␣␣'''
        DATATYPE_DICT = {0: "Integer", 1: "Double", 2: "String",
                         4: "Double␣Array", 5: "Integer␣Array"}

        title = "Property␣Data".center(LINE_SPACE)
        self.ximFile.writelines("\n"*4 + "="*LINE_SPACE + "\n" +
           title + "\n" + "="*LINE_SPACE + "\n")

        thead = "Length".center(6), "|", "Name".center(50), "|",
           \
              "Type".center(15), "|", "Value".center(25)
        thead = "".join(thead)
        self.ximFile.writelines(thead + "\n" + "="*LINE_SPACE + "
           \n")

        tbody = ""
        for length, name, ptype, value in self.propertyDataList:
            if isinstance(value, str):
                value = value.replace('\n', '␣').replace('\r', ',
                   ')
            value = str(value)

            if len(value) > 54:
                if value.startswith('<') :
                    import xml.dom.minidom
                    xml_string = xml.dom.minidom.parseString(
                       value)
```

```
                    pretty_xml_as_string = xml_string.toprettyxml
                        ()
                    valList = pretty_xml_as_string.split("\n")

                    tbody = (str(length).center(6) + "|" + str(
                        name).center(50) + "|" + \
                      (DATATYPE_DICT[ptype]).center(15) + "|\n")

                    for i in range(len(valList)):
                        tbody += ("␣"*73 + "|" + (valList[i]).
                            center(25) + "\n")
                else:
                    valList = textwrap.wrap(str(value), width=80)

                    tbody = (str(length).center(6) + "|" + str(
                        name).center(50) + "|" + \
                              (DATATYPE_DICT[ptype]).center(15) +
                                 "|\n")

                    for i in range(len(valList)):
                            tbody += ("␣"*73 + "|␣␣" + (valList[i
                               ]).center(25) + "\n")

            else:
                tbody = (str(length).center(6) + "|" + str(name).
                    center(50) + "|" + \
                         (DATATYPE_DICT[ptype]).center(15) + "|" +
                             str(value).center(25))

            self.ximFile.writelines(tbody + "\n" + "-"*LINE_SPACE
                + "\n")

        self.ximFile.writelines("="*LINE_SPACE)
        print ("Property␣data␣stored␣into␣file␣successfully.")

    def closeFile(self):
        '''
␣␣␣␣␣␣␣␣Closing␣ximData.txt␣file
␣␣␣␣␣␣␣␣'''
        self.ximFile.close()

    def saveXimInfo(self):
        '''
␣␣␣␣␣␣␣␣Saving␣headerData,␣histogramData␣and␣propertyData␣in␣text
    ␣file
```

```
␣␣␣␣␣␣␣␣'''
        # storing headerData
        self.saveHeaderInfo()

        # storing histogramData
        self.saveHistogramInfo()

        # storing propertyData
        self.savePropertyInfo()

        # Close file
        self.closeFile()

class XimReader():
    '''
␣␣␣␣XimReader␣is␣the␣main␣class␣for␣converting␣an␣xim␣file␣to␣a␣
   two
␣␣␣␣dimensional␣image.␣This␣class␣reads␣header,␣pixel␣data,␣
   histogram
␣␣␣␣and␣properties␣of␣a␣given␣xim␣file.␣If␣the␣xim␣image␣is␣
   compressed
␣␣␣␣then␣HND␣decompression␣algorithm␣is␣used␣to␣for␣decompression
   .
␣␣␣␣Note:␣HND␣is␣a␣lossless␣compression␣algorithm
␣␣␣␣'''

    def __init__(self, filename=None):
        '''
␣␣␣␣␣␣␣␣Open␣the␣given␣file
␣␣␣␣␣␣␣␣:param␣filename:
␣␣␣␣␣␣␣␣'''
        self.filename = filename
        self.openFile()

    def openFile(self):
        '''
␣␣␣␣␣␣␣␣Check␣for␣the␣existence␣of␣the␣xim␣file
␣␣␣␣␣␣␣␣and␣open␣a␣file␣handler
␣␣␣␣␣␣␣␣'''
        try:
            # Open the binary xim file for reading
            self.f = open(self.filename, 'rb')
        except IOError:
            # No xim file by the given name exists
            print ("xim␣file␣doesn't␣exist")
```

```
    def headerData(self):
        '''
␣␣␣␣␣␣␣␣Header␣has␣a␣fixed␣length␣of␣32␣bytes.
␣␣␣␣␣␣␣␣Integers␣and␣floats␣are␣stored␣in␣little-endian␣format
␣␣␣␣␣␣␣␣'''
        self.ximHeader = dict()  # Dictionary of header values
        # on Py3 we need to decode so that we can later use the
           replace
        self.ximHeader['FormatIdentifier'] = self.f.read(8).
           decode()
        self.ximHeader['FormatVersion'] = struct.unpack('<i',
           self.f.read(4))[0]
        self.ximHeader['Width'] = struct.unpack('<i', self.f.read
           (4))[0]
        self.ximHeader['Height'] = struct.unpack('<i', self.f.
           read(4))[0]
        self.ximHeader['BitsPerPixel'] = struct.unpack('<i', self
           .f.read(4))[0]
        self.ximHeader['BytesPerPixel'] = struct.unpack('<i',
           self.f.read(4))[0]
        self.ximHeader['CompressionIndicator'] = struct.unpack('<
           i', self.f.read(4))[0]


    def pixelData(self):
        '''
␣␣␣␣␣␣␣␣Pixel␣values␣in␣an␣HND␣image␣is␣stored␣in␣pixelData␣field
   .␣Pixel␣data␣are␣either
␣␣␣␣␣␣␣␣compressed␣or␣uncompressed␣which␣can␣be␣determined␣by␣the
   ␣"Compression␣indicator"
␣␣␣␣␣␣␣␣field␣in␣the␣header␣data.
␣␣␣␣␣␣␣␣'''
        w = self.ximHeader['Width']
        h = self.ximHeader['Height']
        bpp = self.ximHeader['BytesPerPixel']

        # Image pixels are stored uncompressed in the xim image
           file.
        pprint(self.ximHeader)
        if not self.ximHeader['CompressionIndicator']:
            # Read in int4 (32 bit) image pixe values
            uncompressedPixelBufferSize = struct.unpack('<%i',
               self.f.read(4))[0]
            # Read in pixel values in 1D array
```

```
            uncompressedPixelBuffer = np.asarray(struct.unpack('
               <%ii' % (uncompressedPixelBufferSize / 4), \
                                                                  self
                                                                     .
                                                                     f
                                                                     .
                                                                     read
                                                                     (
                                                                     uncom
                                                                     )
                                                                     )
                                                                     )


        # Decompress the pixelData using HND decompression
           algorithm.
        else:
            self.LUTSize = struct.unpack('<i', self.f.read(4))[0]
                 # Lookup table size
            LUT = np.asarray(struct.unpack('<%iB' % self.LUTSize,
                self.f.read(self.LUTSize)))  # Lookup table
            compressedBufferSize = struct.unpack('<i', self.f.
               read(4))[0]  # Compressed pixel buffer size
            uncompressedPixelBuffer = self.uncompressHnd(w, h,
               bpp, LUT)  # Uncompress the pixel data
            uncompressedBufferSize = struct.unpack('<i', self.f.
               read(4))[0]  # Uncompressed pixel image size

        # Reshape uncompressed image into 2D array
        self.uncompressedImage = np.reshape(
           uncompressedPixelBuffer, (h, w))


    def histogramData(self):

        self.histogram = dict()
        self.histogram['NumberOfBins'] = struct.unpack('<i', self
           .f.read(4))[0]
        self.histogram['Value'] = struct.unpack('<%ii' % self.
           histogram['NumberOfBins'], \
                                            self.f.read(4 * self.
                                               histogram['
                                               NumberOfBins']))
```

```
    def propertiesData(self):
        """
␣␣␣␣␣␣␣␣Get␣property␣data␣for␣images
␣␣␣␣␣␣␣␣"""
        self.propertyDataList = []

        value = None
        propertyValList = []

        propertyCount = struct.unpack('<i', self.f.read(4))[0]

        PROPERTY_TYPE_DICT = {0 : ('<i', 4),
                              1 : ('<d', 8),
                              2 : ('<i', 4),
                              }

        def get_value(fmt, fmt_length):
            """
␣␣␣␣␣␣␣␣␣␣␣␣Getting␣integer␣or␣double␣value␣and␣appending␣it␣into
   ␣property␣value␣list
␣␣␣␣␣␣␣␣␣␣␣␣"""
            try:
                value = struct.unpack(fmt, self.f.read(fmt_length
                   ))[0]
                propertyValList.append(value)
                return value
            except:
                return None

        if propertyCount:
            for i in range(propertyCount):
                if not value:
                    propertyNameLength = struct.unpack('<i', self
                       .f.read(4))[0]
                else:
                    propertyNameLength = value
                    value = None
                    propertyValList = []

                propertyName = struct.unpack('<%is' %
                   propertyNameLength , self.f.read(
                   propertyNameLength))[0]
                propertyType = struct.unpack('<i', self.f.read(4)
                   )[0]
```

```
            if propertyType in PROPERTY_TYPE_DICT.keys():
                propertyValue = struct.unpack(
                   PROPERTY_TYPE_DICT[propertyType][0],
                                                self.f.read(
                                                   PROPERTY_TYPE_DICT
                                                   [
                                                   propertyType
                                                   ][1]))[0]

                if propertyType == 2:
                    propertyValue = struct.unpack('<%is' %
                       propertyValue, self.f.read(
                       propertyValue))[0]

                rstTpl = propertyNameLength, propertyName,
                   propertyType, propertyValue
                self.propertyDataList.append(rstTpl)

            elif propertyType in [4, 5]:
                    if propertyType == 4:
                        fmt, fmt_length = '<d', 8
                    else:
                        fmt, fmt_length = '<i', 4

                    value = get_value(fmt, fmt_length)
                    while value != None:
                        if len(str(value)) == 2:
                            break

                        value = get_value(fmt, fmt_length)

                    rstTpl = propertyNameLength, propertyName
                       , propertyType, propertyValList

                    self.propertyDataList.append(rstTpl)

                    if not value:
                        break
            else:
                print ("Format␣Type␣not␣valid")

    else:
        print ("Property␣not␣exist")
```

```
    def saveInfo(self):
        """
        Storing headerData, histogramData and propertyData into
    txt file and saving plot image.
        """
        kwargs = {"headerDataDict" : self.ximHeader,
                  "histogramDataDict" : self.histogram,
                  "propertyDataList" : self.propertyDataList
                  }

        self.ximFileInfoObj = XimFileInfo(**kwargs)
        self.ximFileInfoObj.saveXimInfo()



    def lut_sizer(self, byte, maximum = None):
        '''
        each lut byte contains 4 two-bit flags, except for at the
    tail end,
        there may be some partial flags left over
        :param byte:  the byte to be decoded into 4 windowsx
        :param maximum:  the maximum number of windows to pull
        annoyingly these suckers seem to be put in backwards for
    some reason
        '''

        # lookup table 'bit' flag to byte conversion
        byte_conversion = {'00':1, '01':2, '10':4}

        bit_flags = '{0:08b}'.format(byte)
        for count, idx in enumerate(range(6, -1, -2)):
            if maximum and count>=maximum:
                raise StopIteration

            pair = bit_flags[idx:idx+2]
            yield byte_conversion[pair]


    def lut_reader(self, w, h, lut):
        '''
        read the lookup table and generate bite sizes for latter
    diff
        Assisted by lut_sizer which actually parses each lut byte
    , this function
```

```
␣␣␣␣␣␣␣␣just␣wraps␣the␣lut_sizer␣and␣yield␣from␣it␣the␣approprate
   ␣byte␣size␣for
␣␣␣␣␣␣␣␣each␣diff␣in␣sequence
␣␣␣␣␣␣␣␣:param␣w:␣Uncompressed␣image␣width
␣␣␣␣␣␣␣␣:param␣h:␣Uncompressed␣image␣height
␣␣␣␣␣␣␣␣:param␣lut:␣look␣up␣table
␣␣␣␣␣␣␣␣'''

        # Determine the number of unused 2-bit flag fields
        # in the last byte of the look up table
        # was dividing by bpp, but should be by 4, as there are 4
            flags per 8
        # bit byte, regardless of underlying bytes per pixel

        complete_bytes, partial_bytes = divmod((w * (h - 1) - 1),
            4)

        for count, b in enumerate(lut):
            if count>= complete_bytes:
                # we have come to the end, so only yield part of
                   the last lut
                # byte
                yield from self.lut_sizer(b, partial_bytes)
            else:
                yield from self.lut_sizer(b)



    def uncompressHnd(self, w, h, bpp, lut):
        '''
␣␣␣␣␣␣␣␣Uncompress␣the␣xim␣file␣based␣on␣HND␣algorithm.␣The␣first
   ␣row␣and␣the
␣␣␣␣␣␣␣␣first␣pixel␣of␣the␣second␣row␣are␣stored␣uncompressed.␣
   The␣remainders
␣␣␣␣␣␣␣␣of␣the␣pixels␣are␣compressed␣by␣storing␣only␣the␣
   difference␣between
␣␣␣␣␣␣␣␣neighboring␣pixels.

␣␣␣␣␣␣␣␣E.g.␣consider␣the␣following␣hypothetical␣12␣pixel␣image:
␣␣␣␣␣␣␣␣␣␣␣␣␣␣␣␣R11␣␣␣␣R12␣␣␣␣R13␣␣␣␣R14
␣␣␣␣␣␣␣␣␣␣␣␣␣␣␣␣R21␣␣␣␣R22␣␣␣␣R23␣␣␣␣R24
␣␣␣␣␣␣␣␣␣␣␣␣␣␣␣␣R31␣␣␣␣R32␣␣␣␣R33␣␣␣␣R34
␣␣␣␣␣␣␣␣Pixels␣R11␣through␣R14␣and␣R21␣are␣stored␣uncompressed,␣
   while␣pixels
```

```
        R22 through R34 are compressed by storing only the
           difference:

        diff = R11 + R22 - R21 - R12

        Exploiting the fact that most images exhibit similarity
           in neighboring
        pixel values, the above difference can be stored using
           fewer bytes,
        e.g. 1, 2 or 4 bytes.

        For decompression, the algorithm needs to know the byte
           size of each
        stored difference. To accomplish this, a lookup table is
           placed at the
        beginning of the image. The lookup table contains a 2-bit
           flag for each
        pixel which defines the byte size for each compressed
           pixel difference.
        So a flag value of 0 means the difference fits into one
           byte while
        1 and 2 mean a two and four byte difference respectively.

        :param w: Uncompressed image width
        :param h: Uncompressed image height
        :param bpp: byte per pixel
        :param lut: look up table
        '''
            print('uncompressHnd called, with args: w= {} h={} bpp={}
               {}'.format(w,h,bpp,lut))
            # Initialize uncompressed image variable
            imagePix = np.zeros((h * w), dtype='int32')

            # Read in the first row
            # ... and the first pixel of the second row
            # which is why we do w + 1
            ind = 0  # Index variable
            for i in range(w + 1):
                imagePix[ind] = struct.unpack('<i', self.f.read(4))
                   [0]
                ind += 1


            # Calculate current pixel value based  on "diff"
            # and adjacent pixel values as following:
```

```
        # R22 (current pixel) = diff + R21 + R12 - R11
        for byte_size in self.lut_reader(w, h, lut):

                # read in appropriate number of bytes
                diff = self.char2Int(byte_size)
                # R22 (current pixel) = diff + R21 + R12 - R11
                imagePix[ind] = diff + imagePix[ind - 1] +
                   imagePix[ind - w] - imagePix[ind - w - 1]
                ind += 1


        print('processed␣{}␣pixels'.format(len(imagePix)))
        return imagePix

    def char2Int(self, sz):
        '''
␣␣␣␣␣␣␣␣Convert␣little-endian␣chars␣to␣a␣32␣bit␣integer
␣␣␣␣␣␣␣␣Character␣size␣can␣be␣1␣byte:␣signed␣char
␣␣␣␣␣␣␣␣␣␣␣␣␣␣␣␣␣␣␣␣␣␣␣␣␣␣␣␣␣␣␣␣2␣bytes␣:␣short
␣␣␣␣␣␣␣␣␣␣␣␣␣␣␣␣␣␣␣␣␣␣␣␣␣␣␣␣␣␣␣␣4␣bytes␣:␣int4
␣␣␣␣␣␣␣␣:param␣sz:
␣␣␣␣␣␣␣␣'''
        if sz == 1:
            value = struct.unpack('<b', self.f.read(1))[0]  # b:
               signed char
        elif sz == 2:
            value = struct.unpack('<h', self.f.read(2))[0]  # h:
               short
        elif sz == 4:
            value = struct.unpack('<i', self.f.read(4))[0]  # i:
               int4

        return value

def process_arguments(args):

    # Construct the parser
    parser = ArgumentParser(description='TrueBeam(TM)␣xim␣image␣
       reader.')

    # Add expected arguments
    # Name of the xim image file
    parser.add_argument('-f', '--filename', dest='fname', type=
       str, required=True, \
```

```
                        help="Please␣enter␣name␣of␣the␣binary␣xim
                           ␣file")

    # Add image display option (optional)
    parser.add_argument('-s', '--showImage', dest='showImage',
       type=int, default=1,
                        help="Show␣xim␣image␣(Optional,␣0␣or␣1)")
    # Version number
    parser.add_argument('-v', '--version', action='version',
       version='%(prog)s␣1.0')

    # Apply the parser to the argument list
    options = parser.parse_args(args)

    return vars(options)

def main():

    # Read the command line argument
    options = process_arguments(sys.argv[1:])
    # Create a file object
    fp = XimReader(options['fname'])
    # Read header data
    print('reading␣header')
    fp.headerData()
    print('reading␣header:␣Done')
    # Read xim image, decompress if needed
    print('pixeldata')
    fp.pixelData()
    print('pixeldata:␣Done')
    # Histogram data
    print('histogramdata')
    fp.histogramData()

    print('histogramdata:␣done')
    # Properties data

    print('propertiesdata:␣start')
    fp.propertiesData()
    print('propertiesdata:␣done')

    # Saving headerData, histogramData and propertiesData.
    print('saveinfo:␣start')
    fp.saveInfo()
    print('saveinfo:␣done')
```

```
    #Now show image
    if (options['showImage']):
        m = np.mean(fp.uncompressedImage.flatten())
        s = np.mean(fp.uncompressedImage.flatten())
        plt.imshow(fp.uncompressedImage, vmin=0, vmax=m + 0.1 * s
           , cmap=plt.gray())
        plt.savefig(os.path.join(fp.ximFileInfoObj.outputFolder,
           XIMREADER_IMG_NAME))
        print ("%s is stored on %s" % (XIMREADER_IMG_NAME,
            fp.ximFileInfoObj.outputFolder))
        plt.show()

if __name__ == "__main__":
    # Let's get started
main()
```

C Appendice 3

Tutorial for operation with quality control data software

This tutorial aims to facilitate the use of the developed software for measurement and management of quality control data which is a free software only available for Windows.

Initialization

The user must start the software by double clicking on the executable file, *main.exe*.

Database

Quality control data management software makes use of SQL technology for storing information. In this way, it is important to understand the basic principles of this technology as well as how the tables were created.

The database is composed by five different tables responsible for storing the data grouped into the following categories: sign in information, imaging systems, general parameters, dosimetry, collimator leaves and geometry parameters. All tables have in common a single parameter, the date. In this situation, the date is the primary key, which means that each date only corresponds to a single value for each parameter.

Set user, date and database directory.

Initiating the program presupposes a set of steps designed to identify the user responsible for the quality control, to save the current date and to define the database directory used to access and to store the measurements.

Thus, after the user typing his name in [1] and the date on which the procedure starts in [2]. A new database can be created in [3] or, alternatively, the selection of an existing one in [4]. Subsequently, once the information necessary for the start is filled in, the data is authenticated in [5], a procedure in which the system verifies the information inserted, is a mandatory requirement to proceed. After checking all the fields, the user can advance to the main menu in [6]. In order to minimize the data loss related to accidental program closing, this feature is locked in the top bar and is only available in the last menu.

Menu

The main menu gives to the user access to a wide range of functions for the acquisition, storage and visualization of data.

Data resulting from measurements obtained using the current daily protocol which means the measurements obtained using external instruments can be stored in [1, 2 and 5]. The user should complete a set of forms adjusted to the different categories of tests that will be presented later. However, the software provides an analysis tool to determine the collimator's leaf positions and replace the current daily visual test. The quality control images can be obtained using the XML code presented in Appendix 1 A. These images are then uploaded to [4] in order to be analysed. The software also establishes a connection to external devices, the electrometer. This device can be connected with the software in [3].

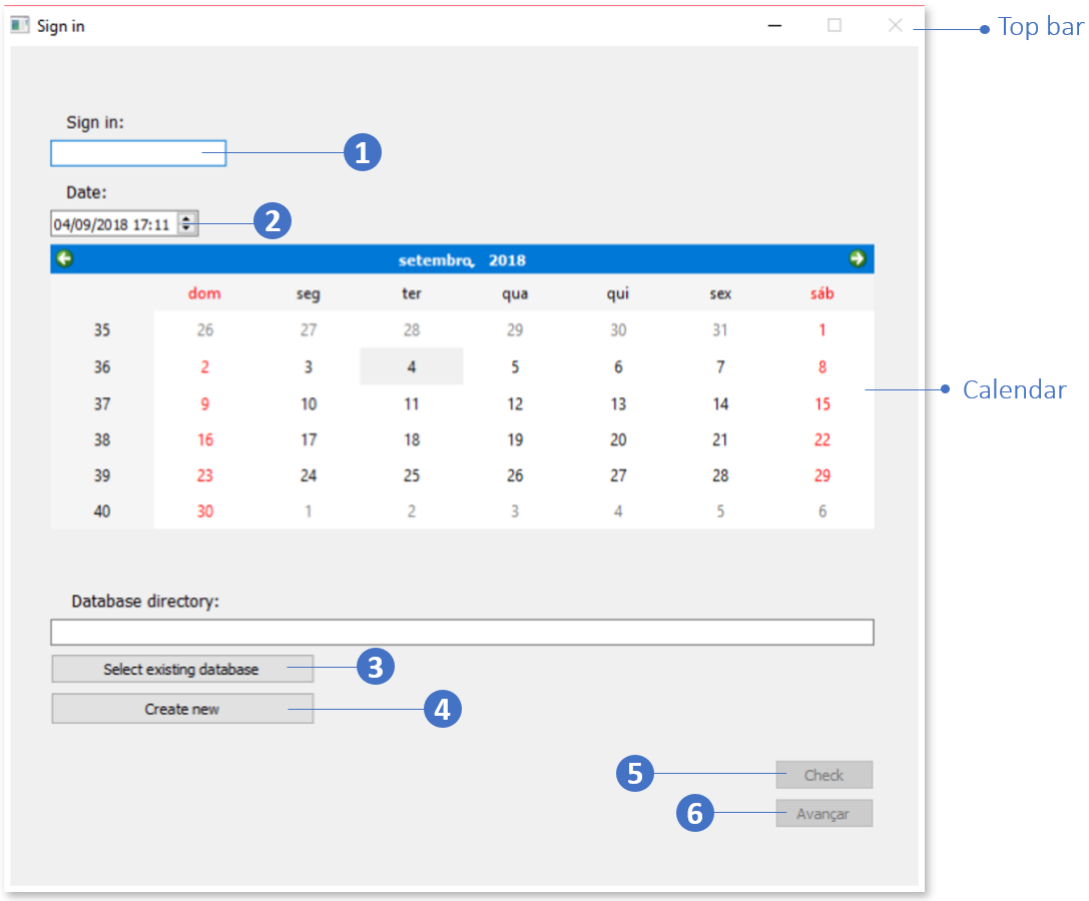

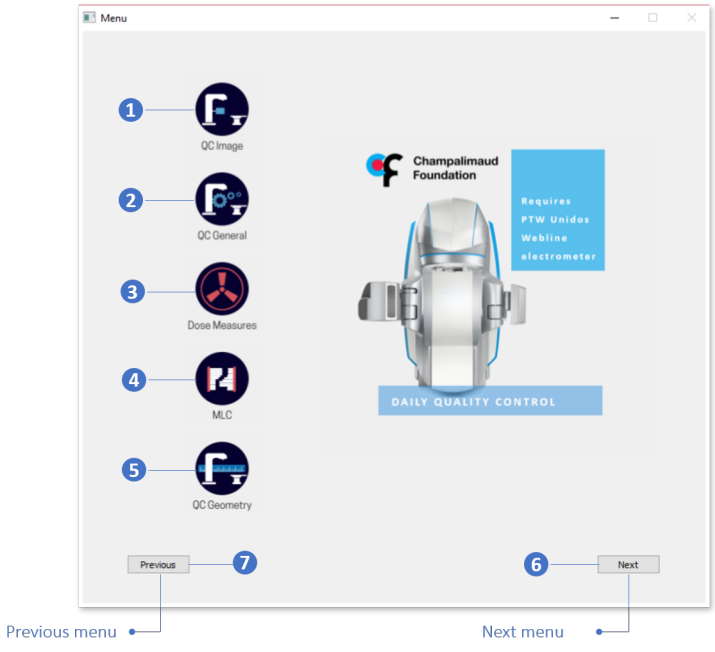

The features included in this software are intended to provide the user with a tool for digitizing data and having the data in a digital format can easier future analyses. In this software, time trends can be accessed in [6].

Storage data

A set of forms is used to introduce quality control data in databases. These forms are available to store the information related to image systems, geometry and linear accelerator general performance.

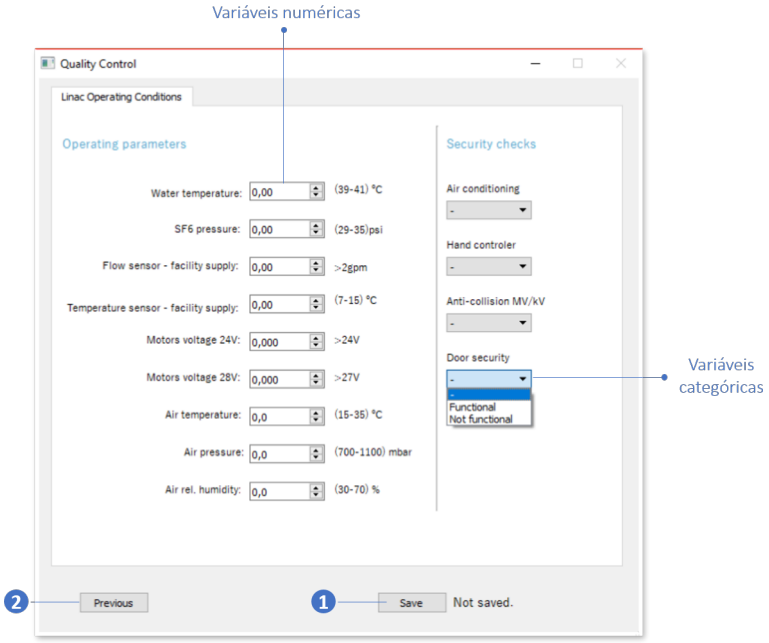

After filling the form, the user should click on [1] to store the data in the database. If the user returns to the main menu by clicking on [2] without saving the data, the information will be lost. It is important to note that in these forms the results can only be saved once per session.

Communication with PTW Unidos^{Webline} electrometer

As mentioned before, the software can be used to facilitate the control of the external electrometer device which is capable of performing readings of the dose values administered by association with an ionization chamber.

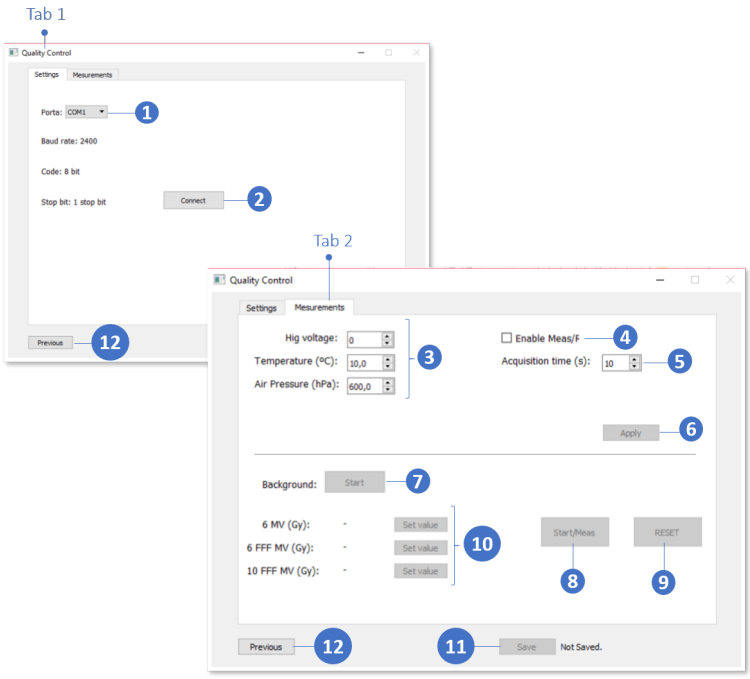

The electrometer must be connected to the computer using RS-232 communication cable. The interaction between the software and the electrometer starts in Settings. After choosing the COM port, [1], the connection must be effective in [2], an action that will activate the features available in Measurements. After the communication between the devices is established, the user can guarantee dose correction by filling the fields in [3]. Subsequently, the user has the possibility to opt for a manual acquisition method in [4] or by an automatic method, whose time interval is defined in [5]. These configurations are applied in [6]. The user should start the measurement process by defining background in [7]. Considering the available energies, the software is prepared to store information related to 6 MV, 6FFF MV and 10FFF MV. To start the measurements the user should click on [8]. In this situation, if the user has chosen the manual method the process will end after clicking on [9]. Then, the user must select the corresponding energy field in [10] and after all, measurements are saved in [11].

Collimator's leaves positions analysis

The positioning of the collimator leaves is performed automatically by analysing features extracted from previously acquired portal images.

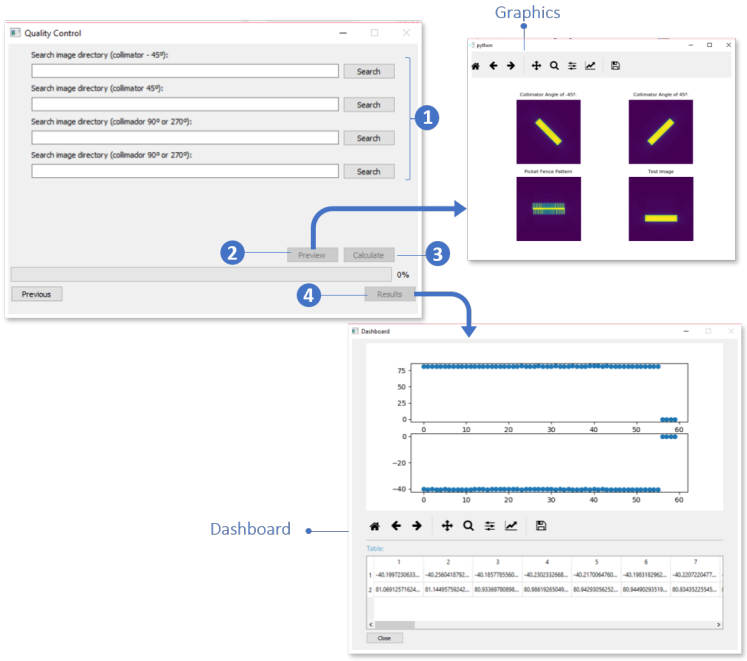

The software is designed to receive images acquired with the EPID positioned in the isocenter. The textboxs in [1] are filed with the correspondent image directory whose specifications are described in the legend above the field. A preview of the images is generated in [2]. After the user confirms the choice of the images, the determination of leaf positions is done in [3]. Since the process is finished, the results can be consulted in [4].

Data visualization

The data saved can be visualized using this software. The user should select the table and the variable to be accessed, as presented in [1] and [2]. The visualization of the time trend is generated by clicking [3].

The dashboard is composed by a graph showing the time variation of the chosen variable and a general overview of all the variables that compose the table chosen.The user can exit in [4].

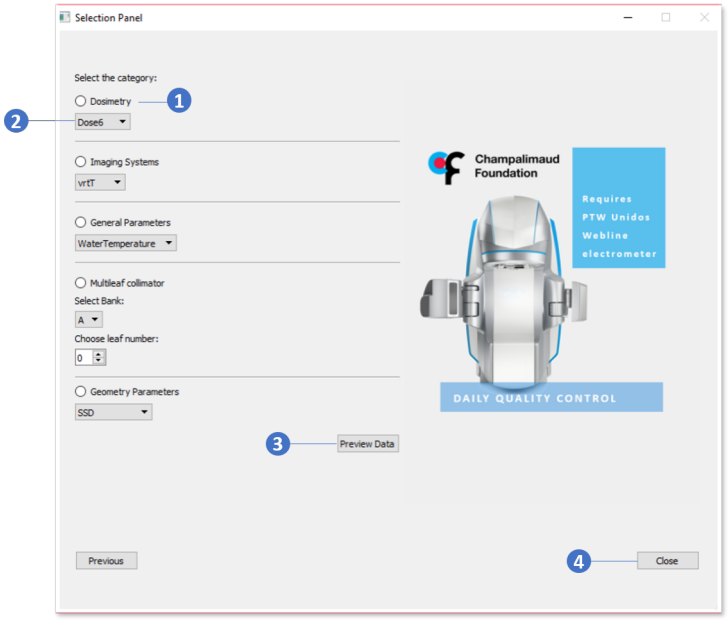

Developer mode

This software was created during a dissertation project developed at the Faculty of Sciences of the University of Lisbon and the Champalimaud Foundation in an academic context. For this reason, and since it is possible to include new features in the software, a brief explanation of how to edit and debug the code is provided.

The user should start by installing the Anaconda®. Anaconda is a free computing tool used for Python content distribution (https://docs.continuum.io/anaconda/). The installation of Anaconda should guarantee the installation of Spyder®, a graphical interface that allows the editing of scripts and debugging in Python.

Then, depending on the Python version, the installation of a set of packages, not provided in the version chosen but required to run the software developed, is needed. The packages can be installed via *conda* or *pip*. In the command line the user should type *conda install <packagename>* or *python -m pip install <packagename>* to proceed with the installation of some package. The user may know that packages are missing from their version of Python by simply running the software on the command line.

In the folder distributed with the application, the user can find all the .py files which can be editable and used to create the executable file.